Hydraulics Research
Wallingford

SELF-CLEANSING CONDITIONS FOR SEWERS CARRYING SEDIMENT

by

R W P May, P M Brown, G R Hare and K D Jones

Report SR 221
December 1989

Registered Office: Hydraulics Research Limited,
Wallingford, Oxfordshire OX10 8BA.
Telephone: 0491 35381. Telex: 848552

This report describes work funded by the Department of the Environment under Research Contract No DGR PECD 7/6/82. It is published on behalf of the Department of the Environment, but any opinions expressed in this report are not necessarily those of the funding Department. The work was carried out in the River Engineering Department of Hydraulics Research, Wallingford headed by Dr W R White. The nominated project officers were Dr R P Thorogood for DoE and Dr W R White for HR.

Published by permission of the Controller of Her Majesty's Stationery Office.

ABSTRACT

An experimental study, funded by the Department of the Environment, was made of the factors governing the deposition of non-cohesive sediment in a 300mm diameter concrete pipe. Tests were carried out with 0.72mm sand using flow velocities between 0.5m/s and 1.5m/s, proportional depths of flow between 3/8-full and pipe-full and volumetric sediment concentrations between 0.3ppm and 440ppm. The 20m length of concrete pipe was installed in a tilting flume equipped with separate re-circulation systems for water and sediment. A new optical device was developed for continuously measuring the rate of sediment transport in the system.

Data for the limit of deposition in the concrete pipe were compared with previous HR results for smooth 77mm and 158mm diameter pipes and with several available formulae. Analysis showed that the limiting sediment concentrations in the concrete pipe were approximately half those expected in a smooth pipe of equal diameter. The reduction in transporting capacity was explained in terms of an increase in the threshold velocity of the sediment in the rougher pipe. A formula for predicting the limit of deposition in both rough and smooth pipes was developed using all the HR data. This can be used to estimate minimum flow velocities for self-cleansing sewers based on pipe size, sediment size, depth of flow and rate of sediment transport.

Tests were also carried out with small depths of sediment deposition. These showed that a mean sediment depth of 1% of the pipe diameter enables a flow to transport significantly more sediment than at the limit of deposition with effectively no increase in head loss. Self-cleansing sewers designed for a 1% sediment depth could therefore be laid at flatter minimum gradients than those designed according to a "no-deposit" criterion.

SYMBOLS

A	Cross-sectional area of flow
C_v	Volumetric sediment concentration
D	Pipe diameter (internal)
D_{gr}	Non-dimensional grain parameter (Equation (12))
d	Mean sediment size (d_{50})
d_{mm}	Sediment size in mm
E	Specific energy of flow
g	Acceleration due to gravity
i	Hydraulic gradient of flow
k	Size of bed roughness
k_s	Hydraulic roughness in Colebrook-White formula
k_{ss}	Composite value of k_s for pipe with sediment
L	Laursen's parameter (Equation (18))
m	Gradient of specific energy line
n	Manning's roughness coefficient
P	Wetted perimeter of flow
Q	Water discharge
Q_s	Volumetric sediment discharge
R	Hydraulic radius of flow (= A/P)
R_e	Reynolds number of flow (= $4VR/\nu$)
S_o	Gradient of pipe invert
V	Mean flow velocity
V_{bs}	Flow velocity at transition from sediment movement as bed-load to suspended-load
V_L	Flow velocity at limit of deposition
V_m	Minimum flow velocity corresponding to specified depth of sediment deposit
V_t	Threshold velocity of isolated sediment particle in pipe
V_{tr}	Value of V_t for rough pipe
V_{ts}	Value of V_t for smooth pipe
w	Fall velocity of sediment particle
X	Parameter defined by Equation (30)
Y	Parameter defined by Equation (32)
y	Depth of flow
θ	Angle of pipe to horizontal (positive upwards)
λ	Darcy-Weisbach friction factor
ν	Kinematic viscosity of water
ν_m	Kinematic viscosity of water-sediment mixture
ρ	Density of water
σ_s	Standard deviation
τ_o	Mean shear stress in pipe

CONTENTS

CONTENTS (CONT'D)

FIGURES

APPENDIX

1 INTRODUCTION

It has long been recognised that sediment deposits in sewers cause loss of flow capacity and can lead to surcharging and sometimes surface flooding. The problems were often considered to be localised and were usually dealt with by means of routine maintenance. However, two recent developments have demonstrated that the adverse effects of sediments in sewers are more serious than previously believed.

Firstly, the increased use of closed-circuit television equipment has shown that large lengths of sewerage systems contain significant deposits. A survey carried out for a CIRIA (1987) research project suggested that up to 25,000km of sewers and drains in the UK may be affected. Even though many such deposits may not be large enough to cause regular surcharging or flooding, they will still reduce the maximum flow capacity of a system and prevent it coping with the flood event for which it was designed.

The second development is the greater emphasis now placed on environmental aspects such as water quality. Stormwater sewerage systems, either separate or combined, are responsible for a significant proportion of the pollution that enters estuaries, rivers and watercourses, particularly in urban areas. Research has shown that many of the pollutants such as those responsible for the biological and chemical oxygen demand become closely associated with the sediment particles in sewers. Thus, sediments discharged directly from separate storm water sewers or from storm sewer overflows in combined systems will cause pollution in the receiving waters. In order to be able to study methods of improving water quality, it is therefore important to understand how sediment is transported through a sewerage system. The build-up of deposits near storm sewer overflows can also cause them to operate more frequently than necessary and thereby produce additional pollution.

Experimental research on sediment movement in sewers has been carried out at Hydraulics Research (HR) since 1975, under two studies funded by the Department of the Environment (DoE). The first study between 1975 and 1982 was concerned principally with developing an improved criterion for the design of self-cleansing sewers. Experiments were made using 77mm and 158mm diameter smooth plastic pipes, and showed how the flow velocity needed to prevent the formation of deposits depended on factors such as the sediment concentration, particle size and pipe diameter. Results of this study were described in reports by May (1975, 1982).

The second study, which is the subject of this report, forms part of the River Basin Management (RBM) programme. This is a co-ordinated programme of research into the effects of sewers on rivers, and covers field work, laboratory studies and the development of computational models. Individual projects are being carried out by the Water Research Centre (WRc), universities and HR, with funding provided by the Regional Water Authorities (and their successor organisations), the Science and Engineering Research Council and the Construction Industry Directorate of DoE.

A major component of the programme is MOSQITO, a computational water quality model for sewers, which is being developed at HR (with DoE funding) for use by the UK water industry. In order to be able to predict variations in water quality in sewers, it is necessary to determine rates of sediment deposition and erosion. The experimental study on sediment movement described in this report therefore has two functions : it extends the scope of the 1975-1982 work on self-cleansing sewers and secondly provides information necessary for the development of MOSQITO.

2 SCOPE OF STUDY

The principal objective of the present study is to aid the development of improved guidelines for the design of self-cleansing sewers carrying sediment.

Current practice for the design of self-cleansing sewers is to ensure that either the flow velocity or the shear stress produced by the flow exceeds a certain limiting value. Typical minimum values are in the range 0.75m/s to 1.0m/s for velocity and 1 N/m^2 to 4 N/m^2 for shear stress. Such limits are usually linked with a requirement that they be achieved at a given depth of flow (eg with the pipe half full) or with a given frequency (eg once a day on average for a combined sewer). These conditions lead to values of minimum gradient below which gravity sewers should not be laid if they are intended to be self-cleansing. A survey of various guidelines for self-cleansing sewers is contained in Appendix G of CIRIA (1987).

Recent laboratory studies, including the work carried out at HR under the first DoE contract, showed that self-cleansing conditions cannot be defined simply in terms of a fixed value of velocity or shear stress but need to take account of the rate of sediment entering the system, the size and density of the sediment, and the diameter of the pipe. Various formulae which include these extra factors have been developed, but they were mostly based on experiments carried out with non-cohesive sediments in smooth pipes of small diameter. Sediments in separate storm water sewers usually remain non-cohesive, but in combined systems they may become coated with biological slimes and greases. Crabtree (1988) classified sewer sediments into five broad categories. Type A material corresponds to the coarser sediment which forms bed deposits in combined sewers; analysis showed that it typically consists of granular sand and gravel with an organic content of about 10%. Rheological tests carried out by Williams et al (1989) on four Type A samples from sewers in Cardiff indicated that the material was cohesive, so results from laboratory studies with non-cohesive sediments may need to be applied with caution to combined systems. However, until the behaviour of non-cohesive sediments is understood properly, it will be difficult to take correct account of cohesive effects.

As mentioned, most studies on self-cleansing conditions have been carried out with smooth pipes of small diameter. Unfortunately, the resulting formulae give widely-differing predictions when extrapolated to pipes significantly larger than those originally tested. The first part of the new study described in this report was, therefore, designed to investigate self-cleansing conditions in concrete pipes of 300mm and 450mm diameter, which are more typical of those used in many sewerage systems. The results are compared with data and equations from previous studies in order to identify more accurately the effects of pipe size and texture.

Although earlier studies have disagreed on the precise flow conditions needed to prevent sediment deposition, most predict that the required flow velocity increases with increasing pipe size. The implication is that the minimum gradients of large sewers (eg having diameters > 0.5m) should be steeper than those specified at present. A change in design guidelines based on recent research could, therefore, significantly increase the costs of new sewerage schemes by requiring pipes to be laid at greater depths; more pumping would also be needed. However, there is a possibility that the criterion usually adopted for "self-cleansing" conditions - namely, no formation of stationary sediment deposits - may be more severe than is actually necessary. If small depths of sediment deposit are permitted under design conditions, it may be possible to reduce the values of minimum flow velocity; this in turn would allow the use of somewhat flatter pipe gradients. It can also be argued that the criterion of no sediment deposition is a fiction because some sediment will always remain in a sewer after a storm and will usually form a stationary deposit until the next storm occurs.

Whether or not a relaxation in the self-cleansing criterion is justified depends on the answers to two questions. Firstly, if sediment deposits are allowed to form, will they remain small or will they grow in size until ultimately the pipe surcharges or becomes blocked? Secondly, will the additional hydraulic resistance due to the deposits be large enough to reduce the hydraulic capacity of the sewer significantly? The second part of the study described in this report was carried out to answer these questions and provide guidance on suitable design criteria for sewers carrying sediment.

3 PREVIOUS STUDIES

3.1 Definitions

Sewers are usually required to be "self-cleansing" but exactly what this means is seldom made clear. Three different definitions can be envisaged:

(a) Threshold of movement. Flow conditions are just sufficient to cause particles to start moving along the pipe (either along the smooth invert of the pipe or over other deposited particles).

(b) Transport without deposition. Flow conditions are sufficient to transport sediment along the pipe at the rate at which it enters without stationary deposits forming (termed "flume traction").

(c) Transport with deposition. Flow conditions are sufficient to transport sediment along the pipe at the rate at which it enters, with the depth of stationary deposits limited to a certain proportion of the pipe diameter.

Although the threshold of movement is of interest, it is not in fact appropriate as a definition of self-cleansing conditions because the rate of sediment transport is effectively zero; sediment entering the system at a finite rate will therefore cause the deposits to increase continuously with time.

The boundary between (b) and (c) is termed the limit of deposition, and has been the subject of most of the recent experimental research on self-cleansing conditions. It provides an appropriate design criterion, but as described in Section 2 it may require relatively steep gradients for larger pipes.

When the limit of deposition is exceeded, separate isolated dunes tend to occur at the flow velocities and sediment concentrations typically found in gravity sewers. The dunes travel slowly along the pipe by means of a caterpillar-track type of motion. Particles at the upstream end of a dune are transported forward by the flow to the downstream end where they are retained by a separation zone formed by the steep leading edge of the dune. The particles below the surface remain stationary until they become exposed at the upstream end, so the dunes can be considered as being effectively stationary. Well beyond the limit of deposition, the sediment forms a continuous bed; particles at the surface are transported by the flow over a layer of other particles which remain stationary.

Previous research relevant to the present study is summarised in the following sections under the three alternative definitions of self-cleansing conditions. A full list of the symbols used is given at the beginning of this report.

3.2 Threshold of movement

Novak & Nalluri (1975) measured conditions at the threshold of movement for individual particles (with sizes in the range d = 0.15mm to 2.0mm) in smooth circular and rectangular channels. The best-fit relation for the threshold velocity V_{ts} on a smooth bed was

$$V_{ts} = 0.61\ [g\ (s-1)\ d]^{\frac{1}{2}}\ (d/R)^{-0.27} \qquad (1)$$

where s is the specific gravity of the particle and R is the hydraulic radius of the flow. When plotted on the well-known Shields diagram for the threshold of movement, the data points lay below the curve for particles resting on a bed of similar particles, as would be expected due to the lower frictional resistance offered by a smooth surface.

Novak & Nalluri (1984) extended their earlier work to rectangular channels with rough beds. The threshold velocity V_{tr} for an individual particle on a rough bed was found to be higher than the corresponding velocity V_{ts} on a smooth one; the relationship established between the two values was

$$(V_{tr}/V_{ts}) = 1 + 1.43\ (d/k)^{-0.4} \qquad (2)$$

where d is the sediment size and k the size of the bed roughness (d varied between 0.6mm and 50mm and was larger than k in all the tests). Experiments were also carried out on small groups of particles. In the case of particles touching in rows across the width of the channel, it was found that the threshold velocity V_t was the same for both rough and smooth channels and given by

$$V_t = 0.50\ [g\ (s-1)\ d]^{1/2}\ (d/R)^{-0.40} \qquad (3)$$

3.3 Transport without deposition

Several experimental studies have been carried out to determine the relationship between flow conditions and sediment transport rate at the limit of deposition. The sediment concentration, C_v, will here be defined in terms of volumetric transport rates so that

$$C_v = \frac{Q_s}{Q + Q_s} \qquad (4)$$

where Q is the water discharge and Q_s the volumetric sediment discharge. Since typical values of C_v in sewers are in the range 10 to 100 parts per million (ppm) by volume, there is no significant difference in using the more usual but less precise definition

$$C_v = \frac{Q_s}{Q} \qquad (5)$$

Laursen (1956) summarised the results of four investigations carried out with 51mm and 152mm diameter smooth pipes using sands with sizes between

0.25mm and 1.6mm. Results for the limit of deposition were presented graphically, but May (1975) showed that these could be approximated by

$$\frac{V_L}{[2\ g\ (s-1)\ y]^{1/2}} = 7.0\ C_v^{1/3} \tag{6}$$

where V_L is the mean velocity in the pipe at the limit of deposition, and y is the depth of flow. Note that the limiting velocity was found not to depend significantly on the sediment size.

Robinson & Graf (1972) carried out tests in 102mm and 152mm diameter smooth pipes flowing full with sediment sizes of 0.45mm and 0.88mm. The sediment concentrations were in the range 10^3 ppm to 7×10^4 ppm, so the results provide a link with other studies on the transportation of sediments at very high concentrations (up to $C_v = 3 \times 10^5$ ppm). The best-fit equation to the results was

$$\frac{V_L}{[2\ g\ (s-1)\ D]^{1/2}} = \frac{0.928\ C_v^{0.105}\ d_{mm}^{0.056}}{(1 - \tan \Theta)} \tag{7}$$

where d_{mm} is the sediment size in mm and Θ is the angle of the pipe to the horizontal (positive for an upwards-sloping pipe).

Tests on the limit of deposition were carried out previously at Hydraulics Research using 77mm and 158mm diameter smooth pipes and sediment sizes between 0.6mm and 7.9mm. May (1982) fitted the results to a semi-theoretical equation and obtained

$$C_v = 2.05 \times 10^{-2}\ (A/D^2)^{-1}\ (d/R)^{0.6}\ [1 - (V_{ts}/V_L)]^4 .$$

$$\left[\frac{V_L^2}{g\ (s-1)\ D}\right]^{3/2} \tag{8}$$

V_{ts} is the threshold velocity of an isolated particle on a smooth bed, and has the value given by Novak & Nalluri's Equation (1); A is the cross-sectional area of the flow.

Macke (1982) measured the limit of deposition in smooth pipes with diameters of 192mm, 290mm and 445mm and used sands with sizes of 0.16mm and 0.37mm. These results, together with data from other sources, were analysed on the assumption that the sediment was transported in suspension, and were found to fit the equation

$$Q_s \rho g (s-1) w^{1.5} = 1.64 \times 10^{-4} \tau_o^3, \text{ for } \tau_o \geq 1.07 \text{ N/m}^2 \tag{9}$$

where w is the fall velocity of the particles and τ_o is the average shear stress around the pipe. The equation is dimensional and SI units should be used. In order to compare it with other formulae for the limiting velocity, Equation (9) can be expressed in the form

$$V_L = 1.98 \lambda^{-0.6} w^{0.3} [(s-1) A C_v]^{0.2} \tag{10}$$

where λ is the Darcy-Weisbach friction factor of the flow.

Mayerle (1988) carried out experiments to determine the limit of deposition using a smooth pipe with a diameter of 152mm and two rectangular channels with widths of 311mm and 462mm; the rectangular channels were tested with both smooth and rough inverts. Six sizes of uniform sediment were used ranging from 0.50mm to 8.7mm (with s = 2.49 to 2.61). Many different data correlations were investigated, and one of the best fits to the data for the smooth circular pipe was given by

$$\frac{V_L}{[g\ (s-1)\ d]^{1/2}} = 0.89\ D_{gr}^{-0.40}\ C_v^{0.19}\ (d/R)^{-0.20}\ \lambda^{-1.05} \tag{11}$$

where D_{gr} is a non-dimensional grain parameter defined as

$$D_{gr} = [g\ (s-1)/\nu^2]^{1/3}\ d \tag{12}$$

Information on the effect of bed roughness in the rectangular channels was also used to develop an alternative equation for circular pipes which it was hoped would be suitable for both rough and smooth pipes. The resulting equation recommended by Mayerle & Nalluri (1989) was

$$\frac{V_L}{[g\ (s-1)\ d]^{1/2}} = 14.43\ D_{gr}^{-0.14}\ C_v^{0.18}\ (d/R)^{-0.56}\ \lambda^{0.18} \tag{13}$$

The value of the friction factor λ can be calculated from the Colebrook-White equation

$$\lambda^{-0.5} = -\ 2\ \log_{10}\ [(2.51\ \lambda^{-0.5}/R_e) + (k_{ss}\ R^{-1}/14.8)] \tag{14}$$

R_e is the Reynolds number of the flow and k_{ss} is the composite roughness of the pipe when carrying sediment at the limit of deposition. The value of k_{ss} can be determined from the following best-fit relation given by Mayerle & Nalluri

$$(k_{ss} - k_s)/R = 0.0130\ D_{gr}^{0.24}\ C_v^{0.40} \tag{15}$$

An alternative approach to predicting the limit of deposition was developed by Ackers (1978, 1984), who analysed the HR data for 77mm and 158mm pipes (see earlier) using the well-established Ackers-White sediment transport equation. Certain necessary changes were made to the latter equation in order to permit its application to pipes (eg replacement of flow depth by hydraulic radius), but otherwise the coefficients (determined from alluvial channel data) were assumed to be unchanged. On this basis, the analysis showed that the sediment transport rates observed in the HR tests at the limit of deposition were consistent with the Ackers-White equation if the effective width of sediment in the invert of the pipe was taken to be approximately equal to 10 particle diameters. A full description of the application of the Ackers-White equation to pipe flow is given in CIRIA (1987).

When comparing results of different studies, it is relevant to know whether, just prior to deposition, the sediment particles were being transported as bed-load or as suspended-load. The dividing line between the two modes of transport is seldom clear cut, but may be estimated by the following criteria due respectively to Newitt et al (1955) and Spells (1955):

$$V_{bs} = 17\ w \tag{16}$$

$$V_{bs}^{1.225} = 0.0251\ g\ (s-1)\ d_{85}\ (D/\nu_m)^{0.775} \tag{17}$$

Here V_{bs} is the pipe-full flow velocity at the transition from bed movement to movement in suspension and ν_m is the kinematic viscosity of the water-sediment mixture; 85% by weight of the particles are finer than the d_{85} size. Values of V_{bs} given by these formulae for a range of particle sizes are compared below (assuming $D = 0.15$m, $\nu_m = 1.14 \times 10^{-6}$ m^2/s and $s = 2.6$).

d (mm)	V_{bs} (Eqn 16) (m/s)	V_{bs} (Eqn 17) (m/s)
0.15	0.23	0.61
0.6	1.5	1.9
1.5	3.6	4.0
6.0	9.7	12.4

Although the two equations do not agree very well, they do indicate that, for flow conditions near the limit of deposition in gravity sewers, particles coarser than about 0.4mm are likely to be moving as bed load.

3.4 Transport with deposition

According to Laursen (1956), the sediment-transporting capacity of a pipe flowing part-full decreases once deposition begins. If the sediment and water discharges are kept constant, the depth of the deposits will continue to increase until the pipe flows full and surcharges. Only then can the sediment-transporting capacity of the flow increase until it matches the rate at which sediment is entering the pipe. Laursen and his co-researchers, therefore, investigated equilibrium conditions for deposited beds only for the case of pipe-full flow. A graphical relationship was established between the proportional depth, y_s/D of the sediment deposit and a parameter

$$L = \frac{Q}{[g\ (s-1)\ D^5]^{\frac{1}{2}}\ C_v^{1/3}} \qquad (18)$$

It is convenient to express the relationship by means of a formula, and a reasonable fit is given by

$$y_s/D = 2\ (L + 1)^{-1/3} - 1 \qquad (19)$$

It is stressed that this equation does not have any particular theoretical basis, but purely describes the shape of the mean experimental curve presented by Laursen. The deviation of Equation (19) from the mean curve is considerably smaller than the experimental scatter about the mean curve.

Data for the alluvial channels and pipes with deposited beds were analysed by Graf & Acaroglu (1968) and fitted to an equation which can be expressed in the form

$$\frac{V}{[8\ g\ (s-1)\ R]^{½}} = 0.732\ \lambda^{-0.624}\ C_v^{0.248}\ (d/R)^{0.252} \qquad (20)$$

R is the hydraulic radius of the free-flow area, and λ is the overall friction factor for the pipe; no attempt was made to apportion the resistance between the deposited bed and the walls of the pipe.

As mentioned in Section 3.3, Ackers (1978) adapted the Ackers-White sediment transport equation to describe the movement of sediment in pipes. For the case of a deposited bed, it was initially assumed that the effective width of sediment transport was equal either to the diameter of the pipe or to the width of the water surface, if the pipe was flowing less than half-full. Other choices, however, can be made, and CIRIA (1987) suggested that the effective width be taken as equal to the actual width of the deposited bed. The greater the depth of deposit in a pipe, the more accurate the predictions of the Ackers-White equation can be expected to be, because conditions then approach more closely those in alluvial channels for which the equation was originally developed. However, a detailed evaluation of the equation for the case of deposited beds in pipes has not yet been made due to the lack of suitable experimental data.

Perrusquia (1987, 1988) carried out experiments with various depths of sediment deposit in a 225m diameter concrete pipe using sand sizes of 0.5mm and 1.0mm. In the first stage of the study, tests were made with a plane stationary bed in order to verify methods for apportioning the overall frictional resistance between the pipe walls and the sediment bed : the method due to Vanoni & Brooks (1957) gave satisfactory results. In the second stage, tests were carried out at low rates of sediment movement in order to study the development of bed forms and their effect on flow resistance. It was found that the dimensions of the ripples/dunes were reasonably predicted by a method due to Fredsoe (1982) and the flow resistance by a method due to Engelund & Hansen (1972). However, further work was considered necessary to develop relationships specific to sediment deposits in pipes.

4 TEST ARRANGEMENT

4.1 General layout

The experiments were carried out in a converted 2.44m wide tilting flume (see Figure 1) in which flow was supplied to the test pipe by up to three pumps having a total capacity of around $0.25m^3/s$. Pipes up to 450mm diameter can be installed, but initially a 300mm diameter concrete pipe was studied. The pipe was mounted in one half of the flume, the other half acting as a bypass channel. Flow into the head of the system passed into the sewer pipe over a 1.22m wide rectangular thin plate weir; part of the flow from the pumps could be diverted into the bypass channel by means of an adjustable tilting weir. This system allowed the flow rate entering the sewer pipe to be varied rapidly for accurate simulation of floods. The sediment was recirculated separately with a small proportion of the liquid discharge, by a slurry pump whose discharge was measured using an electro-magnetic current meter. The sediment concentration in the recirculation pipe was measured using an infra-red sensor (see 4.2).

The test pipe was made up of 2.52m long ROCLA spun-concrete pipes with a nominal internal diameter of 300mm and a total length of 21m. It was measured to have a mean internal diameter of 298.83mm, with a standard deviation of σ_s = 2.89mm (see Figure 2). The individual pipes had spigot-and-socket joints, which would normally be assembled with the spigots pointing downstream. For practical reasons it was necessary to fix the pipe to the bulkhead at the upstream end, so the pipe was laid with sockets pointing downstream. This caused the joints to present a small (approx 2-3mm) expansion in the downstream direction, which was considered beneficial because otherwise sediment deposition might have occurred prematurely at the steps. Internal gaps between the pipe lengths varied from zero to approximately 20mm depending on the fit at individual joints. The pipe was laid on wooden blocks such that the invert was as level as possible when the flume was level. The invert levels were checked along the pipe, and it was found that at the gauge positions the deviations Δ from the mean level were in the range $-0.2 \leq \Delta \leq 2.1$mm; for the pipe as a whole the range was $-4.9 \leq \Delta \leq 2.4$mm. The flume could be tilted to give a maximum pipe slope of around 1/100.

Each pipe length had two 900 x 90mm slots cut in the top to allow observation of bed conditions along the length of the pipe. Flush-fitting, transparent lids were built to re-seal the pipe for tests at pipe-full flow, whilst still allowing observation of the bed.

The depth of flow in the pipe was controlled initially using an adjustable sluice gate at the downstream end.

The gate was later replaced by restrictors which allowed more precise depth control. These were vertical panels which were introduced from both sides of the pipe outlet. Flow from the pipe discharged freely into a hopper where the sediment was allowed to settle. The sediment was extracted, with a small proportion of the flow, from the bottom of the hopper, and recirculated by the slurry pump to the head of the sewer. The remaining flow discharged over the sill of the hopper into an outer tank, thus maintaining a constant head over the slurry pump. Mesh screens around the sill prevented sediment in suspension from escaping into the outer tank. Water jets were used to prevent the build-up of sediment deposits in the hopper and the clogging of the screens.

The hydraulic gradient along the pipe was measured using five electronic digital depth gauges mounted above the pipe at 2.52m intervals along part of its length. The point gauges were fitted with a battery-powered electronic detector circuit, which emitted an audible "squeak" when the tip of the gauge was in contact with the water. This was of particular assistance in the tests with part-full flow when the water surface was measured directly, and fluctuations caused the gauge to "dip" into and out of the water. For pipe-full flow the level was measured in stilling wells mounted on the transparent perspex lids. These stilling wells were connected with the pipe via 0.5mm diameter holes, which were small enough to reduce periodic fluctuations in water level to around ±1mm.

The sand bed profile was measured with a portable electronic point gauge with digital read out, which was zeroed on the pipe invert. The accuracy of the measurements was approximately ±0.25mm.

4.2 Sediment concentration measurement

In the earlier HR tests with the 77mm and 158mm diameter pipes, dry sand was added at the upstream end of the pipes using a vibrating screw sediment injector, and removed at the downstream end by collecting it in a hopper. This was found to have a number of drawbacks. The screw-injector tended to grind the sand, reducing its size as the testing continued. Also, it was necessary to keep drying large quantities of sand after every test before it could be re-used, and the injector could not be relied upon to maintain a constant rate of supply.

In order to achieve the much higher transport rates expected in the larger diameter pipes, without demanding huge quantities of dry sand for every test, a new method was devised for the present set of experiments. This used a re-circulating sediment system and a new instrument which measures sediment concentration by the interruption of an infra-red light beam. The instrument is similar in type to the Partech device which is widely used for measuring silt concentrations. Development tests showed that the instrument would satisfactorily register much coarser sand particles. This was essential to the concept of the test rig, because it enabled the concentration of the wet re-circulated sand to be measured continuously without affecting equilibrium conditions in the sewer pipe.

The sand from the hopper at the downstream end of the sewer pipe was pumped at a pre-set velocity to the head of the system via a 75 mm diameter pipe. The flow velocity in this sediment return pipe was measured using an electro-magnetic current-meter (ECM) which was not affected by small sediment concentrations.

The sediment return pipe contained a 1m long perspex section, with an infra-red light source mounted against the invert on the outside of the pipe (see Figure 3). The source shone a "pencil" beam across the diameter of the pipe to a sensor opposite it, also mounted on the outside of the pipe. Sand passing along the pipe interrupted the beam, and reduced the strength of signal arriving at the sensor. The sensor signal was fed to an amplifier unit which converted it to a voltage, which was nominally in the range 0-1 volts but could be varied using gain and balance settings. For the sediment tests these were set to give an output of .988 V for no signal reaching the sensor, down to around 0.1V for clear water. From the amplifier, the signal was fed both to a chart recorder to produce a hard copy, and through a voltage-frequency converter to a counter. The counter could be set to count over a given time period from 1 second up to 9999 seconds to give a mean reading for that period. After passing the sensor the sand and water were fed back into the head of the sewer pipe (downstream of the thin-plate weir), thus maintaining a constant mean sediment transport rate through the system. Figure 4 shows schematically the layout of the measurement and recording system.

The response of the infra-red device was found to be dependent on both sediment size and flow velocity in the sediment pipe. The dependence on flow velocity was advantageous, in that a wide range of transport rates could be covered by only a few pipe velocities: increasing the pipe velocity reduces sediment concentration for a given transport rate, and therefore reduces the response of the infra-red sensor. The flow velocity and sediment concentration in the sediment pipe could be altered to suitable values without affecting the corresponding conditions in the sewer pipe.

Before the system could be used, it was necessary to calibrate the infra-red sensor over a range of sediment concentrations and sediment pipe flow velocities. Based on expected transport rates for the range of sewer velocities to be studied, two calibration velocities were initially chosen, and tested over the full response range of the sensor using 0.72mm sand.

Before and after each calibration a sensor reading was taken with no sediment present. This, the "clear-water" reading, was found to vary by a few percent from one test to another. At the other end of the scale, a reading was taken with the infra-red source switched off. This reading was found to be constant, confirming that ambient light levels were not affecting the readings.

The sediment sensor calibrations were carried out using a 2 litre plastic beaker, with holes of various sizes drilled in the base to allow a range of injection rates. The holes were taped over, and the beaker filled with sand and weighed. It was then mounted above the hopper at the downstream end of the sewer pipe, with a funnel and vertical pipe to catch the sand from the beaker and carry it directly down to the slurry pump intake. With the return pipe set at the required calibration velocity, tape was removed from one or more holes, and a stop watch was started. Sand was then added to the beaker from a pre-weighed supply, to keep it topped up to a constant level. When all the pre-weighed sand had been used, the holes were resealed and the stopwatch stopped. The beaker was then reweighed, and the mean injection rate calculated as

$$\frac{\text{initial beaker sand} + \text{pre-weighed sand} - \text{final beaker sand}}{\text{duration of test}}$$

The amount of pre-weighed sand was chosen to give a test duration of at least five minutes - at the very highest injection rates the amount of sand required made a longer calibration impracticable. A hard copy of the calibration output was retained from the chart recorder, but actual sensor readings were obtained from the counter, which was set at a 100s counting period. The chart record served only as a check on the counter output, and was useful in determining how steady the sand supply rate remained during the test.

It was found that the lowest transport rates (below approx 2g/s) could not be achieved using this arrangement as the sand tended to arch above the hole in the beaker if it was smaller than about 4mm, and a steady rate of supply could not be relied upon. Therefore a simple vibrating wire, driven by a small electric motor, was added to permit a smaller beaker and hole diameter to be used. This allowed calibrations to be carried down to 0.16 g/s, which was equivalent to the lowest sediment transport rate expected in the sewer pipe.

It was necessary to normalise the sensor output in some way to account for variations in the clear-water reading. These variations could be ascribed to two main causes:

1. Changes in the sensitivity of the sensor, due to temperature and power fluctuations.

2. Changes in the transmissivity of the water due to presence of fines and air.

Other possible factors included electrical interference from other equipment and physical movement of the heads, but these were not thought to be significant.

If one introduces a theoretical "pure water" reading - ie. the reading which is obtainable from water with no air or fines present - then the normalised reading will be equal to the change in signal due to the presence of sediment, divided by the full range of the instrument

$$\text{i.e. } \frac{\text{actual reading - clear water reading}}{\text{source off reading - pure water reading}}$$

If the sensitivity of the sensor changes, then all readings below "source off" should change proportionately, including the "pure water" reading. Therefore, if it were assumed that all fluctuations in clear water reading were due to changes in sensitivity only, then the quantity

$$\frac{\text{source off reading - clear water reading}}{\text{source off reading - pure water reading}}$$

should be constant, and it is appropriate to normalise the output as

$$\frac{\text{actual reading - clear water reading}}{\text{source off reading - clear water reading}}$$

If all fluctuations were due only to changes in the transmissivity of the water, then the "pure water" reading would be constant and the normalised readings would be proportional to

actual reading - clear water reading

Early calibrations tests yielded a very non-linear relationship between sensor output and concentration, with the sensor showing a tendency to "saturate" at concentrations well below those required. This non-linear response was unacceptable because, if short-term variations were meaned with respect to time, the calculated mean concentration would have been distorted from its true value. By reducing the strength of the source it was possible to achieve an approximately linear response over about 70% of the sensor range. (i.e from clear water up to a concentration giving 70% of the signal for "source off"). For concentrations beyond the linear range, increases in concentration produced progressively smaller changes in output signal. This was expected, because once the concentration exceeds a certain value, some of the sand particles will blanket others, reducing their net effect on the signal strength reaching the sensor. This did not, however, present a problem because it was possible to stay within the linear range at the higher transport rates by suitably increasing the velocity in the sediment return pipe.

Calibrations were obtained over a range of velocities which gave consistent results covering sediment transport rates from 0.16 up to around 50g/s. The calibrations were determined using both the normalizing techniques described above, and very little difference was found between them, both giving a response which could be regarded as approximately linear over 70% of full range, and both having a standard deviation of 8.4%. It was decided that there was more evidence that fluctuations were due to changes in the transmissivity of the water than to changes in the sensitivity of the measuring system, so the calibrations were those calculated using

actual reading - clear water reading

Figure 5 shows the calibration obtained at velocity = 1.39m/s in the sediment return pipe.

Once some initial problems were overcome, the infra-red sensor worked well and saved much drying and weighing of sand samples. By allowing the system to settle for around 30 minutes before using it for measurements, variations in clear-water reading were reduced to below 5%. Errors were further reduced by taking clear-water readings before and after each test.

5 EXPERIMENTAL PROCEDURE

5.1 Clear-water roughness

Before any experiments with sediment took place, a series of clear-water tests was carried out, in order to obtain an estimate of the value of k_s (Nikuradse equivalent sand roughness) for the 299mm diameter concrete pipe, and in order to develop a workable system for setting uniform flow conditions at part-full. Clear-water roughness was also measured immediately prior to each limit of deposition test with the same discharge and depth of flow.

The procedure adopted in all these tests was to set a particular discharge without sediment present, then adjust the flow depth to the required value, and take a measurement of hydraulic gradient using the digital point gauges. For pipe-full tests, the slope of the pipe was set at some convenient value such that the water levels at the gauging points were within the stilling wells, and as low as possible to minimise leakage around the lids. The pipe was surcharged by gradually adjusting the downstream sluice gate (or flow restrictors) until this state was reached. The slope was not changed from one test to the next unless necessary for this reason. A "still-water" reading was taken at each flume slope setting, this reading acting as a datum for calculation of hydraulic gradient. The reading was obtained by stoppering the sewer at the downstream end and filling it slowly until a still water level could be measured in each of the gauged stilling wells. These still-water readings were checked periodically to ensure that the gauges had not moved.

For part-full tests, the slope was adjusted to achieve conditions as close as possible to uniform flow. This was not always easy, particularly if normal depth was near to critical depth for the required velocity. Disturbances of the flow at entry and exit from the pipe caused the water surface to fluctuate periodically by 2-3mm at the gauge positions. Also, irregularities in pipe section at the joints and elsewhere created standing waves with amplitudes of up to 15mm for subcritical flows, and as much as 20mm when the flow was supercritical. The criteria for adjustment of flume slope and gate setting were therefore necessarily flexible.

Generally adjustments were made until at least three of the five gauges gave the required depth to within ±2mm. The five gauges were then read, and the average hydraulic gradient calculated using, in most cases, all five values. Prior to studying the limit of deposition for each test condition, two sets of depth readings were taken to determine the clear-water roughness.

5.2 Threshold of movement

Tests were carried out to obtain an approximate value for the velocity at which isolated sand particles would start to move in the sewer pipe. The procedure was to set a flow depth and velocity, then add a few sand particles by hand and see whether they continued to move having fallen to the bed. If the particles failed to move the velocity was marginally increased and the slope re-set in order to obtain approximately uniform flow conditions. This process was continued until movement was observed. The rig was not specifically designed for such measurements, and it was not practicable to position particles carefully on the invert, nor to carry out tests for pipe-full flow. Two readings were obtained, at approximately ¼ full and ½ full conditions.

5.3 Limit of deposition

Once the gradient and sediment sensor readings had been recorded for clear water conditions, sediment was gradually added to the system. The sediment used in all the tests described in this report was a narrow-graded sand with d_{50} = 0.72mm and a specific gravity of 2.62; the grading is shown in Figure 6. In order to prevent immediate formation of dunes, it was found that the best method was to add sand by hand into the jet as it fell into the hopper from the downstream end of the sewer pipe. This allowed the sand to mix with the water in the hopper before being extracted by the slurry pump, rather than travelling along the sediment pipe as one "slug". At first it was found that large quantities of sediment were escaping over the sill of the hopper, so the mesh screens were added, and the back of the tank was raised to accommodate the additional head difference across the mesh. Another difficulty was that some of the sand deposited on the sides of the hopper rather than falling to the bottom, this despite the steep (45°) sides and considerable turbulence within the hopper. This became most apparent with the part-full tests, when the discharge from the sewer pipe was reduced and there was less turbulence in the hopper. In order to minimise this deposition, water jets were added in the corners of the hopper to wash the sand off the sides and back into suspension where it could be collected by the pump.

Sand was added until the limit of deposition was observed. At low flow velocities (below around 1m/s), this was taken to be the point at which particles would bunch together and cease to move for a few seconds before being dispersed and carried away by the flow. This condition could be satisfactorily observed from above - in the case of pipe-full tests, very easily through the transparent windows in the top of the pipe. At higher velocities, it was found that as more sand was added there was a gradual transition from flume traction to flow over a continuous moving bed. In this case, although particles on the invert might be in continuous motion, they were not transported directly by the flow, but were moved by impacts with particles in the layer above. The limit of deposition was taken to be the condition when particles on the invert were still just being moved directly by the flow. A small increase in concentration would cause the particles on the invert to become closely packed and move only as a result of shear forces transmitted by the layer above. Eventually, when the concentration in the flow was high enough, the moving deposit would thicken until the shear force exerted on the particles on the invert became less than the frictional resistance and they ceased to move. In this instance it was not possible to judge the limit of deposition solely by observations from above, as the particles on the invert were obscured by a continuous moving bed. For this reason windows were installed along the invert of the pipe to allow observation from below.

It was necessary to decide which section of the pipe should be used for determining the limit of deposition, as local disburbances in the flow caused certain sections to deposit before others. A particular section around mid-length was chosen, which seemed to be "typical" in terms of how soon it would form a deposit relative to other parts of the pipe.

Judgement was primarily based on the conditions at this point, but the full length of the pipe was always checked to ensure that local dunes had not formed elsewhere.

Once it was decided that the flow was at the limit of deposition, a minimum of about 15 minutes was allowed for the system to reach equilibrium. A series of 5-10 consecutive readings were recorded from the concentration sensor, each reading representing the mean concentration for a 100s period. The hydraulic gradient was measured again, and for part-full tests the slope was adjusted, if necessary, to restore uniform flow conditions. Two sets of water level readings were taken for each test, as with the clear-water measurement. The fluctuations in water level already described tended to make it difficult to detect the small increases in roughness between clear water and the limit of deposition.

In most of the tests, limit of deposition conditions were maintained for ten to fifteen minutes whilst the concentration and head loss readings were being recorded. In these cases, the limiting sediment concentration was calculated as above from the mean of all readings. Sometimes however, it was not easy to identify the limit of deposition and achieve steady conditions. An inevitable consequence of reaching the limit of deposition is that more sediment accumulates in the pipe, so that the downstream portion is starved of sediment and the flow there will not be at the limit of deposition. The system of recirculating the sediment to the head of the pipe inevitably causes a certain degree of unsteadiness in the rate of sediment supply, and it is only the mean concentration over several minutes that remains constant. In some cases the limit of deposition would be observed, but then due to this starvation effect, the concentration would subsequently fall to a lower value. If this occurred, only the readings taken when the flow was actually observed to be at the limit of deposition were included in the calculation. Similarly, water level readings were only used with the corresponding concentration reading taken for the same period.

Once the necessary readings had been taken at the limit of deposition, the sluice gate was lowered to act as a weir and retain the sediment in the sewer pipe. The slurry pipe was then allowed to continue running until clear water flowed past the infra-red sensor. The clear-water sensor reading was recorded for comparison with the equivalent reading at the beginning of the test. The sand concentration at the limit of deposition was then calculated using the appropriate calibration curve (Section 4.2).

5.4 Deposited bed

At the start of each test, clear water was conveyed through the experimental rig and readings taken on the concentration sensor. The sediment was then introduced into the hopper at the downstream end of the sewer pipe and distributed uniformly around the system by tilting the flume steeply and using a high discharge. The distribution was considered to have reached equilibrium when the sediment sensor reading averaged over 1000 seconds was constant. The discharge and flume slope were then set, and the downstream flow restrictors adjusted until uniform flow was achieved in the sewer pipe. Two sediment sensor readings were taken over 1000 seconds and a further ten sets of readings taken over 100 seconds. Water depth and temperature measurements were recorded during the 1000 second interval. If dunes were present, then their speed along the pipe was determined and the time interval for the sensor reading extended to take into account the irregular movement of the sand bed.

Three different depths of sediment bed were tested with this technique: 0.044m, 0.010m and 0.0022m. Some deposited bed tests were later carried out as a continuation of the limit of deposition tests, and bed thicknesses thus varied from zero to 0.009m. The procedure for these tests was to reach the limit of deposition of the sediment (as described in Section 5.3), and then gradually inject additional sediment until a deposited bed had formed.

Once the relevant hydraulic measurements had been made, the flow was slowed to a non-transporting velocity and the deposited bed preserved by closing the downstream flow restrictors and reducing the discharge simultaneously. If the sediment bed was continuous, five measurements of the deposit width were taken along each pipe section. If the bed was not continuous and intermittent dunes were formed, twenty width measurements were made along each pipe section. The average depth of sediment was calculated from bed width and pipe geometry.

6 EXPERIMENTAL RESULTS

Details of the experiments carried out with the 299mm diameter concrete pipe are listed in Tables 1, 2 and 3. Table 1 shows the measurements taken for clear water analysis of the pipe roughness, Table 2 lists the limit of deposition data and Table 3 the deposited bed data.

6.1 Pipe friction

For pipe-full tests, the hydraulic gradient was taken to be the mean water surface slope with respect to the still-water reading. This was calculated directly from water levels in the stilling wells, using least squares regression. If one point gauge was clearly in disagreement with the others it was excluded from the regression.

The method used to determine the hydraulic gradient i for part-full tests was as follows. Mean flow velocity was calculated at each gauge position, based on the recorded flow depth and total discharge. Specific energy, E at each point could then be determined from:-

$$E = y + V^2/2g \qquad (21)$$

where y is the flow depth at the centreline. V is the mean velocity at the section, calculated as discharge divided by flow area at the section, and g is the gravity constant. The best-fit energy gradient, m (positive for E increasing in the downstream direction) was determined using least-squares regression on all the points.

All points were normally used so as not to bias the calculation of mean velocity and because it was found that omitting points gave less consistent roughness values. The hydraulic gradient i was then found from:-

$$i = S_o - m \qquad (22)$$

where S_o is the slope of the pipe invert.

In both pipe-full and part-full cases, the Darcy-Weisbach friction factor was calculated from:-

$$\lambda = 8gRi/V^2 \qquad (23)$$

where R is the hydraulic radius corresponding to the mean depth along the profile.

A "measured" value of k_s could then be determined from the Colebrook-White formula for commercial pipes

$$k_s = 14.8R\ (10^{-1/2\sqrt{\lambda}} - 2.51/R_e\sqrt{\lambda}) \qquad (24)$$

where R_e is the Reynolds number (=4VR/ν)

For comparison, values of Manning's n were also calculated from

$$n = R^{2/3}\ i^{1/2}/V \qquad (25)$$

A large number of measurements was made to determine the clear-water roughness value, k_s, of the concrete pipe to be used in the Colebrook-White resistance formula. It was expected that the value of k_s would remain approximately constant over the full range of flow conditions to be studied. These measurements covered flow velocities in the range 0.18 to 2.09m/s, at flow depths approximating to ¼ full, ½ full, ¾ full, pipe full, and just below pipe full (y/D = 0.95). The measurements at y/D = 0.95 were made in an attempt to assess any influence the lids might have had on the roughness. The hydraulic gradient was also measured immediately before each limit of deposition test, with the same flow velocity and depth as that to be studied. The previous HR tests (with the 77mm and 158mm pipes) had shown that this measurement was necessary if the increase in head loss due to sediment was to be observed accurately; it was not sufficient to rely on a predicted value of λ, or even on values measured at the same flow conditions but at a different time.

All clear-water results are included in Table 1, and calculated values of k_s are shown plotted against R_e in Figure 7. The results are reasonably consistent over a wide range of Reynolds numbers, although there are several outliers, occurring particularly at low velocities. The overall mean value of k_s from all measurements is $\bar{k}_s$ = 0.192mm with a standard deviation of $\sigma_s = 0.235$mm. This suggests that it is highly improbable that any roughness measurement greater than 0.663mm (being $k_s + 2\sigma_s$) is correct, and it is therefore justifiable to exclude such outlying values from the analysis.

The mean of all clear water measurements included in the analysis is $\bar{k}_s = 0.147$mm with $\sigma_s = 0.113$mm; the estimated standard error of the mean is $\sigma_n = 0.012$mm.

By treating the results for different values of y/D separately, the mean value of k_s can be observed to vary from 0.296mm at y/D = 0.75 to 0.093mm at y/D = 0.375, see Table 4. These variations in k_s, whilst in some cases determined from relatively few values, are statistically significant at 50% confidence levels.

The predicted values of Manning's n and the Darcy-Weisbach friction factor λ, calculated assuming $k_s = 0.147$mm for pipe full conditions, are compared in Figures 8 and 9 with the measured values. The scatter of the measured points about a mean can be appreciated from the standard deviations listed in Tables 5 and 6 for various flow depths. The overall mean roughness values of the pipe for clear-water conditions were n = 0.0099 with $\sigma_s = 0.00058$, and $\lambda = 0.0185$ with σ_s = 0.00202.

An additional analysis was carried out to determine how closely the measured n and λ data for pipe-full conditions fitted the predicted curve for $k_s = 0.147$mm. The mean value of the ratio n-observed/n-predicted was 0.99 with $\sigma_s = 0.042$, i.e all the observed pipe-full data lay between 91% and 107% of the predicted curve in Figure 8. Similarly the mean value of the ratio λ-observed/λ-predicted was 1.00 with $\sigma_s = 0.085$, so that measured friction factors for pipe-full conditions lay between 83% and 117% of the predicted curve in Figure 9.

Some of the variation in the value of k_s with flow depth may be because the hydraulic radius R used in the Colebrook-White equation does not fully describe the characteristics of part-full flow. This parameter is sufficient only if the velocity and shear stress distributions are uniform around the wetted perimeter of the channel. This is not the case for a circular pipe flowing part-full, so an additional "shape factor" is needed when estimating its resistance from a formula for pipe-full flow.

Several studies have been carried out in the past to determine suitable shape factors for open-channel flows. Engelund (1964) proposed the use of a "resistance radius" in place of hydraulic radius, and developed a theory based on certain assumptions about the distributions of velocity and shear stress. The method involves rather lengthy calculations, and Engelund made a number of simplifying assumptions applicable to wide channels in the fully rough region. These assumptions would not hold for the part-circular section considered here. Kazemipour & Apelt (1979) carried out numerous experimental studies on channels of various cross-sections, and also used data from other researchers to derive an essentially empirical correction, which would allow the friction factor for open channels to be determined from standard pipe resistance formulae. A further study by Kazemipour & Apelt (1980) concentrated on semi-circular channels. Following on from this, Nalluri & Adepoju (1985) used this data, along with data from May (1982) and further measurements of their own, to develop a formula which was applicable to flow depths greater than 0.5D. The drawback to both these studies on pipe channels is that they were empirically derived from smooth pipe data. The Kazemipour formula shifts values of λ to fit the Karman-Prandtl equation

$$1/\sqrt{\lambda} = 2\log_{10} Re\sqrt{\lambda} - 0.8 \qquad (26)$$

and Nalluri & Adepoju compared their data with the Blasius equation

$$\lambda = 0.316/ R_e^{0.25} \qquad (27)$$

Nalluri & Adepoju suggested an equation of the same form as the Blasius equation, but incorporating a shape factor y/P, and using a modified Reynolds number, $R_{ey} = Vy/\nu$. Although Nalluri & Adepoju's formula is intended for direct use only in smooth pipes, a correction factor can be calculated by comparing their formula with the Blasius equation.

Hare (1988) compared the resistance data obtained in the present study with the values predicted by the methods due to Kazemipour & Apelt and Nalluri & Adepoju. He found that neither method fitted very well the present results for flow in the transition region, but that variations were generally smaller than for smooth pipes.

Comparing the k_s values for each flow depth, shown in Table 4, it can be seen that the effective roughness increases with proportional depth up to a maximum at y/D = 0.75 and then reduces towards pipe full. In terms of n and λ, the maximum roughness occurs at y/D = 0.95. The overall mean value of k_s = 0.147mm is consistent with the design value of k_s = 0.15mm recommended by HR (1983) for spun-concrete pipes in normal condition.

6.2 Threshold of movement

Two tests were carried out to measure the threshold velocity of the sand particles but were intended as only an approximate indication for the particular conditions tested. The results are shown in Table 7 together with threshold velocities predicted by Equations (1), (2) and (3) due to Novak & Nalluri (see Section 3.2).

It can be seen that the observed velocities were higher than those given by Equation (1) but lower than those given by (2) and (3). This is not unexpected because the first equation was developed for smooth channels and the other two equations for rougher surfaces than occur in concrete pipes. These exploratory results, therefore, suggest the need for further work to determine threshold velocities in commercial pipes with intermediate types of surface texture.

6.3 Limit of deposition

Measurements of the sediment concentration and hydraulic gradient at the limit of deposition were obtained for both part-full and pipe-full conditions, and are presented in Table 2. In some cases it was decided at the time of the observations that conditions were either slightly beyond or slightly below the limit of deposition, as defined in section 5.3, and these results are labelled >LD or <LD as appropriate. As previously mentioned, once the limit of deposition had been reached, two readings of hydraulic gradient were taken in order to determine the head-loss gradient. In the first test carried out, a number of readings were also taken at concentrations below the limit of deposition, in the hope that the variation of head-loss with increasing concentration could be observed. The results showed that this was not feasible because the variations were small relative to the overall scatter, so in

subsequent tests readings of the hydraulic gradient were taken only at the limit of deposition.

Figure 10 shows the change in head loss caused by the sediment when the flow is at the limit of deposition. The proportionate change in the friction factor λ relative to the equivalent clear water value λ_o is plotted against the limiting flow velocity V_L; the ratio $(\lambda - \lambda_o)/\lambda_o$ is also equal to the proportionate change in head loss. It is hard to detect any definite trend in the data, except that the change in resistance is usually greater for part-full flow than for pipe-full flow. Negative values of the head-loss ratio are considered to be unlikely, and are probably due to errors in the water level measurements caused by fluctuations and standing waves in the pipe. The average proportionate increase in head loss for all the data is only 0.73%; this is equivalent to a change in the mean value of k_s from 0.147mm for clear water to 0.155mm at the limit of deposition.

During each test a mean sediment concentration C_v (ppm) was determined from the infra-red sensor over an appropriate length of time. A corresponding mean flow depth, nominally y/D = 1, 0.75, 0.5, 0.38 was calculated accurately from the five depth gauges, and from this a mean value of the limiting velocity V_L (m/s) determined. Figure 11 shows the resultant relationship between C_v and V_L for the 299mm concrete pipe for both full and part-full conditions. In Figures 12 to 15, the experimental data for each flow depth are shown separately, and are compared with several alternative equations for predicting the limit of deposition.

Figure 12 shows all the measured pipe full data compared with three versions of May's equation.

Version number 1 is the equation described in Section 3.3 which was derived from earlier HR tests on 77mm and 158mm diameter smooth pipes, and has the form

$$C_v = \frac{2.05}{100} (D^2/A) \ (d/R)^{0.6} \ [V_L^2/g(s-1)D]^{1.5} \ (1-V_{ts}/V_L)^4 \tag{28}$$

where V_{ts} = threshold velocity given by Novak & Nalluri's Equation (1). This equation overpredicts the limiting sediment concentrations in the 299mm pipe in all cases. Agreement is reasonably good over the central range of velocities between 0.6m/s and 1.0m/s, but at the extremes the equation overpredicts by a factor of 2. For the three part-full conditions tested a similar trend is apparent (Figures 13 to 15); predicted values are in all circumstances higher than measured, particularly at the two shallowest depths. At half-full flow, the experimental results are less consistent with measured concentrations scattered over a much wider range for a given velocity than for the pipe-full results. Some of these variations occurred near the critical flow velocity of V_c = 1.07m/s when the existence of standing waves along the pipe made it difficult to judge the limit of deposition precisely.

Version number 2 in Figures 12 to 15 is a modified form of Equation (8) which was intended to be suitable for both rough and smooth pipes. The major change is the calculation of the threshold velocity from Novak & Nalluri's Equation (3) in place of Equation (1). Equation (3) applies to small groups of particles instead of isolated ones, and has the advantage of being valid for both rough and smooth pipes. The earlier HR data for the 77mm and 158mm diameter pipes (but not the new 299mm data) were therefore re-analysed using Equation (3). The resulting best-fit equation was

$$C_v = \frac{1.03}{100}(D^2/A)\ (d/R)^{0.253}\ [V^2/g\ (s-1)D]^{3/2}\ (1 - \frac{V_t}{V_L})^4 \quad (29)$$

which is similar to Equation (8) except for the numerical constant and the power of the parameter (d/R). It can be seen in Figures 12 to 15 that Equation (28) gives steeper curves of C_v versus V_L than does the original Equation (8). For pipe-full flow, version 2 underpredicts at velocities below about 0.7m/s but overpredicts increasingly at velocities above this value. For part-full conditions, Equation (28) overpredicts in nearly all cases, and at high values the discrepancies become substantial.

Version number 3 is based on the original Equation (8) but uses the observed threshold velocity of V_t = 0.256m/s which was measured in the 299mm diameter concrete pipe when flowing approximately half-full (see Section 6.2). Version 3 is plotted in Figure 14, and shows a better fit to the experimental data than versions 1 and 2, although it still overpredicts at the higher velocities. This result confirms the view that threshold velocities in commercial pipes are somewhat higher than the values given by Equation (1) (which was based on tests with only smooth pipes and channels).

The experimental data for the 299mm diameter concrete pipe are compared in Figures 16-19 with several other formulae for the limit of deposition; those selected from Section 3.3 are:

(1) Laursen (1956), Equation (6)
(2) Robinson & Graf (1972), Equation (7)
(3) Macke (1982), Equation (10)
(4) Mayerle (1988), Equation (11)
(5) Mayerle & Nalluri (1989), Equation (13)

The values of λ used in the last three equations were average values measured in the 299mm diameter concrete pipe at each flow depth. The fall velocity w of the sand particles and the kinematic viscosity ν of the water were calculated from the equations given in Appendix A.

The following conclusions can be drawn from the comparisons.

(1) Laursen This equation overpredicts the limiting sediment concentrations by factors between about 2.5 and 4.0; the discrepancies become larger as the flow depth decreases. The slope of the equation is approximately parallel to the data at the highest velocities, ie. $C_V \alpha V_L^3$.

(2) Robinson & Graf

The equation is valid only for pipe-full flow, and Figure 16 shows that its line passes through the experimental data at a flow velocity of 1.0m/s. However, the gradient of the line is much too steep, causing it to overpredict the limiting concentrations substantially at higher velocities.

(3) Macke This equation gives very similar results to version number 1 of May's formula (ie the original Equation (8)). Macke's equation therefore overpredicts the limiting sediment concentrations in nearly all cases; agreement is better for the pipe flowing full and 3/4-full and becomes worse as the proportional depth of flow decreases.

(4) Mayerle and (5) Mayerle & Nalluri Although these two equations were derived from basically the same set of data, they give suprisingly different

predictions when applied to the 299mm pipe. Mayerle's equation overpredicts in most cases, and shows bigger discrepancies than Macke's equation for pipe-full flow. However, in the case of half-full flow, Mayerle's formula fits the data quite well for velocities below 0.9m/s. By contrast, Mayerle & Nalluri's equation generally underpredicts by a factor of about 2-3 but gives a better fit to the 3/8-full data than the other equations.

In Figures 20 to 22 the complete sets of HR data for the limit of deposition in 77mm, 158mm and 299mm diameter pipes are combined and compared with the formulae due to May (Equation (8), ie version number 1 in Figures 12-15), Macke (Equation (9), equivalent to (10)), and Mayerle & Nalluri (Equation (13)). The measured value of the friction factor λ in each test was used when calculating the plotting positions for Equations (9) and (13). Each of the three Figures has been arranged so that the value on the vertical axis is linearly proportional to the sediment concentration; this enables direct comparisons to be made between the predictions of the three equations. The overall performance of each equation is presented statistically in Table 8.

Not suprisingly, May's Equation (8) in Figure 20 provides a reasonable fit to the results for the 77mm and 158mm pipes since this was the data set from which the equation was derived. In the case of the 299mm pipe, as already seen, the equation significantly overpredicts the limiting sediment concentration when the pipe is flowing at half-depth or less.

Macke's Equation (9) in Figure 21 gives a satisfactory fit to the data for sand in the 77mm and 158mm diameter pipes. According to Macke, the equation is not valid for values of shear stress $\tau_o < 1.07$ N/m², but the plot indicates reasonable agreement for these two pipe sizes down to a value of $\tau_o = 0.5$ N/m². It can readily be seen that the equation is unsuitable for much coarser particles since it underestimates the limiting concentrations of the gravels by a factor of about 40. In the case of the 299mm diameter pipe, Macke's equation overpredicts the concentrations, particularly at the lower values of shear stress; its performance is similar to that of May's equation.

Mayerle & Nalluri's Equation (13) in Figure 22 underestimates the sediment concentrations in nearly all the tests with sand but overestimates for the two gravels. Agreement is better at the higher velocities, but the differences are quite substantial, with the predicted concentrations varying from the measured values by factors of about 2 to 5. The method of plotting in Figure 22 does, however, correlate the data for the three sizes of pipe reasonably well.

6.4 Unsteady flow conditions

After studying conditions at the limit of deposition for steady flows, two additional tests were carried out to determine the effect of time-varying flows.

In the first test, the pipe was arranged to flow full at a steady mean velocity of 1.26m/s, and sediment was then added to the recirculation system until conditions were just at the limit of deposition. Next, the tilting weir was lowered to divert some of the discharge into the bypass channel (see Figure 1), so that the 299mm diameter pipe was now flowing half-full with a mean velocity of 1.0m/s. This reduced the sediment transporting-capacity of the flow in the 299mm pipe and resulted in a deposited bed with dune features. The unsteady-flow test was then started by gradually raising the side weir so that the discharge and depth of flow in the pipe returned to the original pipe-full conditions. This procedure was carried out over a period of 22 minutes so as to simulate a typical storm flow event in a sewer. It was observed that the bed deposits became smaller as the discharge increased, and when pipe-full conditions were reached the sediment was found to be moving again in flume traction at the limit of deposition.

The second test was carried out in a generally similar way, but with a flow velocity of 0.8m/s when the pipe was flowing full at the limit of deposition and 0.6m/s when flowing half-full. At the half-full condition, the sediment formed a single large dune which moved very slowly along the pipe. As the flow rate was increased, the dune became shorter; after 65 minutes, when the pipe was again flowing full, the dune had disappeared and the sediment was moving at the limit of deposition.

These tests showed that the limit of deposition occurred at the same flow conditions whether it was approached from below (flume traction) or from above (deposited bed); there was therefore no hysteresis effect. Also, varying the flow rate fairly slowly with time did not alter the conditions for deposition. Inertial effects might affect the limit if the flow velocity were to vary very rapidly, but this is unlikely to occur under typical storm conditions in sewers.

6.5 Deposited bed

Measurements of the rate of sediment transport and the hydraulic gradient for flow conditions beyond the limit of deposition in the 299mm concrete pipe are presented in Table 3. In most tests the sediment formed isolated dunes separated by sections of clear pipe. After each test, the bulk volume of sediment in the pipe was determined. The corresponding value of sediment depth, y_s, given in Table 3 is the mean depth which would have resulted if the deposited material had been distributed uniformly along the measured section of pipe. When the amount of sediment contained in the recirculation system was kept constant, it was found that the value of y_s was not greatly affected by changes in water discharge and flow depth. This enabled the relationship between flow velocity and sediment transport rate to be studied for a series of approximately constant depths of bed deposit. The tests were carried out with the pipe flowing either full or half-full. Each velocity given in Table 3 and the related Figures takes account of the deposited bed and is obtained by dividing the discharge by the net cross-sectional area of the flow.

Figures 23 and 24 show how the sediment transport rate (expressed in terms of the volumetric sediment concentration) varied with flow velocity and the depth of the deposited bed when the pipe was flowing full and half-full. Both plots also contain the corresponding measurements for the limit of deposition (see 6.3), together with best-fit curves through these points (see 7.1). Just beyond the limit of deposition, the pipe contained only one or two small isolated dunes. Therefore, when the volume of the dunes was averaged along the length of the pipe, the resulting mean sediment depth, y_s, was often small and of the same order as the particle size.

Only relatively few measurements were taken with the pipe flowing full, and the data in Figure 23 show some scatter. However, it can be seen that generally as y_s/D increases, C_v increases from its value at the limit of deposition. Also shown in the plot are lines corresponding to two equations which apply to pipe-full flow with a deposited bed : Equation (19) developed from Laursen's results and Graf & Acaroglu's Equation (20), see Section 3.4. The two equations are in reasonable agreement, but overestimate the rate of sediment transport. Laursen's formula overpredicts the values of C_v at the limit of deposition by factors of between 3 and 10, but underestimates the increases in C_v produced by increases in the depth of deposit. The form of Graf & Acaroglu's equation suggests that it is probably not suitable for depths of sediment deposit as small as those studied here. The only parameter in Equation (20) which relates to the depth of sediment is the hydraulic radius R of the free flow area. At small values of y_s/D, the value of R does not alter significantly so the equation predicts little change in C_v until the relative depth of deposit becomes large.

A larger number of tests was carried out with the pipe flowing half-full, and the results in Figure 23 show more clearly the effect of deposit depth on the rate of sediment transport. Just beyond the limit of deposition ($y_s/D \leq 0.001$), it appears that the values of C_v remain close to those at the limit of deposition; some points correspond to a slight reduction in C_v but the changes are not larger than the overall scatter in the data. When the sediment depth reaches $y_s/D = 0.006$, a clear trend becomes established of increasing C_v with increasing y_s/D. Anomalies in the data are apparent at flow velocities around 1m/s, and these may be due to the effect of standing waves which formed when the Froude number of the flow was close to unity. Ignoring these anomalies, curves drawn through the data for y_s/D = 0.006, 0.03 and 0.13 show a similar pattern. At lower velocities, the curves are approximately parallel to but displaced from the mean line through the limit-of-deposition data; at higher velocities, the curves become flatter and tend towards the limit-of-deposition line. This is to be expected because as the flow velocity is increased, sediment movement will occur through a greater depth of deposited bed; when the particles at the invert start to move, conditions correspond to those at the limit of deposition.

The experimental results for deposited beds are compared in Figure 25 with the sediment concentrations predicted by the Ackers-White transport equation (see 3.4). Values of C_v were calculated using the measured hydraulic gradient and an effective bed width W_e corresponding to the mean sediment depth y_s. Figure 25 shows that the Ackers-White equation consistently overestimates the rate of transport, and it can be seen that agreement is poorer for the pipe-full data than for the half-full data; the mean ratios between predicted and observed concentrations are 3.13 and 1.93 respectively. This margin of error is fairly common in studies of sediment transport in alluvial channels for which the Ackers-White equation was originally developed. It should also be remembered that in the present tests, the sediment bed was not usually continuous along the pipe; the bed width corresponding to the mean sediment depth may not therefore be the most appropriate when calculating transport rates.

The effects of bed deposits on the hydraulic resistance of the 299mm diameter concrete pipe are shown in Figures 26 and 27. In Figure 26, changes in resistance are expressed in terms of the proportionate increase in the friction factor λ relative to the corresponding mean clear-water value λ_o (see Table 6); the quantity $(\lambda - \lambda_o)/\lambda_o$ is also equal to the proportionate increase in the hydraulic gradient, $(i - i_o)/i_o$. In Figure 27, the changes in resistance are shown in terms of the composite k_{ss} value of the pipe; as described in Section 6.1, the mean clear-water roughness was found to be $k_s = 0.15$mm. It can be seen from these plots that deposition has no significant effect on flow resistance until the mean sediment depth exceeds a value of about $y_s/D = 0.074$. When the bed depth reaches $y_s/D = 0.034$, the mean k_s value is about 0.54mm compared with the clear-water value of 0.15mm. As an example, this change in k_s would reduce the flow capacity of a 300mm pipe laid at a slope of 1/500 by about 11%; alternatively, to maintain the same capacity, the slope of the pipe would need to be increased to about 1/400.

7 DISCUSSION

7.1 Limit of deposition

Analysis of the experimental data drew attention to the effect which the proportional depth of flow in a pipe has on conditions at the limit of sediment deposition. The equation developed by May (1982) from the earlier HR study on 158mm and 77mm pipe was

$$C_v = 2.05\times10^{-2}\ (A/D^2)^{-1}\ (d/R)^{0.6}\ [1 - (V_{ts}/V_L)]^4 \cdot \left[\frac{V_L^2}{g\ (s-1)\ D}\right]^{3/2} \qquad (8)$$

For a given flow velocity, this formula predicts that the limiting sediment concentration in a pipe flowing half-full should be twice that in a pipe flowing full. Equation (10) due to Macke (1982) also predicts a similar change. By contrast, Equations (11) and (13) developed respectively by Mayerle (1988) and Mayerle & Nalluri (1989) relate C_v to R (instead of A), and therefore predict that, for the same velocity, the limiting concentrations should be equal in pipes flowing full and half-full. The results for the 299mm pipe showed that the effect of part-full flow on the limit of deposition was in fact intermediate between these two predictions.

This prompted first a re-analysis of the earlier HR data for the 158mm and 77mm pipes. Referring to Equation (8), it can be seen that the quantity

$$X = C_v\ (A/D^2)\ [1 - (V_t/V_L)]^{-4}\ [\frac{V_L^2}{g\ (s-1)\ D}]^{-3/2} \qquad (30)$$

should depend on the relative sediment size (d/R). Figure 28 shows the data plotted in the form of X versus (d/R), together with the best-fit line corresponding to Equation (8); the values are also listed in Table 9. Each point in Figure 28 is the mean value of X for a given test condition (ie pipe size, sediment size and proportional depth). In most cases there was a significant amount of scatter about each mean point, but this method of presentation makes it easier to identify the main trends in the data. Taking the proportional depth of flow (y/D) into account, it was found that the data for the 158mm diameter pipe flowing part full were well correlated by the quantity

$$Y = X\ (y/D)^{-0.36} \qquad (31)$$

Values of Y are listed in Table 9 and plotted against (d/R) in Figure 29. The scatter in the data for the 158mm pipe is considerably reduced compared with that in Figure 28, and the resulting best-fit equation for the 77mm and 158mm pipes becomes

$$C_v = 2.11\text{x}10^{-2}\ (y/D)^{0.36}\ (A/D^2)^{-1}\ (d/R)^{0.6}\ [1 - (V_t/V_L)]^{4}\ [\frac{V_L^2}{g\ (s-1)\ D}]^{3/2} \qquad (32)$$

The value of the numerical constant was determined so as to minimise the proportionate errors in the predicted values of C_v. Equation (32) represents only a minor revision of the original Equation (8), but provides a better description of the effects of part-full flow on the limit of deposition.

As demonstrated in Section 6.3, Equation (8) significantly overpredicts the limiting sediment concentrations in the 299mm diameter pipe. Two possible reasons for this can be envisaged. Firstly, the general form of the equation may be incorrect so that it does not take proper account of the effect of pipe size. Secondly, the discrepancies could be due to the rougher surface texture of the 299mm concrete pipe relative to that of the smooth 77mm and 158mm pipes tested previously. The first reason is considered less likely because Equation (8) was found to correlate data satisfactorily for a two-fold variation in pipe size (from 77mm to 158mm); there is no obvious reason why a further two-fold increase (from 158mm to 299mm) should not follow a similar pattern.

According to the theoretical model which led to Equation (8), see May (1982), an increase in the surface roughness of a pipe can be expected to affect the transport of sediment along the invert in two ways. Firstly, it increases the hydraulic resistance, and causes the local velocity around the particles to decrease relative to the mean velocity of the flow; this reduces the driving force exerted on the particles by the flow. Secondly, the coefficient of friction between the particles and the pipe increases so that a larger driving force is needed to keep them in motion. Referring to Equation (8), the first factor can be expected to reduce the value of the numerical constant and the second factor can be expected to increase the effective threshold velocity. Both factors serve to reduce the amount of sediment that can be transported by a rough pipe relative to an equivalent smooth one. By contrast, Macke's Equation (10) and Mayerle's Equation (11) indicate that an increase in the pipe friction factor λ should increase the limiting sediment concentration; this prediction is not supported by the results of the present study.

As explained in Section 6.2, no suitable equation is yet available for determining the threshold velocity of an isolated sediment particle in a commercial pipe with a non-smooth finish (eg concrete). Estimates of the effective threshold velocity V_t in the present tests with the 299mm pipe can be obtained by analysing the results according to the framework provided by Equation (32). For a given proportional depth of flow, the equation suggests that

$$C_v = \text{constant} \cdot \frac{(V_L - V_t)^4}{V_L} \qquad (33)$$

Regression analysis of the data in Table 2 (excluding one anomalous test at y/D = 0.5) thus enabled best-fit values of V_t to be determined, as shown in Table 7. The results for the pipe flowing part-full are suprisingly consistent given the variability of the data, but are higher than the value for pipe-full flow; the actual threshold velocities measured in the pipe were intermediate between these two limits.

Weighting the results of the regression analysis according to the number of tests gave an overall mean threshold velocity of V_t = 0.30m/s. This figure was then used in Equations (30) and (31) to calculate mean values of the quantity Y; these are listed in Table 9 and plotted against (d/R) in Figure 29, together with the corresponding data for the 158mm and 77mm pipes. It can be seen that the 299mm results now fall quite close to the best-fit line given by Equation (32).

All the HR data are shown plotted against Equation (32) in Figure 30, and statistical information on the degree of fit is summarised in Table 8.

Overall, the results indicate that Equation (32) provides a reasonable estimate of conditions at the limit of deposition, provided the effective threshold velocity can be determined correctly. For smooth pipes, V_{ts} should be calculated from Equation (1). For concrete pipes, the present study indicates that V_t is approximately equal to $4V_{ts}/3$, but it is not known over what range of conditions this relationship holds.

Equation (32) has been briefly compared with Macke's data for sand sizes of 0.16mm and 0.37mm, and was found to underestimate the measured sediment transport rates significantly. This is believed to be because the sands were fine enough to be transported in suspension at the flow velocities used in the experiments. By contrast, Equation (32) relates specifically to bed-load transport, and it is therefore recommended that it should not be applied for sand particles finer than about 0.4mm to 0.5mm (see also the discussion of the conditions for suspended-load transport in Section 3.3). Equation (32) and Macke's Equation (10) appear to behave fairly similarly for medium sands in smooth pipes, but for coarser particles Macke's equation significantly underestimates the rate of transport. Equation (32) also gives a better fit to the new data for the 299mm concrete pipe, but further tests are needed to determine the effective threshold velocity of sediment in such pipes.

7.2 Deposited bed

The results in Figures 23 and 24 show that the transition from flume traction to movement with a deposited bed does not significantly decrease the sediment-transporting capacity of the flow. Beyond the limit of deposition, the transport rate increases as the mean sediment depth y_s increases; as explained in 6.4, y_s is the uniform depth of deposit which would result if the sediment in the pipe were distributed uniformly with distance. This finding is important because it means that the start of deposition in a pipe flowing part-full need not produce an unstable situation in which deposition continues until the pipe surcharges (assuming constant water and sediment discharges). However, it is necessary to take account of the change in hydraulic resistance caused by deposition when considering results such as those for half-full flow in Figure 24. An increase in resistance will make the water flow deeper and reduce its velocity; this will tend to offset some or all of the gain in sediment-transporting capacity due to the increased width of deposited bed. However, Figure 25 shows that for the 299mm pipe there was no significant increase in hydraulic resistance until the mean sediment depth reached about $y_s = 0.03$ D.

The results of the present study therefore suggest that the "no-deposit" criterion for self-cleansing sewers could be usefully relaxed without adverse effects. For a deposited sediment depth of $y_s/D = 1\%$, Figure 24 indicates that the limiting sediment concentration would be about 7 times the value at the limit of deposition when the flow velocity is 0.6m/s and about 2 times when the velocity is 1.2m/s. The effect on minimum velocities and gradients for sewers can be illustrated by an example of a 300mm concrete pipe required to cater for a volumetric sediment concentration of 25ppm when flowing half-full. Assuming, conservatively, a two-fold increase in sediment-transporting capacity relative to that at the limit of deposition, the required minimum velocity would be reduced from about 0.85m/s to 0.75m/s; this would allow the minimum gradient of the pipe to be decreased by about 20%, which would be worthwhile economically.

Based on the present findings, it is suggested that a mean deposited depth of $y_s/D = 1\%$ could provide a suitable criterion for the design of self-cleansing sewers. This depth would not increase the hydraulic resistance of a pipe significantly but would increase the sediment-transporting capacity of the flow by a factor of at least two relative to the "no-deposit" criterion. A conservative method of estimating the minimum flow velocity V_m consistent with a sediment depth of $y_s/D = 1\%$ could therefore be obtained by applying a factor of about two to Equation (32) to give

$$C_v = 4.0 \times 10^{-2} \, (A/D^2)^{-1} \, (y/D)^{0.36} \, (d/R)^{0.6} \left[1 - (V_t/V_m)\right]^4 \left[\frac{V_m^2}{g\,(s-1)\,D}\right]^{3/2} \qquad (34)$$

This suggestion is obviously based on a limited number of tests and should be reviewed as more experimental data become available. Future studies on sediment transport in pipes with deposited beds may also provide alternative formulae for predicting the relationship between minimum flow velocity, sediment concentration and depth of sediment deposit.

8 CONCLUSIONS

(1) Previous HR test data on the limit of sediment deposition in 158mm and 77mm diameter smooth pipes were re-analysed to determine more precisely the effect of proportional flow depths. The resulting best-fit equation for predicting the flow velocity required at the limit of deposition is given by Equation (32).

(2) New tests have been carried out to study the limit of deposition in a 299mm diameter concrete pipe using 0.72mm sand, flow velocities between 0.5m/s and 1.5m/s, volumetric sediment concentrations between 0.3 ppm and 440 ppm, and proportional depths of flow between 3/8-full and pipe-full.

(3) Analysis of the new data showed that, for a given velocity and depth of flow, the limiting sediment concentration in the concrete pipe was typically half that expected in a smooth pipe of the same diameter.

(4) The lower transporting capacity of the concrete pipe is considered to be due to greater frictional resistance between the sediment particles and the pipe invert and to changes in the velocity profile in the pipe. These factors cause an increase in the threshold velocity needed to start and maintain individual sediment particles in motion along the pipe.

(5) The data analysis indicated that the effective threshold velocity in the concrete pipe was approximately 33% greater than in a smooth pipe of similar diameter. Using this adjusted threshold velocity, it was found that the results for the 299mm pipe fitted Equation (32) satisfactorily. This suggests that the equation is suitable for both rough and smooth pipes provided the threshold velocity of the sediment is assessed correctly. Equation (32) assumes that the sediment is transported as bed-load, and it should not therefore be applied for sand sizes finer than about 0.4mm to 0.5mm.

(6) Limited tests were made to study the effect of unsteady flows on the limit of deposition. The

transition between flume traction and deposition was not altered by gradually varying flows, and the limit remained the same when approached from above or below.

(7) Tests were also carried out in the 299mm concrete pipe to measure hydraulic resistance and rates of sediment transport for various small depths of bed deposit. Slightly beyond the limit of deposition, the sediment formed a series of isolated dunes which travelled slowly along the pipe. The volume of deposited sediment was measured for each test condition and converted to an equivalent mean depth, y_s, distributed uniformly along the pipe.

(8) The results showed that the sediment transporting capacity of the flow was not reduced significantly by the onset of deposition; beyond this limit, the transporting capacity increased as the mean sediment depth increased. With the pipe flowing half-full and a deposit depth of $y_s/D = 1\%$, the sediment concentration at a flow velocity of 1.2m/s was about two times that at the limit of deposition; at a flow velocity of 0.6m/s, the ratio increased to about seven times. The effect of the sediment deposits on hydraulic resistance did not become significant until y_s/D reached about 3%; at this point, the average k_s value of the pipe was 0.55mm compared with a mean clear-water value of 0.15m.

(9) Based on these findings, it is suggested that a deposit depth of $y_s/D = 1\%$ could provide a satisfactory criterion for the design of "self-cleansing" sewers. It would allow a worthwhile reduction in minimum velocities and gradients, particularly for larger pipes,

compared with the previous "no-deposit" criterion, and would not result in any significant reduction in hydraulic capacity. Equation (34) provides a possible method of determining minimum velocities for a deposit depth of $y_s/D = 1\%$, and should give conservative results.

(10) These suggestions should be reviewed as more experimental data become available on sediment transport in pipes with deposited beds.

9 ACKNOWLEDGEMENTS

The experimental measurements were carried out by Mr G R Hare and Mr K D Jones. The data were analysed by Mrs P M Brown and Mr R Payne. The project was supervised by Mr R W P May, and carried out in the River Engineering Department headed by Dr W R White.

10 REFERENCES

ACKERS P (1978). Urban drainage : the effects of sediment on performance and design criteria. Proc 1st Intern Conf on Urban Storm Drainage, Southampton, England, April, pp535-545.

ACKERS P (1984). Sediment transport in sewers and the design implications. Intern Conf on Planning, Construction, Maintenance and Operation of Sewerage Systems, BHRA/WRC, Reading, England, September, pp215-230.

CIRIA (1987). Sediment movement in combined sewerage and storm-water drainage systems. Construction Industry Research and Information Association, Project Report 1.

CRABTREE R W (1988). A classification of combined sewer sediment types and characteristics. WRc Engineering, Ref 8808041.

ENGELUND F (1964). Flow resistance and hydraulic radius. Acta Polytechnica Scandinavica. Civil Engng and Bldg Constr, Series No 24.

ENGELUND F & HANSEN E (1972). A monograph on sediment transport. Teknisk Forlag, Copenhagen, Denmark.

FREDSOE J (1982). Shape and dimensions of stationary dunes in rivers. Jnl of Hydr Div, Amer Soc Civ Engrs, Vol 108, No 8.

GRAF W H & ACAROGLU E R (1968). Sediment transport in conveyance systems; Part 1. Bull Intern Assoc Sci Hydr, XIII annee, No 2, June, pp20-39.

HARE G R (1988). Sediment movement in sewers : interim report. Hydraulics Research, Wallingford, Report SR 179.

HYDRAULICS RESEARCH (1983). Tables for the hydraulic design of pipes and sewers, 4th edn. Telford International Ltd, London.

KAZEMIPOUR A K & APELT C J (1979). Shape effects on resistance to uniform flow in open channels. Jnl Hydr Res, Vol 17, No 2, pp129-147.

KAZEMIPOUR A K & APELT C J (1980). Shape effects on resistance to flow in smooth semi-circular channels. University of Queensland, Research Report No CE 18, November.

LAURSEN E M (1956). The hydraulics of a storm-drain system for sediment-transporting flow. Bull No 5, Iowa Highway Res Board.

MACKE E (1982). About sedimentation at low concentrations in partly filled pipes. Mitteilungen, Leichtweiss - Institut für Wasserbau der Technischen Universität Braunschweig, Heft 76/1982, pp1-151 (in German).

MAY R W P (1975). Deposition of grit in pipes : Literature survey. Hydraulics Research Station, Report INT 139.

MAY R W P (1982). Sediment transport in sewers. Hydraulics Research Station, Report IT 222.

MAYERLE R (1988). Sediment transport in rigid boundary channels. PhD thesis, Dept Civ Engng, University of Newcastle upon Tyne, England.

MAYERLE R & NALLURI C (1989). Sediment transport with no deposition in rigid boundary channels. Proc XXIIIrd IAHR Congress, Ottawa, Canada, August, ppB561-566.

NALLURI C & ADEPOJU B A (1985). Shape effects on resistance to flow in smooth channels of circular cross-section. Jnl Hydr Res, Vol 23, No 1, pp37-46.

NEWITT D M et al (1955). Hydraulic conveying of solids in horizontal pipes. Trans Inst Chem Engrs, Vol 33/2.

NOVAK P & NALLURI C (1975). Sediment transport in smooth fixed bed channels. Jnl of Hydr Div, Amer Soc Civ Engrs, Vol 101, HY9, September, pp1139-1154.

NOVAK P & NALLURI C (1984). Incipient motion of sediment particles over fixed beds. Jnl Hydr Res, Vol 22, No 3, pp181-197.

PERRUSQUIA G, LYNGFELT S & SJÖBERG A (1987). Flow capacity of sewers with a sediment bed. Proc 4th IAHR Intern Conf on Urban Storm Drainage, Lausanne, Switzerland.

PERRUSQUIA G (1988). Part-full flow in pipes with a sediment bed. Part one : bedform dimensions; Part two : flow resistance. Dept of Hydraulics, Chalmers University of Technology, Göteborg, Sweden, Report series A:17.

ROBINSON M P & GRAF W H (1972). Pipelining of low concentration sand-water mixtures. Jnl of Hydr Div, Amer Soc Civ Engrs, Vol 98, HY7, July, pp1221-1241.

SPELLS K E (1955). Correlations for use in transport of aqueous suspensions of fine solids through pipes. Trans Inst Chem Engrs, Vol 33/2.

VANONI V A & BROOKS N H (1957). Laboratory studies of the roughness and suspended load of alluvial channels. California Inst of Tech, Report No E-68.

WILLIAMS D J A, WILLIAMS P R & CRABTREE R W (1989). Preliminary investigation into the rheological properties of sewer sediment deposits and the development of a synthetic sewer sediment material for laboratory studies. Foundation for Water Research, Medmenham, England, Ref 8907104/LB.

TABLES

TABLE 1 Experimental results for 299mm pipe - clear water resistance

TEST No	y/D	ks	Re	n	V m/s	lambda	T °C
T1CLR	0.50	0.2388	177980	0.01045	0.705	0.02040	13.7
T2CLR	0.50	0.1505	200352	0.01005	0.804	0.01884	13.8
T3CLR	0.52	0.2772	226702	0.01053	0.862	0.02054	14.6
T4CLR	0.50	0.0408	252521	0.00929	0.990	0.01612	14.0
T5CLR	0.50	0.0095	278084	0.00896	1.099	0.01498	13.7
T6CLR	0.50	0.0218	302745	0.00902	1.200	0.01516	14.0
T7CLR	0.50	0.2555	324034	0.01034	1.290	0.01989	13.6
T8CLR	0.50	0.0220	250044	0.00915	1.002	0.01563	14.3
T9CLR	0.50	0.0103	279492	0.00897	1.096	0.01500	14.6
T10CLR	0.50	0.1702	349600	0.00945	1.392	0.01841	14.5
T11CLR	0.50	0.0770	386241	0.00935	1.511	0.01628	14.6
T12CLR	0.50	0.0833	303828	0.00950	1.191	0.01680	14.4
T14CLR	0.50	0.1458	152868	0.01017	0.600	0.01927	14.7
T15CLR	0.50	0.4771	128738	0.01125	0.503	0.02364	14.3
T16CLR	0.75	0.4981	155535	0.01139	0.500	0.02270	14.4
T17CLR	0.75	0.1912	249287	0.01032	0.804	0.01863	14.8
T18CLR	0.75	0.0316	343427	0.00926	1.102	0.01502	14.4
T20CLR	0.38	0.1156	166201	0.00977	0.802	0.01903	14.1
T21CLR	0.38	0.1292	230515	0.00969	1.102	0.01874	14.7
T22CLR	0.50	0.3790	134470	0.01100	0.498	0.02253	15.8
T23CLR	0.75	0.6289	161412	0.01166	0.501	0.02378	15.8
T24CLR	0.75	0.2327	355838	0.01036	1.104	0.01881	15.8
T25CLR	0.75	0.8294	249691	0.01946	0.803	0.02497	14.4
T26CLR	0.38	0.0632	133827	0.00962	0.595	0.01844	17.0
T27CLR	0.38	0.0533	127593	0.00960	0.595	0.01836	15.1
T28CLR	0.38	0.1056	298251	0.00945	1.409	0.01784	16.8
T29CLR	0.50	0.1121	411624	0.00957	1.499	0.01704	16.8
T30CLR	0.50	0.2821	129909	0.01074	0.499	0.02146	16.8
T31CLR	0.75	0.3769	194377	0.01102	0.599	0.02124	16.8
T32CLR	1.00	0.0222	359132	0.00891	1.401	0.01480	15.8
1	0.93	0.2657	377378	0.01045	1.286	0.01934	13.6
2	0.94	0.1135	274899	0.00987	0.925	0.01731	14.4
3	0.95	0.3940	162807	0.01108	0.545	0.02185	14.8
6	0.50	0.2149	131479	0.01051	0.520	0.02057	13.5
7	0.51	0.2716	134298	0.01069	0.520	0.02125	14.2
8	0.51	0.0816	196338	0.00972	0.730	0.01758	15.7
9	0.50	0.1194	271942	0.00976	1.020	0.01777	15.9
10	0.51	0.2089	377974	0.01011	1.382	0.01899	16.4
11	0.51	0.2941	541483	0.01039	1.950	0.02007	16.9
12	0.25	0.1789	259036	0.00966	1.735	0.02085	14.2
13	0.25	0.0661	206888	0.00901	1.370	0.01810	14.5
14	0.25	0.1545	115224	0.00981	0.757	0.02148	14.8
15	0.25	0.1323	116415	0.00971	0.757	0.02095	14.8
16	0.25	0.0502	75359	0.00956	0.493	0.02032	14.7
17	0.75	0.6995	139934	0.01183	0.458	0.02449	13.7
18	0.75	1.2911	142707	0.01272	0.461	0.02834	14.2
19	0.75	0.1867	228639	0.01033	0.731	0.01869	14.6
20	0.76	0.0997	310610	0.00978	0.981	0.01675	15.0
21	0.73	0.0750	443755	0.00945	1.396	0.01568	15.5
22	0.75	0.0741	657992	0.00930	2.090	0.01514	14.9
23	1.00	0.3667	126960	0.01098	0.494	0.02249	14.3

TABLE 1 (contd)

TEST No	y/D	ks	Re	n	V m/s	lambda	T °C
23B	1.00	0.8009	129324	0.01191	0.494	0.02646	15.0
24B	1.00	0.0538	398968	0.00914	1.524	0.01559	15.0
25B	1.00	0.1092	256663	0.00973	1.023	0.01765	13.4
26B	1.00	0.1276	164927	0.01005	0.630	0.01881	15.0
27A	1.00	0.0465	123041	0.00983	0.470	0.01802	15.0
27B	1.00	-0.0735	121175	0.00915	0.469	0.01560	14.5
28A	1.00	0.0647	434437	0.00920	1.638	0.01577	15.5
28B	1.00	0.0398	447115	0.00896	1.643	0.01496	16.5
R27A	1.00	0.0792	116650	0.01006	0.470	0.01885	13.0
R27B	1.00	0.1296	116650	0.01026	0.470	0.01964	13.0
R28A	1.00	0.0494	400425	0.00910	1.609	0.01545	13.1
R28B	1.00	0.0595	400176	0.00919	1.608	0.01575	13.1
R26A	1.00	0.1948	162194	0.01033	0.643	0.01990	13.6
R26B	1.00	0.1107	161185	0.00998	0.639	0.01857	13.6
R25A	1.00	0.1047	257544	0.00970	1.021	0.01755	13.6
R25B	1.00	0.0982	256412	0.00967	1.022	0.01742	13.4
N3	1.00	1.5381	42746	0.01324	0.180	0.03268	11.4
N4	0.49	0.1560	183904	0.01010	0.779	0.01911	11.7
N5	0.25	0.0879	69514	0.00982	0.494	0.02138	11.4
A1CLR	1.00	0.2017	205651	0.01026	0.901	0.01962	10.0
A1CLR1	1.00	0.1109	205651	0.00985	0.901	0.01807	10.0
A1CLR2	1.00	0.1384	207915	0.00998	0.898	0.01856	10.5
A1CLR3	1.00	0.0973	207915	0.00977	0.898	0.01779	10.5
A1CLR4	1.00	0.1072	212663	0.00981	0.898	0.01794	11.3
A1CLR5	1.00	0.1332	212663	0.00994	0.898	0.01842	11.3
A2CLR	1.00	0.1209	230248	0.00984	1.003	0.01806	10.2
A2CLR1	1.00	0.1371	230248	0.00992	1.003	0.01836	10.2
A3CLR	1.00	0.1327	183942	0.01001	0.799	0.01868	10.3
A3CLR1	1.00	0.1243	183942	0.00997	0.799	0.01853	10.3
A4CLR	1.00	0.0880	159317	0.00988	0.698	0.01819	10.0
A4CLR1	1.00	0.1922	159317	0.01033	0.698	0.01990	10.0
A5CLR	1.00	0.1420	113243	0.01033	0.499	0.01990	9.8
A5CLR1	1.00	0.1123	113243	0.01022	0.499	0.01946	9.8
A6CLR	1.00	0.1412	137239	0.01021	0.603	0.01943	9.9
A6CLR1	1.00	0.1676	137239	0.01031	0.603	0.01983	9.9
A10CLR	1.00	0.1210	252745	0.00980	1.101	0.01791	10.2
A10CLR	1.00	0.1180	252745	0.00978	1.101	0.01785	10.2
A11CLR	1.00	0.1479	124231	0.01030	0.549	0.01976	9.7
A11CLR	1.00	0.1682	124231	0.01037	0.549	0.02005	9.7
A12CLR	0.50	0.1524	230473	0.01000	0.997	0.01863	10.4
A14CLR	0.25	0.0652	136599	0.00923	0.994	0.01896	10.8
A15CLR	0.74	0.3264	281559	0.01075	1.019	0.02027	10.2
A16CLR	0.49	0.0896	231817	0.00966	1.019	0.01744	10.2
A17CLR	0.50	0.0220	164434	0.00948	0.704	0.01677	10.9
A18CLR	0.49	0.1304	185467	0.00998	0.814	0.01865	10.3
A20CLR	0.49	0.2152	262515	0.01022	1.131	0.01954	11.0
A21CLR	0.50	0.0255	280543	0.00911	1.195	0.01545	10.9
A22CLR	0.50	0.1493	301242	0.00989	1.270	0.01817	11.0

TABLE 2 Experimental results for 299mm pipe - limit of deposition

TEST No	D (m)	d50 (m)	LAMBDA	y/D	V_L (m/s)	Cv (ppm)	T °C
A1SED10	0.29883	0.00072	0.01850	1.0	0.893	29.86	13.5
A2SED	0.29883	0.00072	0.01817	1.0	1.006	45.50	10.4
A3SED	0.29883	0.00072	0.01934	1.0	0.800	14.50	10.3
A4SED	0.29883	0.00072	0.01971	1.0	0.698	7.56	10.0
A5SED	0.29883	0.00072	0.01979	1.0	0.500	0.67	9.8
A6SED	0.29883	0.00072	0.01890	1.0	0.603	4.07	9.9
A9SED	0.29883	0.00072	0.01752	1.0	1.196	69.75	9.8
A10SED	0.29883	0.00072	0.01784	1.0	1.099	55.29	10.2
A11SED	0.29883	0.00072	0.02084	1.0	0.549	2.13	9.6
A12SED	0.29883	0.00072	0.01896	0.511	0.972	70.10	9.5
A13SED	0.29883	0.00072	0.01886	0.504	0.896	22.18	11.0
A15SED	0.29883	0.00072	0.01784	0.734	1.016	42.54	10.2
A16SED	0.29883	0.00072	0.01769	0.490	1.021	32.67	10.5
A17SED	0.29883	0.00072	0.01803	0.499	0.702	6.68	10.9
A18SED	0.29883	0.00072	0.01815	0.494	0.812	27.52	10.3
A19SED	0.29883	0.00072	0.02027	0.513	0.870	30.47	10.0
A20SED1	0.29883	0.00072	0.01638	0.498	1.108	51.52	11.0
A21SED	0.29883	0.00072	0.01583	0.502	1.191	55.73	10.9
A22SED	0.29883	0.00072	0.01932	0.519	1.237	135.54	11.4
T1SED	0.29883	0.00072	0.01885	0.49	0.714	9.57	13.7
T2SED	0.29883	0.00072	0.01639	0.49	0.822	20.76	13.8
T3SED	0.29883	0.00072	0.01981	0.52	0.864	29.42	14.6
T4SED	0.29883	0.00072	0.01668	0.51	0.983	24.07	14.0
T5SED	0.29883	0.00072	0.01597	0.51	1.066	35.17	13.7
T6SED	0.29883	0.00072	0.01739	0.52	1.119	87.47	14.0
T7SED	0.29883	0.00072	0.02026	0.50	1.290	220.73	13.6
T8SED	0.29883	0.00072	0.01790	0.52	0.948	35.40	14.3
T9SED	0.29883	0.00072	0.01648	0.53	1.035	47.24	14.6
T10SED	0.29883	0.00072	0.01950	0.50	1.386	230.45	14.5
T11SED	0.29883	0.00072	0.01670	0.50	1.498	251.22	14.6
T12SED	0.29883	0.00072	0.01678	0.50	1.191	110.00	14.4
T13SED	0.29883	0.00072	0.01382	0.50	1.294	174.51	13.4
T14SED	0.29883	0.00072	0.01595	0.50	0.599	4.44	14.7
T17SED	0.29883	0.00072	0.01842	0.75	0.805	8.27	14.8
T18SED	0.29883	0.00072	0.01746	0.73	1.129	41.56	14.4
T20SED	0.29883	0.00072	0.01889	0.38	0.801	19.50	14.1
T21SED	0.29883	0.00072	0.01902	0.38	1.100	98.04	14.7
T22SED	0.29883	0.00072	0.02336	0.50	0.499	1.00	15.8
T23SED	0.29883	0.00072	0.02231	0.75	0.502	0.31	15.8
T24SED	0.29883	0.00072	0.01646	0.75	1.107	66.15	15.8
T25SED	0.29883	0.00072	0.02241	0.74	0.809	20.69	14.4
T26SED	0.29883	0.00072	0.01829	0.37	0.598	7.99	17.0
T27SED	0.29883	0.00072	0.01880	0.38	0.597	2.47	15.1
T28SED	0.29883	0.00072	0.01884	0.38	1.396	443.00	16.8
T29SED	0.29883	0.00072	0.01721	0.50	1.497	280.00	16.8
T30SED	0.29883	0.00072	0.02034	0.50	0.495	4.50	16.8
T31SED	0.29883	0.00072	0.02015	0.75	0.603	1.55	16.8
T32SED	0.29883	0.00072	0.01509	1.00	1.386	98.66	15.8

TABLE 3 Experimental results for 299mm pipe - deposited bed

Test No	V (m/s)	y/D	ys/D	Re	ks (mm)	So*100	Cv (ppm)	T °C
DB1	0.609	0.501	0.1479	145466	2.8222	0.2904	280.36	17.2
DB2	0.700	0.502	0.1332	168377	2.1885	0.3412	330.19	16.5
DB3	0.834	0.503	0.1386	198024	1.5254	0.4364	422.91	16.3
DB4	0.972	0.505	0.1497	226258	1.2197	0.5647	542.09	16.0
DB5	1.140	0.500	0.1623	257026	0.3203	0.5778	1186.68	16.0
DB6	1.522	0.501	0.0322	396410	0.1922	0.7508	1165.08	15.3
DB7	1.417	0.502	0.0293	362634	0.4050	0.7568	1112.45	14.5
DB8	1.317	0.503	0.0265	342540	0.5376	0.6975	800.98	15.0
DB9	1.215	0.502	0.0342	313268	0.2419	0.5052	543.68	14.9
DB10	1.123	0.501	0.0360	288097	0.1881	0.4157	356.49	14.8
DB11	1.014	0.500	0.0332	267181	0.3099	0.3808	355.23	15.2
DB12	0.921	0.501	0.0338	234767	0.5033	0.3422	327.30	14.5
DB13	0.823	0.501	0.0428	199448	0.7003	0.2994	325.06	12.9
DB14	0.735	0.499	0.0505	182498	0.7103	0.2430	236.14	14.1
DB15	0.602	0.503	0.0286	150697	1.1646	0.1810	107.21	13.6
DB16	0.516	0.499	0.0340	129883	1.5882	0.1466	52.38	14.0
DB17	1.495	0.504	0.0120	381994	0.2681	0.7594	410.47	14.0
DB18	1.399	0.502	0.0087	355134	0.2486	0.6577	437.42	13.8
DB19	1.296	0.502	0.0062	332834	0.4326	0.6361	310.76	14.2
DB20	1.192	0.502	0.0073	306117	0.3515	0.5152	282.01	14.2
DB21	1.092	0.502	0.0077	281150	0.2047	0.3916	176.46	14.3
DB22	1.003	0.502	0.0069	267854	0.1704	0.3215	151.58	15.7
DB23	1.003	0.499	0.0064	258693	0.1182	0.3069	109.26	14.5
DB24	0.893	0.503	0.0067	230900	0.2053	0.2647	113.51	14.5
DB25	0.799	0.504	0.0089	206187	0.1272	0.1061	76.18	14.3
DB26	0.694	0.501	0.0072	178677	-0.0821	0.1100	30.66	14.3
DB27	0.596	0.502	0.0078	154270	0.1195	0.1142	24.54	14.5
DB28	0.500	0.502	0.0003	130864	0.0872	0.0796	21.17	14.8
DB29	1.008	0.500	0.0018	238317	0.0692	0.2935	53.20	11.2
DB30	0.993	0.502	0.0016	232736	0.1857	0.3223	56.06	10.8
DB31	0.902	0.503	0.0010	211579	0.1862	0.2677	29.51	10.8
DB32	0.801	0.500	0.0001	186825	0.1161	0.2011	11.63	10.7
DB33	0.795	0.503	0.0009	185378	0.1017	0.1945	23.31	10.6
DB34	0.699	0.503	0.0	162187	-0.0345	0.1278	5.68	10.4
DB35	0.602	0.502	0.0	139372	0.0760	0.1129	11.02	10.4
DB36	1.000	1.0	0.0152	230535	0.1109	0.3062	61.86	10.4
DB37	0.902	1.0	0.0013	205477	0.0311	0.2277	64.66	9.9
DB38	1.001	1.0	0.0008	231113	0.1243	0.2533	34.99	10.4
DB39	1.105	1.0	0.0	255164	0.0296	0.3292	21.73	10.4
DB40	1.104	1.0	0.0281	252768	0.1197	0.3748	162.12	10.3
DB41	1.209	1.0	0.0314	275638	0.0715	0.0314	143.42	10.2
DB42	1.297	1.0	0.0030	297750	0.1159	0.5043	203.84	10.2
DB43	1.412	1.0	0.0290	322157	0.3527	0.7294	319.80	10.2
DB44	1.009	1.0	0.0369	232194	0.5208	0.4115	142.21	10.6

TABLE 4 : Values of k_s for clear water in 299mm pipe

y/D	N	$\bar{k}_s$ (mm)	σ_s	σ_n
1.0	37	0.116	0.0676	0.0111
0.95	3	0.258	0.1404	0.0810
0.75	12	0.296	0.2481	0.0716
0.50	30	0.150	0.1089	0.0199
0.375	5	0.093	0.0333	0.0149
0.25	7	0.105	0.0500	0.0189
	94	0.147	0.1135	0.0117

<u>All data</u>

Mean $\bar{k}_s$ for 99 points = 0.192mm

σ_s = 0.236mm

$\bar{k}_s + 2\sigma_s$ = 0.664mm

All values ≥ 0.664mm were eliminated from analysis leaving the 94 values detailed above

TABLE 5 : Values of n for clear water in 299mm pipe

y/D	N	$\bar{n}$	σ_s	σ_n
1.0	37	0.00987	0.00046	0.000075
0.95	3	0.01047	0.00060	0.00035
0.75	12	0.01033	0.00082	0.00024
0.50	30	0.00988	0.00059	0.00011
0.375	5	0.00963	0.00012	0.00005
0.25	7	0.00955	0.00031	0.00012
	94	0.0099	0.00058	0.000060

TABLE 6 : Values of λ for clear water in 299mm pipe

y/D	N	$\bar{\lambda}$	σ_s	σ_n
1.0	37	0.0182	0.0016	0.00027
0.95	3	0.0195	0.0023	0.0013
0.75	12	0.0188	0.0029	0.0009
0.50	30	0.0183	0.0021	0.00039
0.375	5	0.0185	0.00045	0.00019
0.25	7	0.0202	0.0012	0.00048
	94	0.0185	0.00202	0.00021

TABLE 7 : Measured and predicted threshold velocities in 299mm pipe

	Threshold velocities (m/s)			
$\bar{y}/d$	Measured	Predicted Eqn (1)	Predicted Eqn (2)	Predicted Eqn (3)
0.268	0.224	0.201	0.353	0.282
0.489	0.256	0.228	0.401	0.339

$\bar{y}/d$	Effective threshold velocity* (m/s)	Number of tests
1.0	0.206	10
0.744	0.330	7
0.506	0.322	25
0.374	0.344	5
weighted mean	0.301	47

* calculated from limit of deposition data (see 7.1)

TABLE 8 Measured and predicted concentrations at limit of deposition - all HR data

	D (mms)	d50 (mms)	y/D	Cv(meas)/Cv(pred)	o	o(%)
May (Eqn 8)						
	76	0.57	1	0.987	0.110	11.1
	158	0.64	1	1.054	0.197	18.7
	158	0.64	0.75	0.868	0.180	20.7
	158	0.64	0.5	0.804	0.170	21.1
	158	0.64	0.375	0.736	0.578	78.5
	158	5.8	1	1.027	0.127	12.4
	158	7.9	1	0.842	0.181	21.5
	299	0.72	1	0.707	0.155	21.9
	299	0.72	0.75	0.595	0.311	52.3
	299	0.72	0.5	0.501	0.237	47.3
	299	0.72	0.375	0.361	0.215	59.5
				0.791	0.221	32.0
May (Eqn 32)						
	76	0.57	1	0.959	0.114	11.9
	158	0.64	1	1.024	0.195	19.0
	158	0.64	0.75	0.933	0.221	23.7
	158	0.64	0.5	1.001	0.236	23.6
	158	0.64	0.375	1.011	0.787	77.8
	158	5.8	1	0.998	0.138	13.8
	158	7.9	1	0.818	0.196	23.9
	299	0.72	1	1.270	0.423	33.3
	299	0.72	0.75	1.015	0.373	36.7
	299	0.72	0.5	1.075	1.002	93.2
	299	0.72	0.375	0.789	0.288	36.5
				1.029	0.450	42.9
Macke (Eqn 9)						
	76	0.57	1	0.730	0.130	17.8
	158	0.64	1	1.079	0.243	22.5
	158	0.64	0.75	0.981	0.150	15.3
	158	0.64	0.5	1.020	0.212	26.7
	158	0.64	0.375	0.856	0.699	81.6
	158	5.8	1	(30.38)*	(3.61)*	(11.9)*
	158	7.9	1	(35.62)*	(5.11)*	(14.3)*
	299	0.72	1	0.742	0.199	26.8
	299	0.72	0.75	0.759	0.266	35.0
	299	0.72	0.5	0.595	0.242	40.7
	299	0.72	0.375	0.907	0.147	16.2
				0.795+	0.256+	34.83+

+ Excluding points marked with *

TABLE 8 (contd)

	D (mms)	d50 (mms)	y/D	Cv(meas)/Cv(pred)	σ	σ(%)
Mayerle (Eqn 11)						
	76	0.57	1	1.424	0.249	17.5
	158	0.64	1	1.227	0.416	33.9
	158	0.64	0.75	2.155	0.319	14.8
	158	0.64	0.5	2.878	0.874	30.4
	158	0.64	0.375	2.041	1.882	92.2
	158	5.8	1	0.859	0.123	14.3
	158	7.9	1	0.595	0.113	19.0
	299	0.72	1	0.505	0.134	26.5
	299	0.72	0.75	0.435	0.373	85.7
	299	0.72	0.5	0.751	0.523	69.6
	299	0.72	0.375	0.431	0.089	20.6
				1.113	0.473	43.6
Mayerle & Nalluri (Eqn 13)						
	76	0.57	1	2.035	1.265	62.2
	158	0.64	1	3.259	1.296	39.8
	158	0.64	0.75	4.329	1.914	44.2
	158	0.64	0.5	5.506	1.002	18.2
	158	0.64	0.375	4.693	5.335	113.6
	158	5.8	1	0.297	0.052	17.5
	158	7.9	1	0.171	0.053	31.0
	299	0.72	1	2.210	0.947	42.8
	299	0.72	0.75	3.298	2.002	60.7
	299	0.72	0.5	2.546	1.893	74.3
	299	0.72	0.375	1.513	0.306	20.2
				2.802	1.389	52.5

TABLE 9 : Analysis of data for limit of deposition

D (mm)	d (mm)	$\bar{y}/d$	$d/\bar{R}$	N	$\bar{X}$	$\bar{Y}$	$\bar{Y}\,(\bar{R}/d)^{0.36}$
76.7	0.57	1.0	2.973×10^{-2}	8	2.450×10^{-3}	2.450×10^{-3}	2.019×10^{-2}
158.3	0.64	1.0	1.617×10^{-2}	38	1.805×10^{-3}	1.805×10^{-3}	2.144×10^{-2}
158.3	0.64	0.750	1.340×10^{-2}	8	1.423×10^{-3}	1.578×10^{-3}	2.098×10^{-2}
158.3	0.64	0.501	1.615×10^{-2}	5	1.386×10^{-3}	1.777×10^{-3}	2.113×10^{-2}
158.3	0.64	0.379	1.966×10^{-2}	7	1.420×10^{-3}	2.014×10^{-3}	2.127×10^{-2}
158.3	5.8	1.0	1.466×10^{-1}	5	7.097×10^{-3}	7.097×10^{-3}	2.246×10^{-2}
158.3	7.9	1.0	1.996×10^{-1}	5	7.085×10^{-3}	7.085×10^{-3}	1.863×10^{-2}
298.8	0.72	1.0	9.639×10^{-3}	10	1.606×10^{-3}	1.606×10^{-3}	2.602×10^{-2}
298.8	0.72	0.745	7.997×10^{-3}	7	9.187×10^{-4}	1.021×10^{-3}	1.851×10^{-2}
298.8	0.72	0.505	9.573×10^{-3}	25	8.793×10^{-4}	1.124×10^{-3}	1.829×10^{-2}
298.8	0.72	0.375	1.181×10^{-2}	5	9.624×10^{-4}	1.370×10^{-3}	1.966×10^{-2}

weighted mean - D = 76.7, 158.3mm	2.111×10^{-2}
weighted mean - D = 298.8mm	2.011×10^{-2}
weighted mean - all data	2.073×10^{-2}

FIGURES

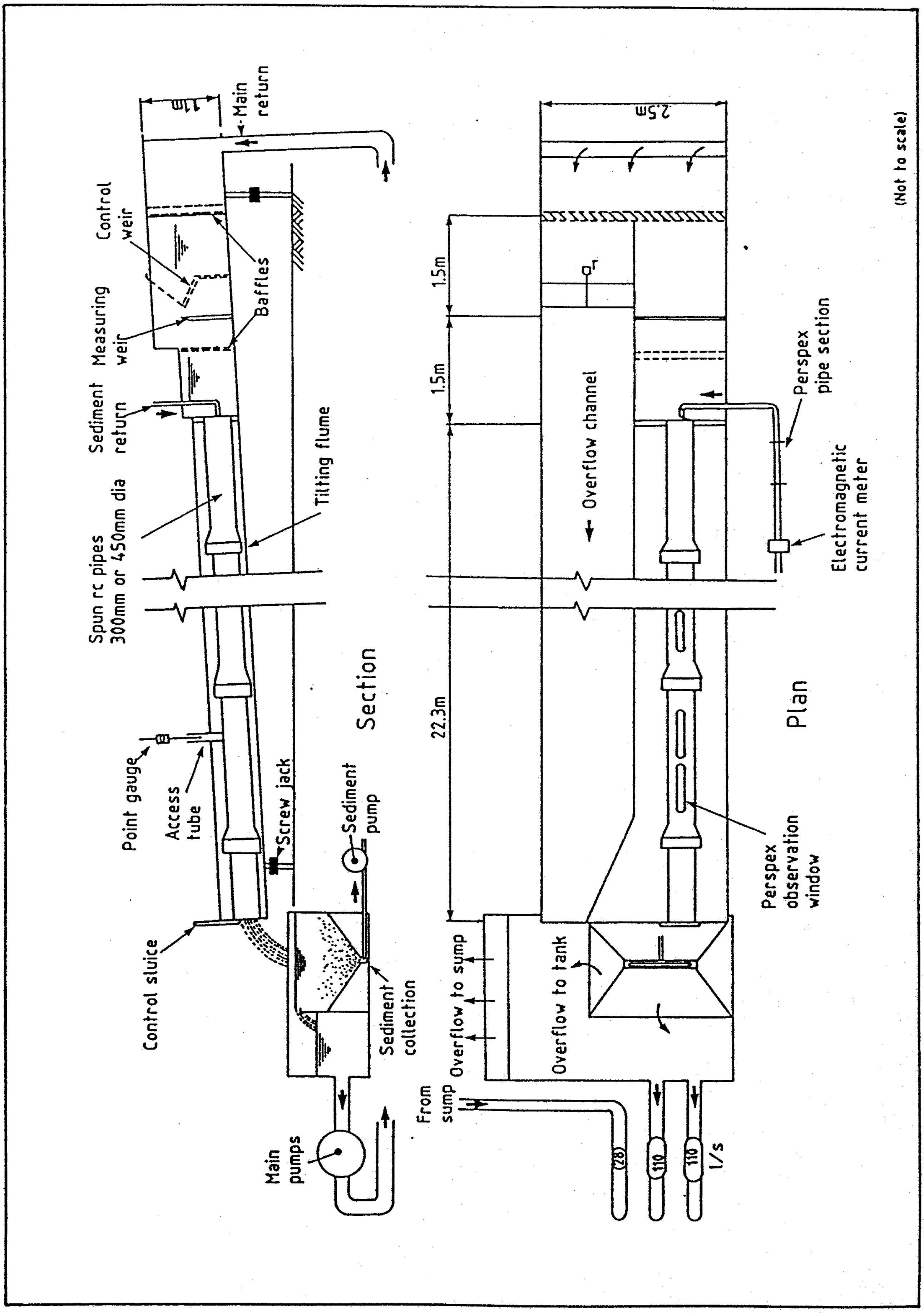

Fig 1 Layout of test rig

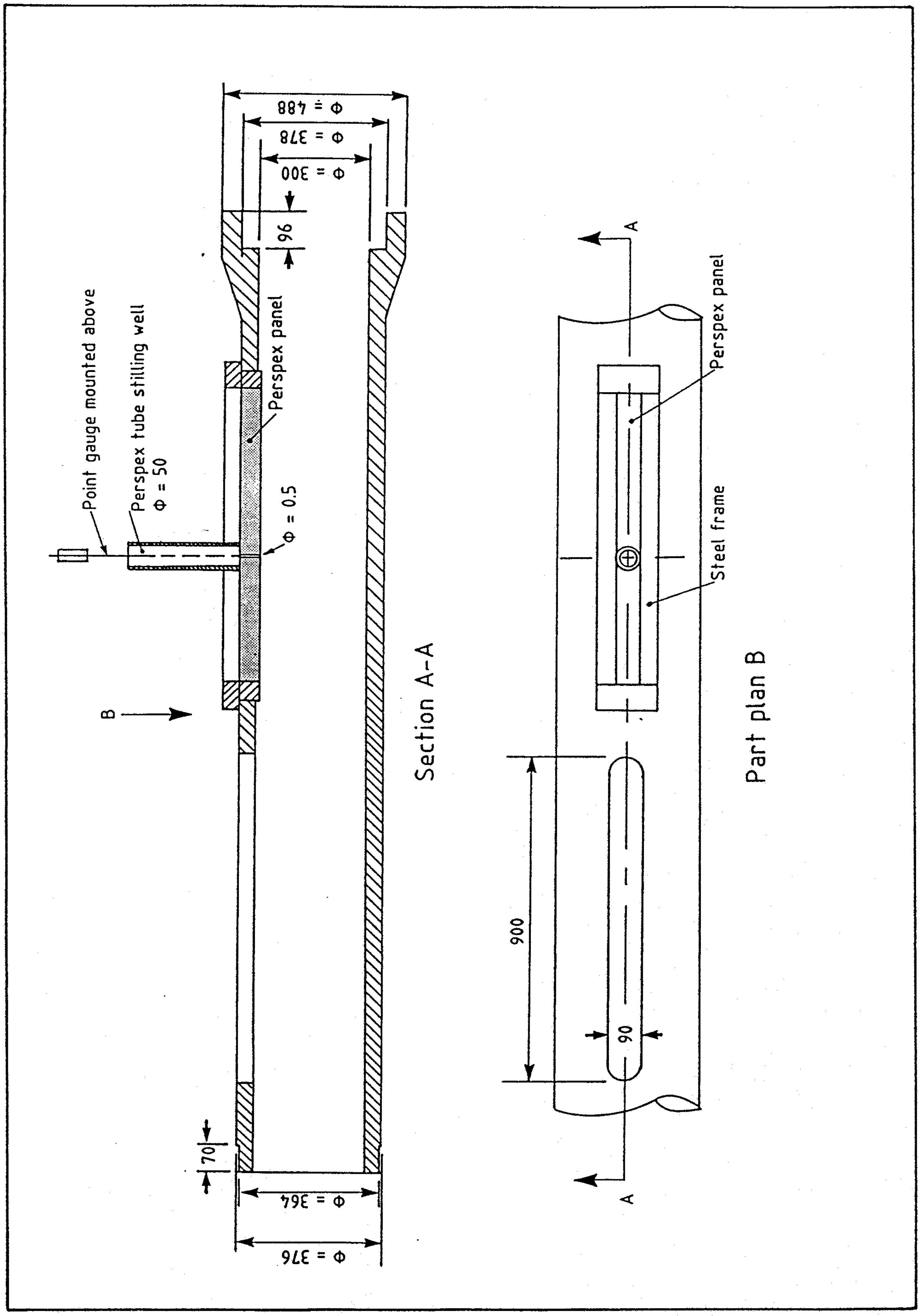

Fig 2 Detail of concrete pipe section showing slots and removable lids

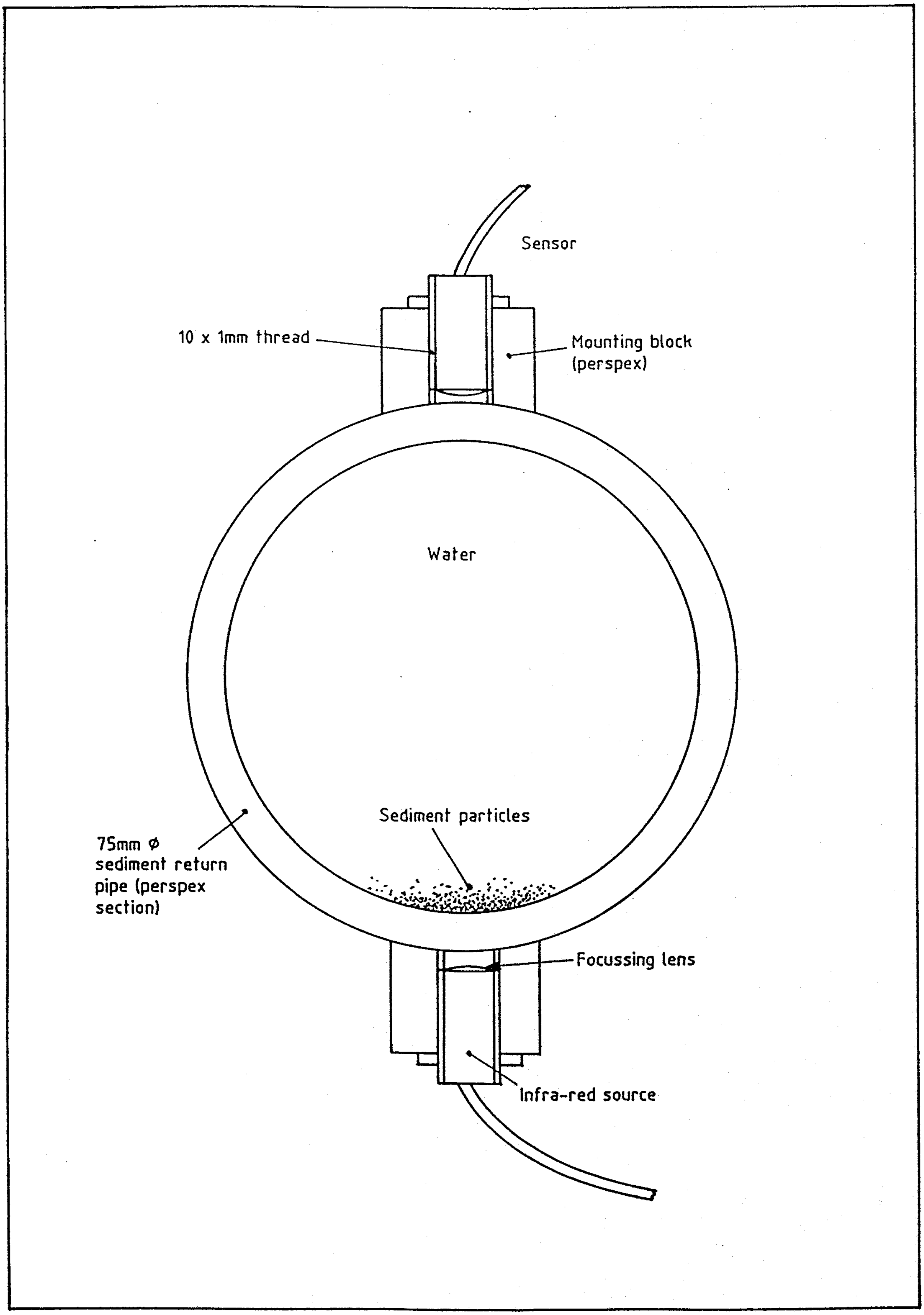

Fig 3 Cross-section through sediment sensor

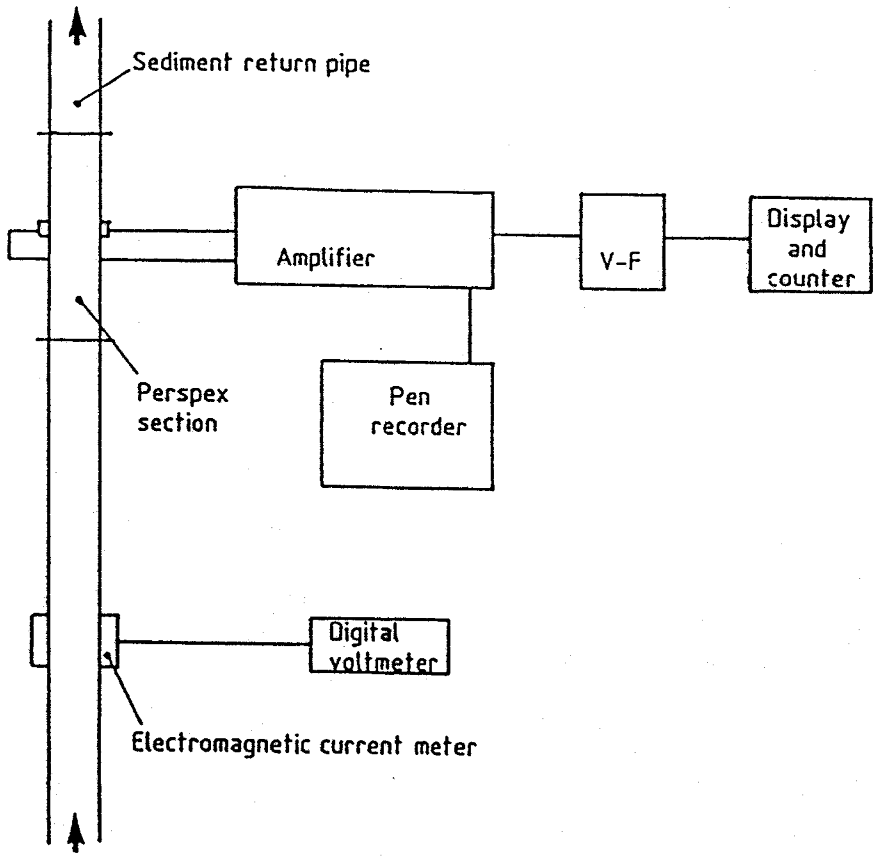

Fig 4 Schematic layout of sensor equipment

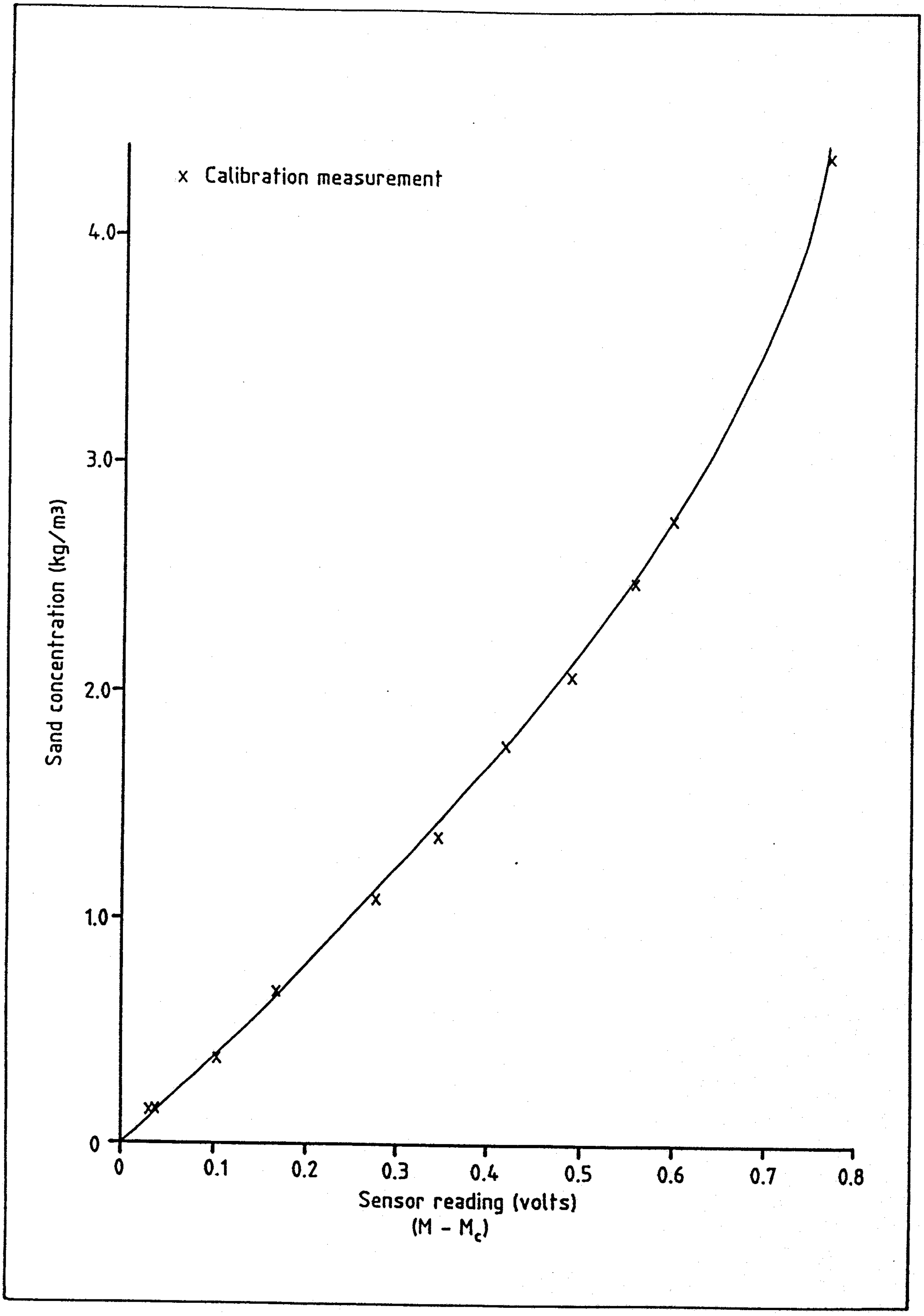

Fig 5 Sensor calibration at 1.39m/s Q = 0.00613 m^3/s

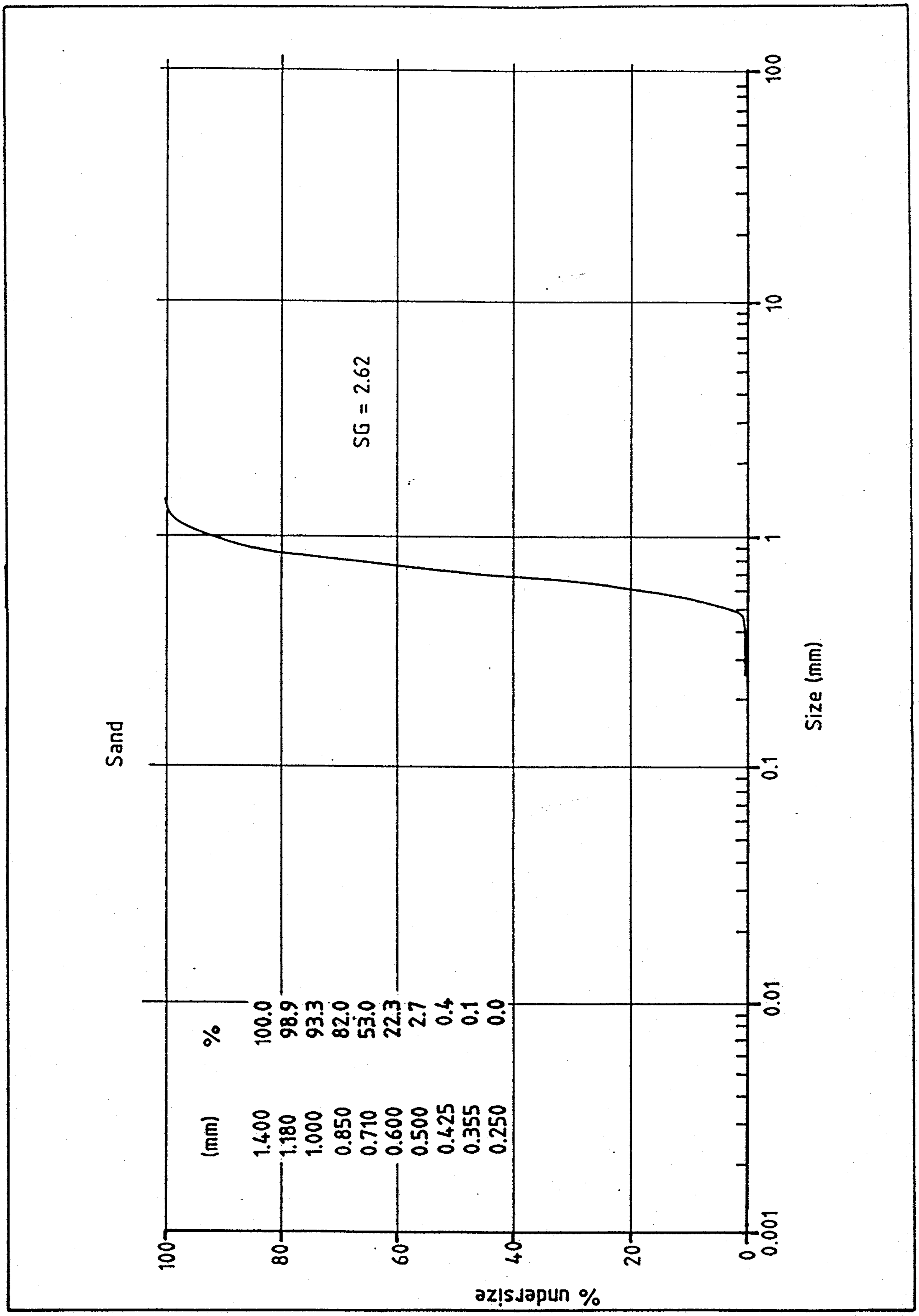

Fig 6 Sand grading

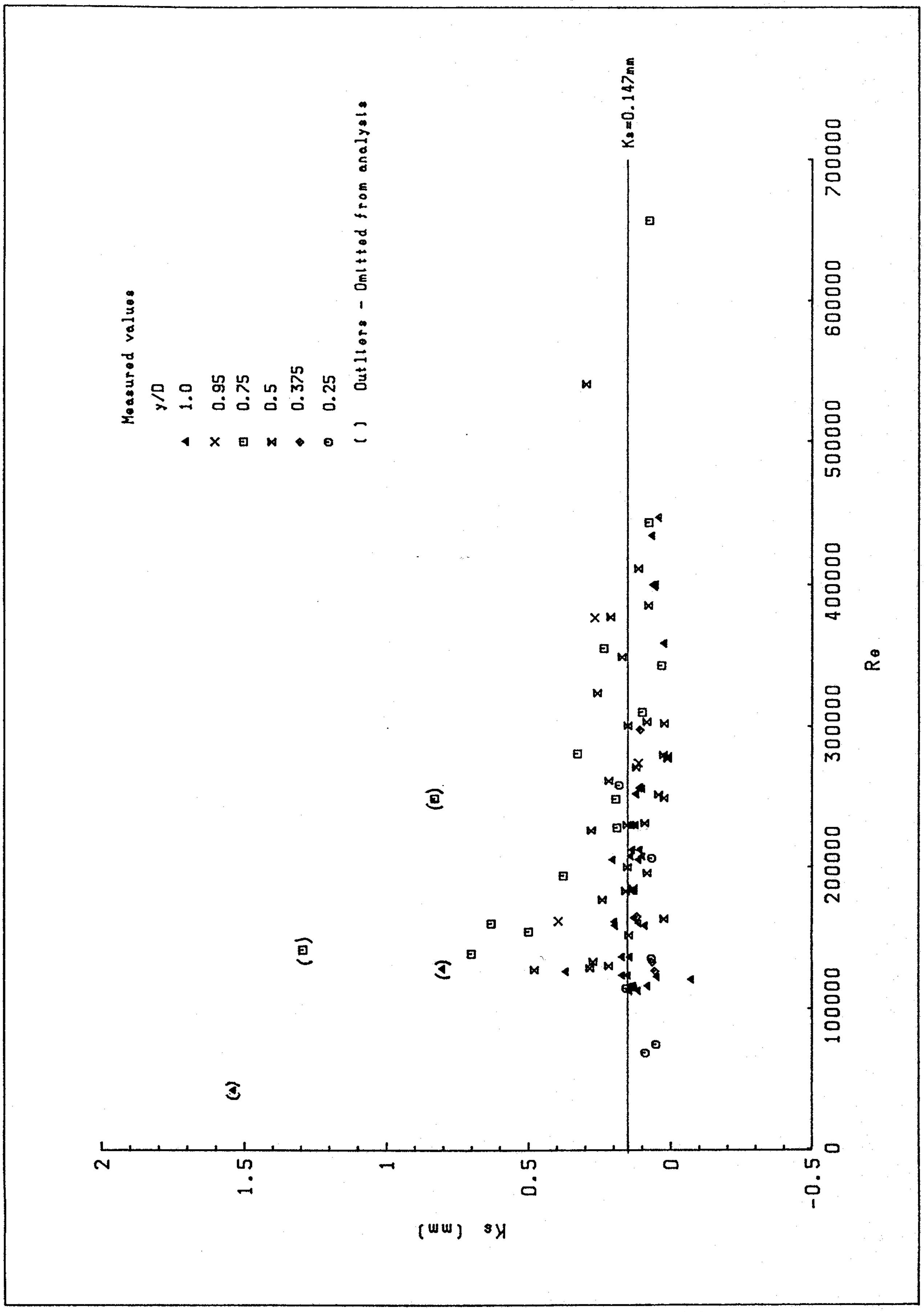

Fig 7 ks versus Reynolds number for clear water in 299 mm pipe

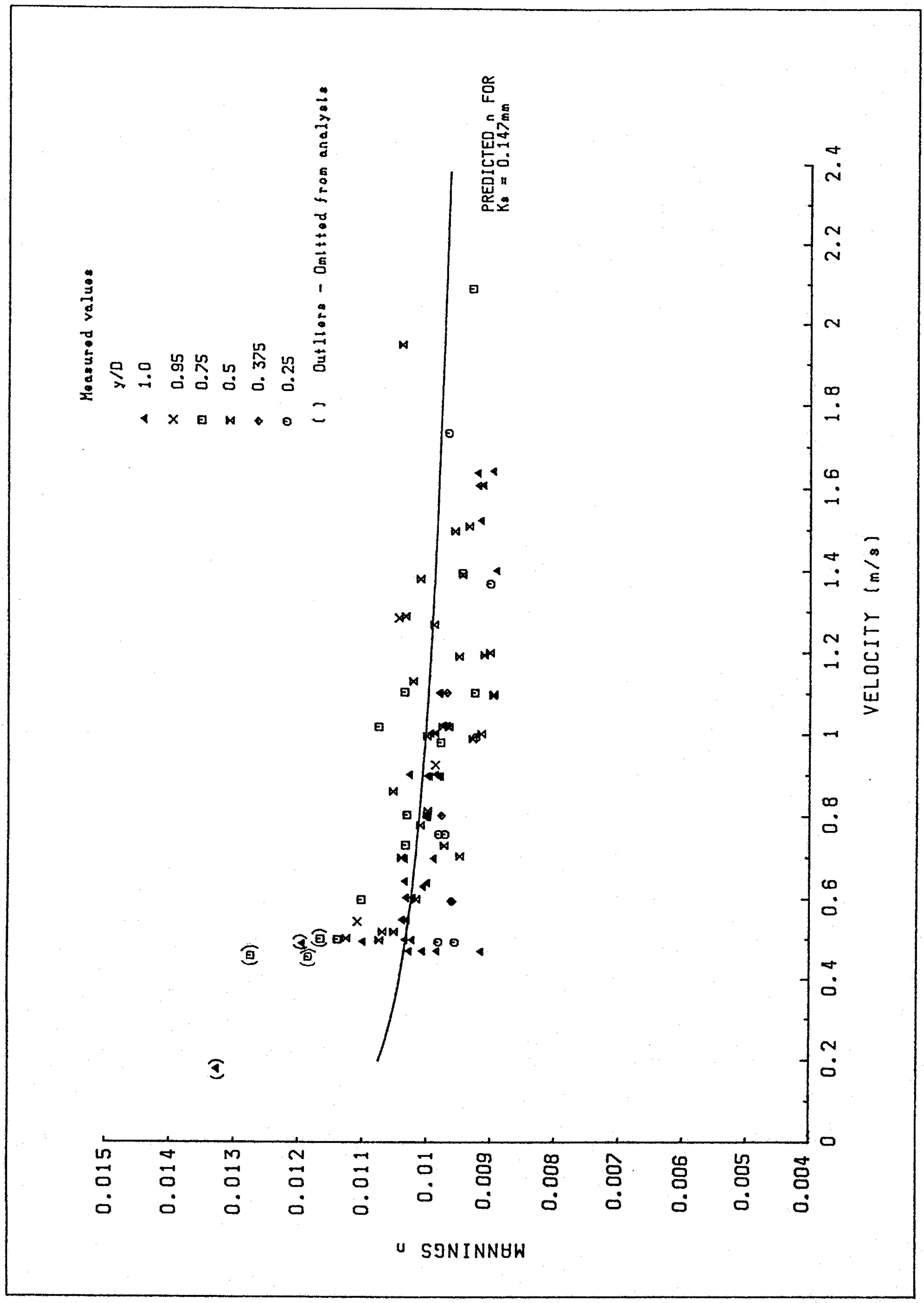

Fig 8 Mannings n versus clear-water velocity in 299 mm pipe

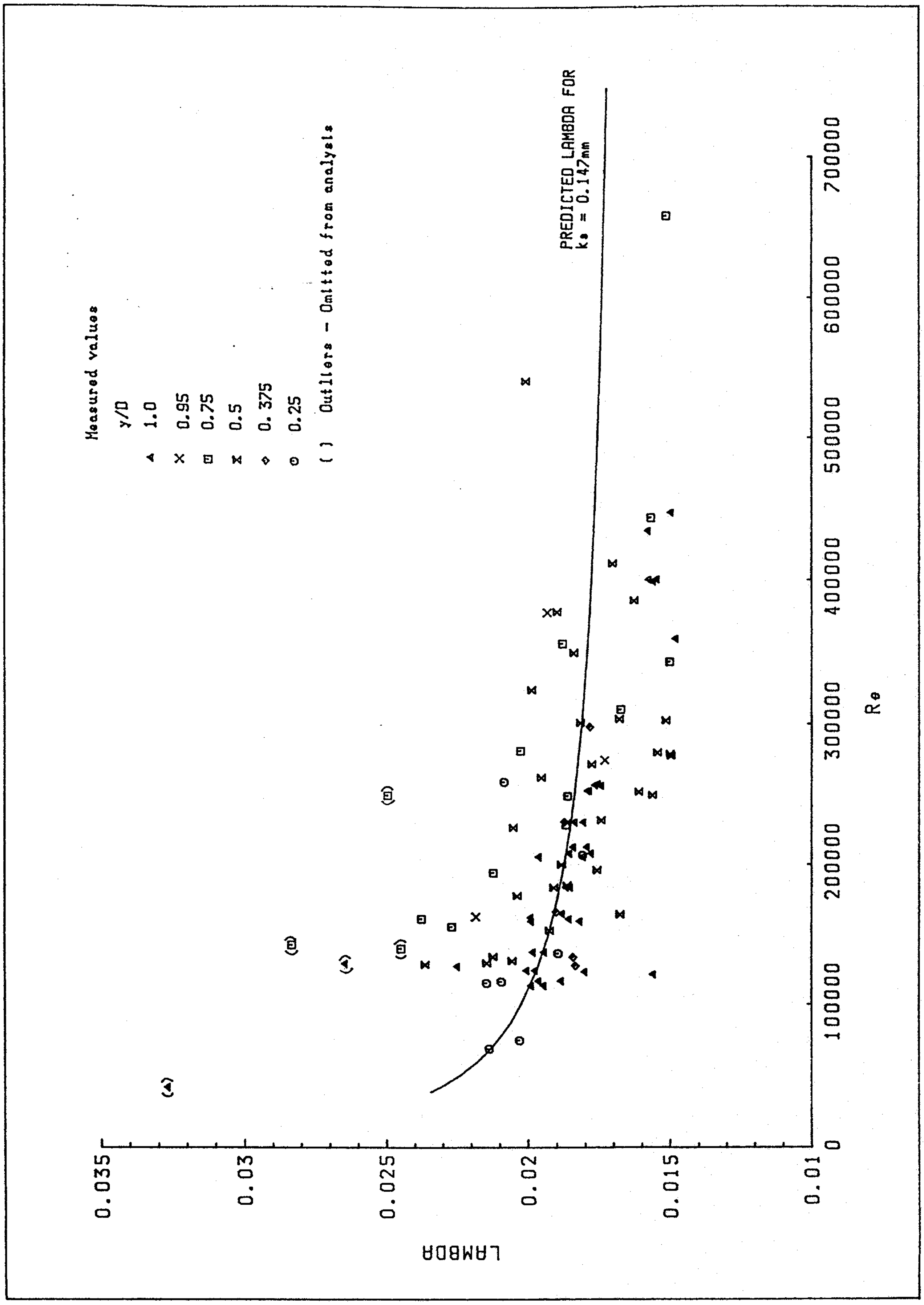

Fig 9 Lambda versus Reynolds number for clear-water in 299 mm pipe

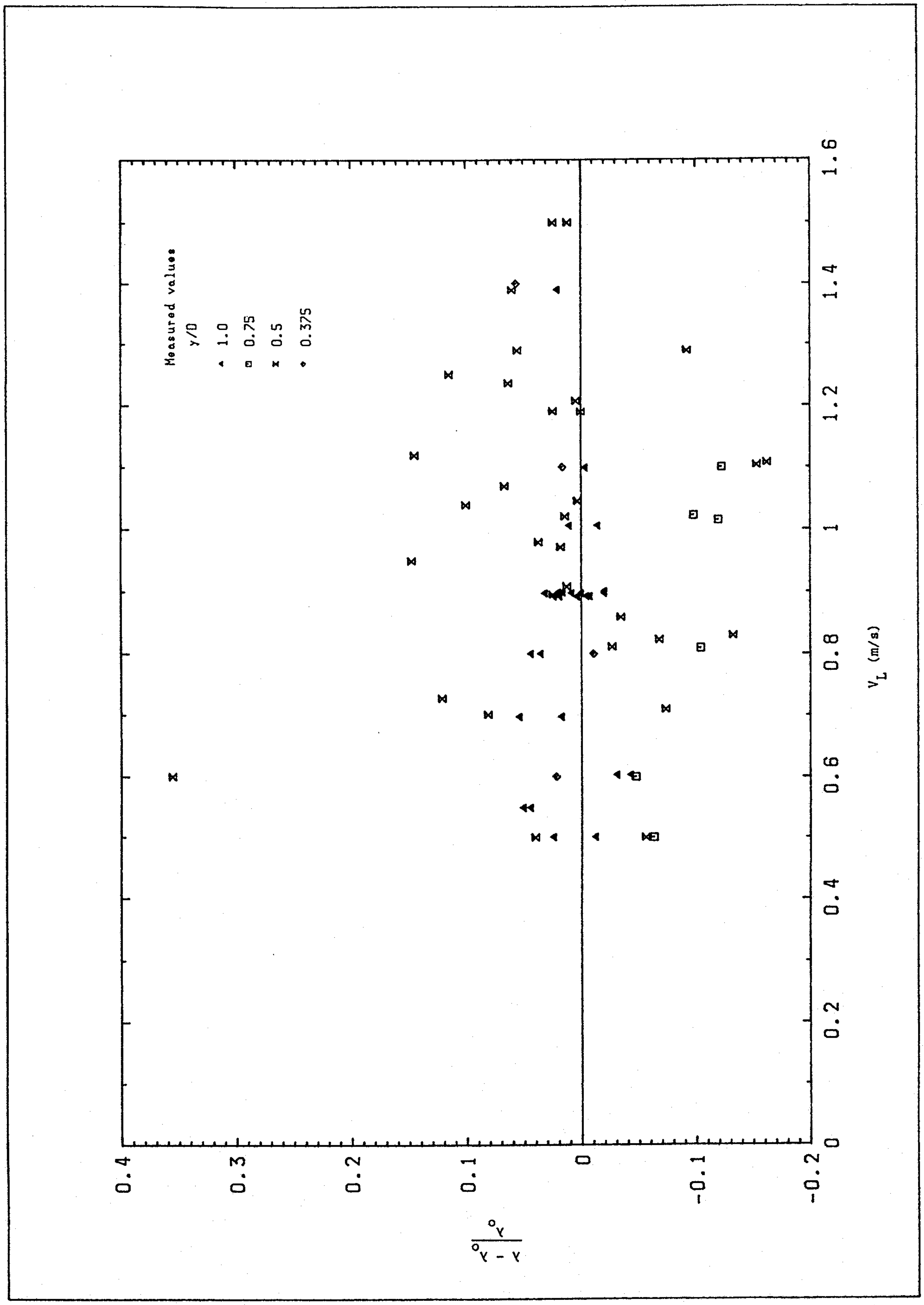

Fig 10 HEAD LOSS AT LIMIT OF DEPOSITION - Experimental data

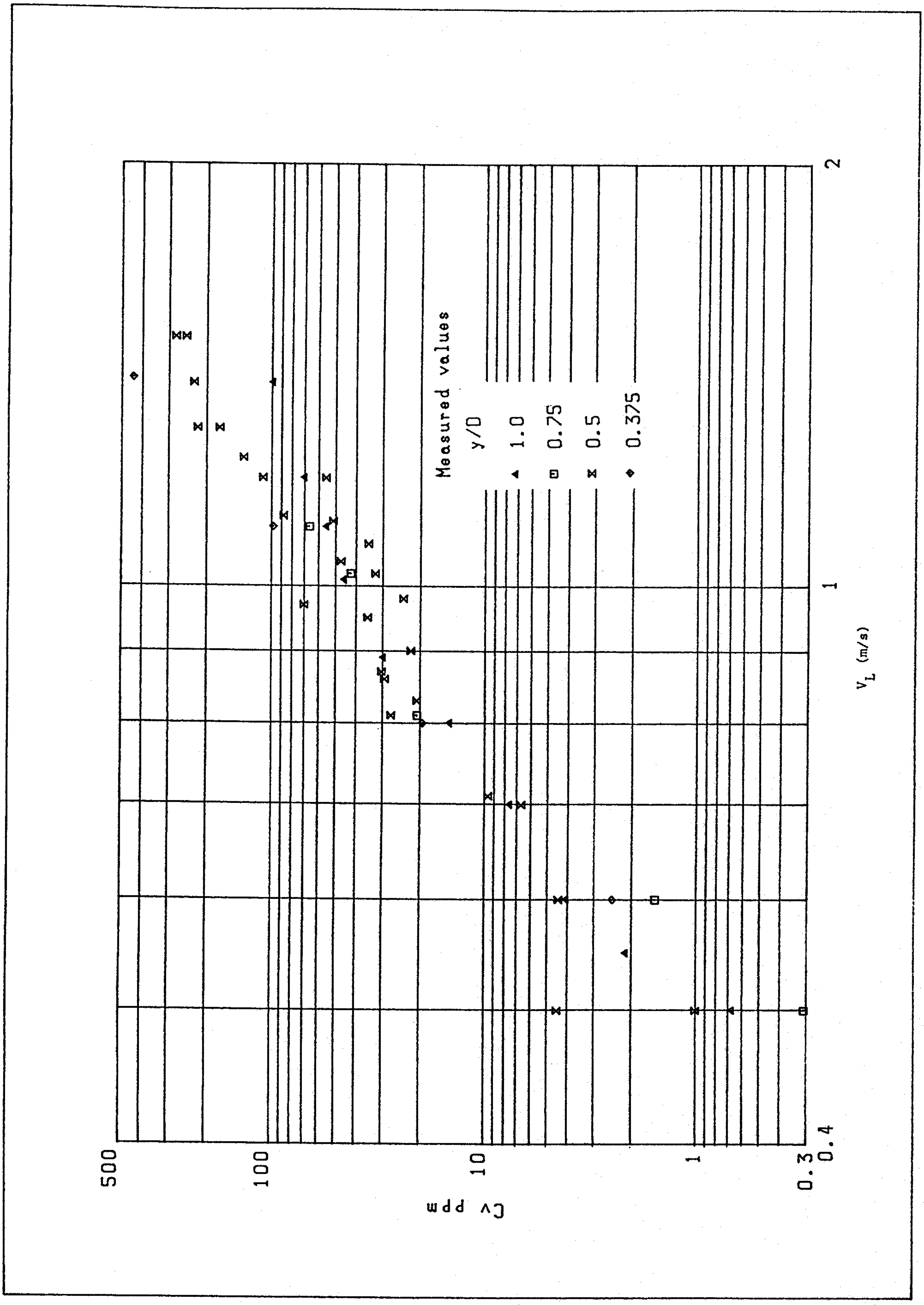

Fig 11 SEDIMENT CONCENTRATION AT LIMIT OF DEPOSITION - Experimental data for 299 mm pipe

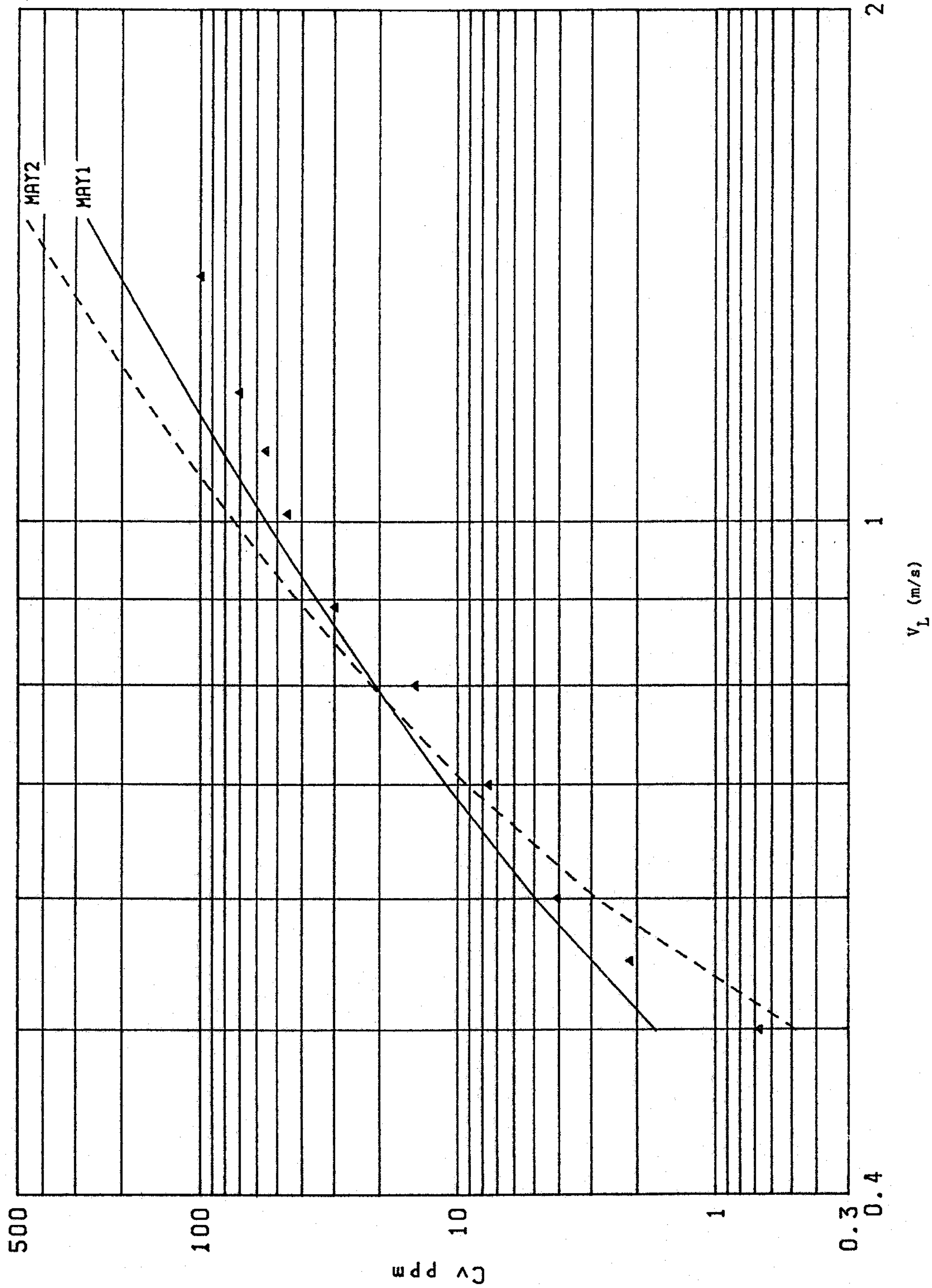

Fig 12 LIMIT OF DEPOSITION - Comparison of experimental data for 299mm pipe with May's equations (pipefull)

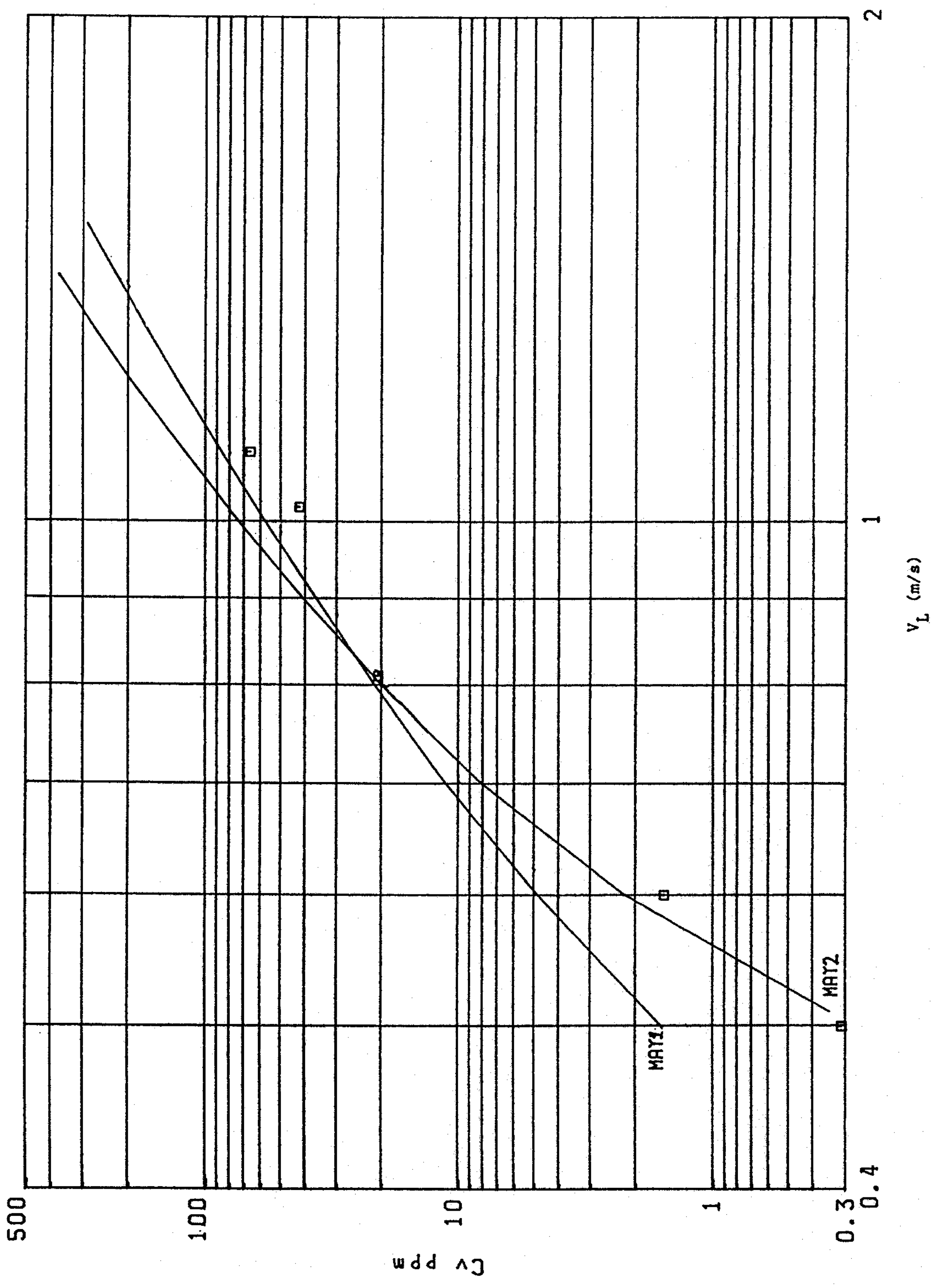

Fig 13 LIMIT OF DEPOSITION - Comparison of experimental data for 299mm pipe with May's equation (3/4 full)

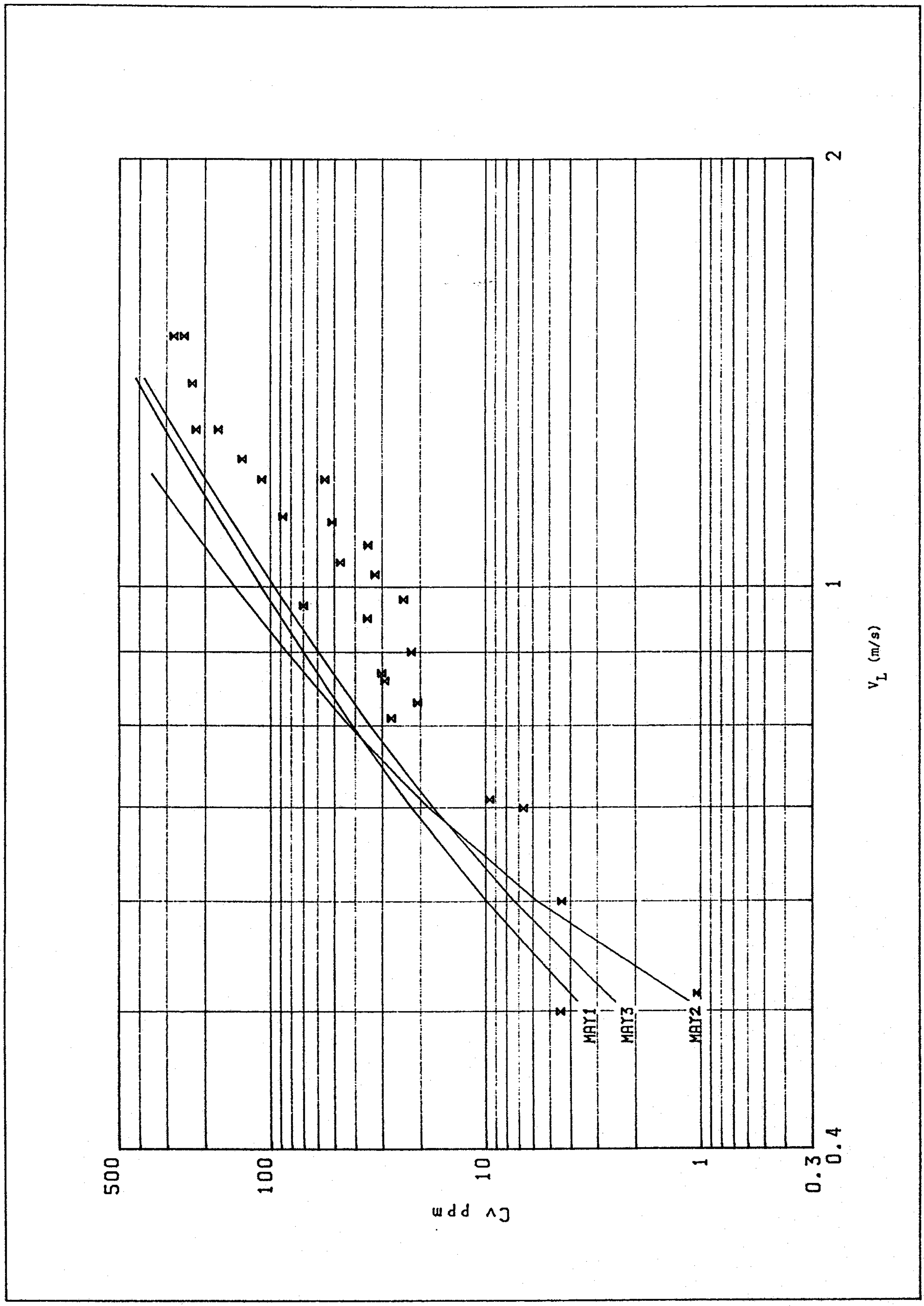

Fig 14 LIMIT OF DEPOSITION - Comparison of experimental data for 299mm pipe with May's equations (1/2 full)

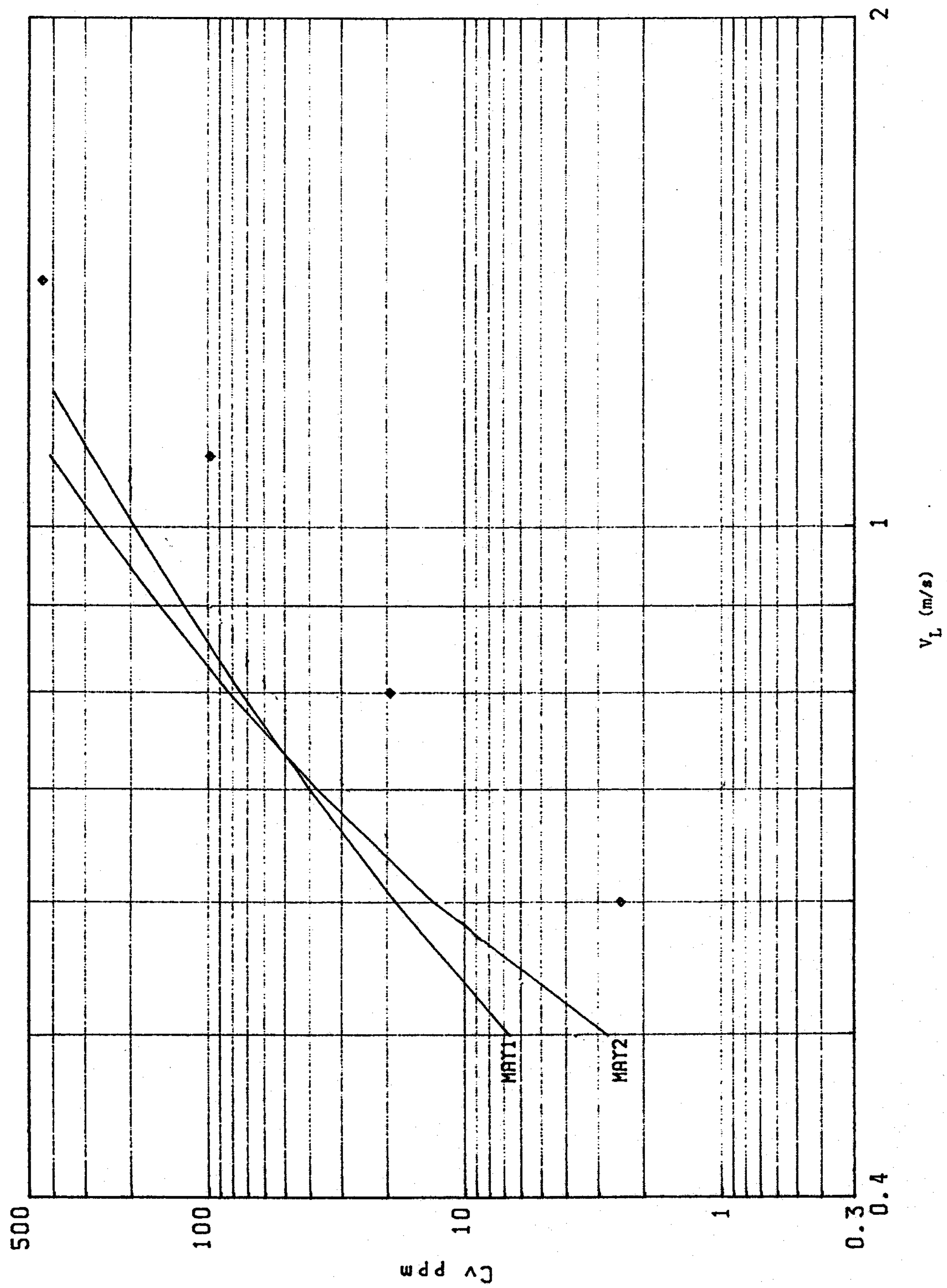

Fig 15 LIMIT OF DEPOSITION - Comparison of experimental data for 299mm pipe with May's equations (3/8 full)

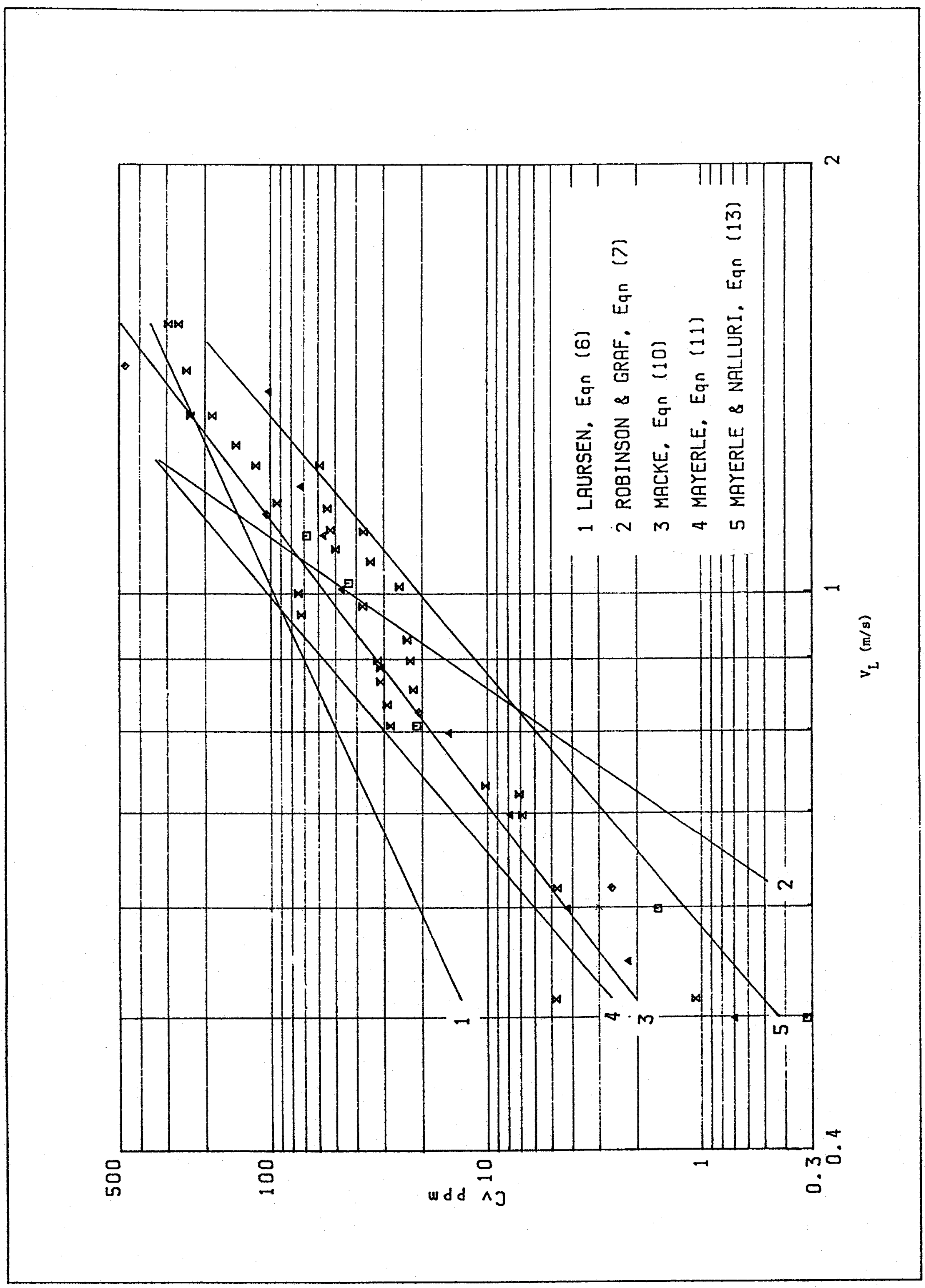

Fig 16 LIMIT OF DEPOSITION - Comparison of experimental data for 299mm pipe with other eqns (pipe-full)

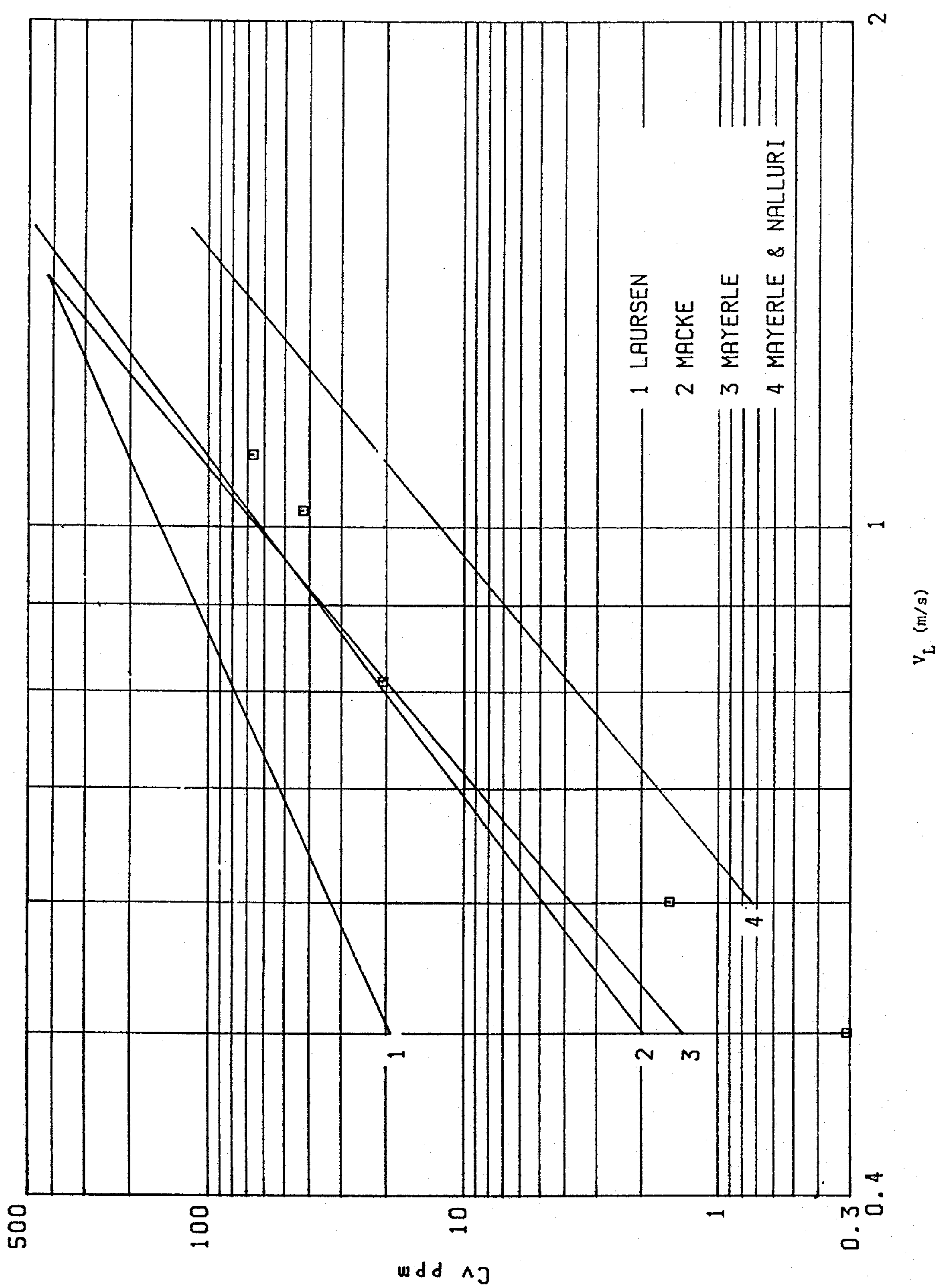

Fig 17 LIMIT OF DEPOSITION - Comparison of experimental data for 299mm pipe with other eqns (3/4 full)

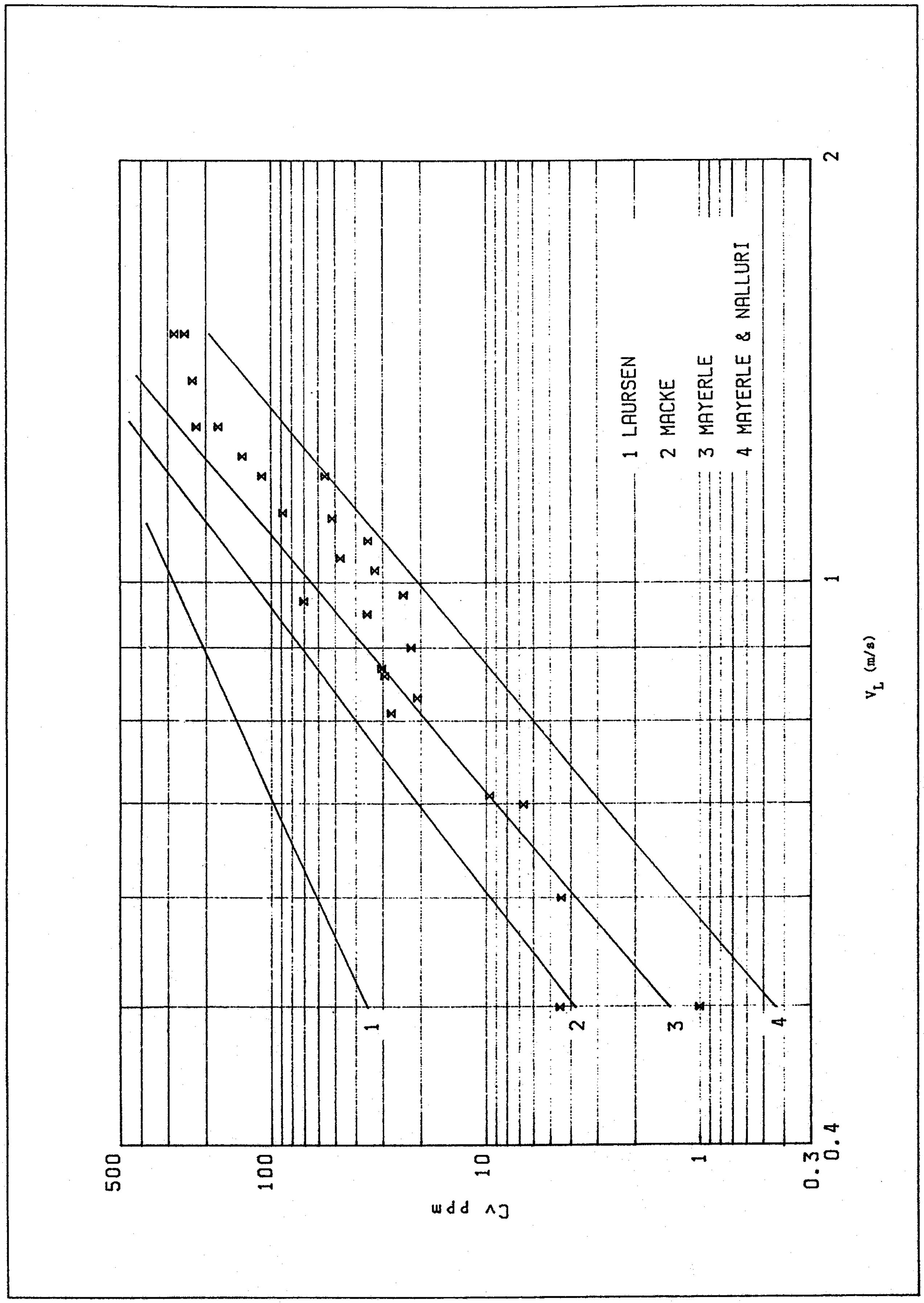

Fig 18 LIMIT OF DEPOSITION: - Comparison of experimental data for 299mm pipe with other eqns (1/2 full)

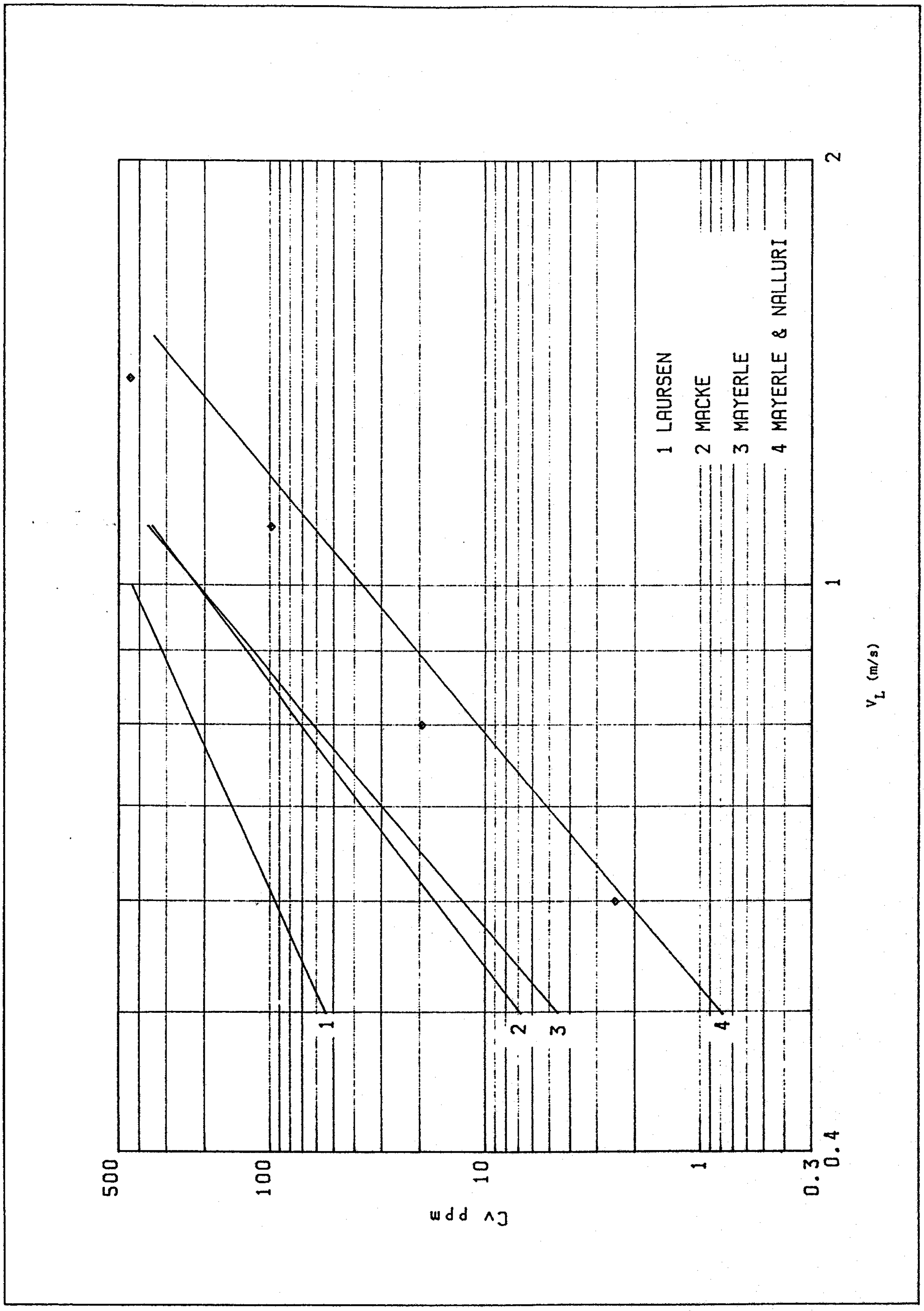

Fig 19 LIMIT OF DEPOSITION - Comparison of experimental data for 299mm pipe with other eqns (3/8 full)

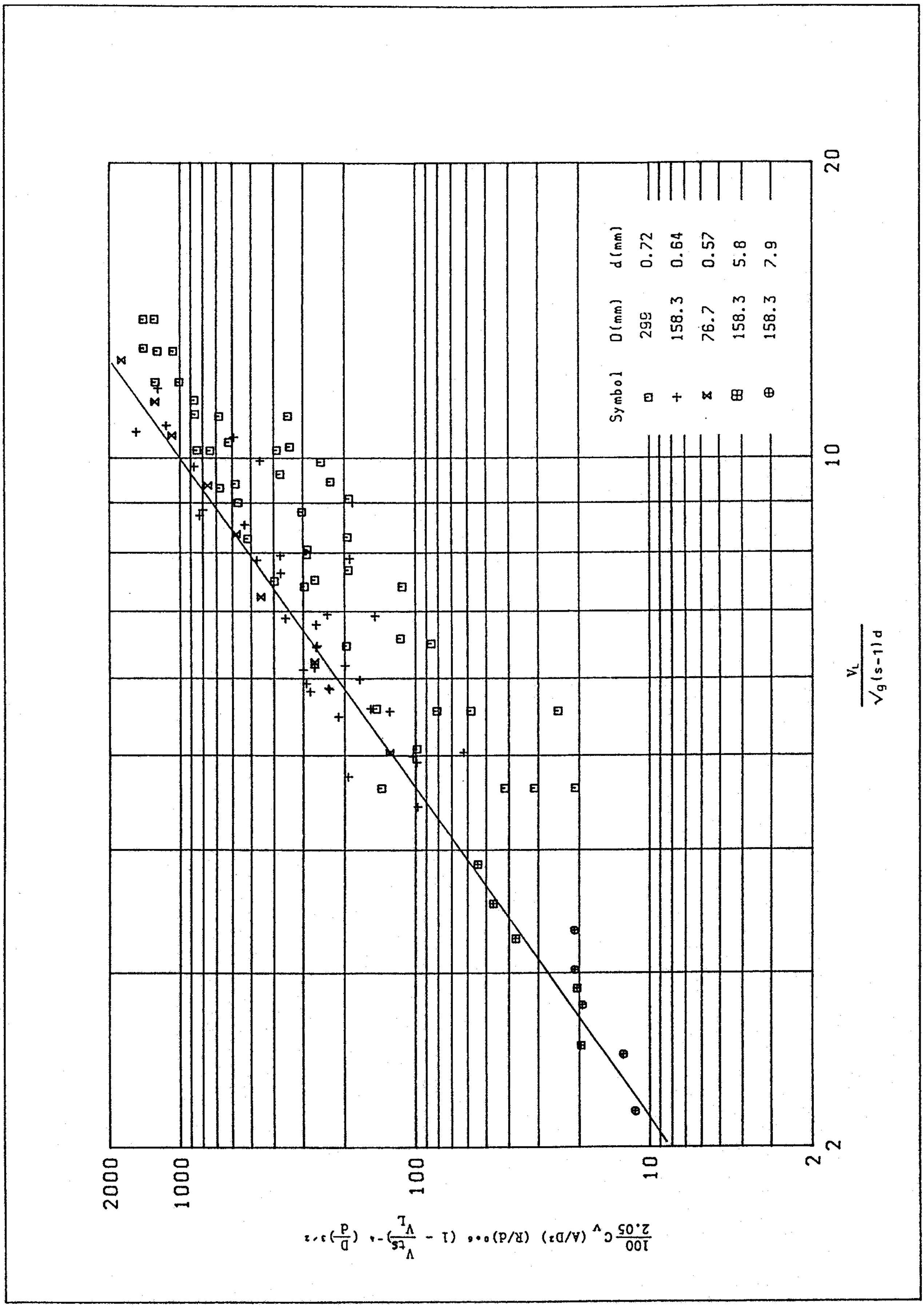

Fig 20 LIMIT OF DEPOSITION - HR data for 299 mm, 158 mm and 77 mm pipes in May format

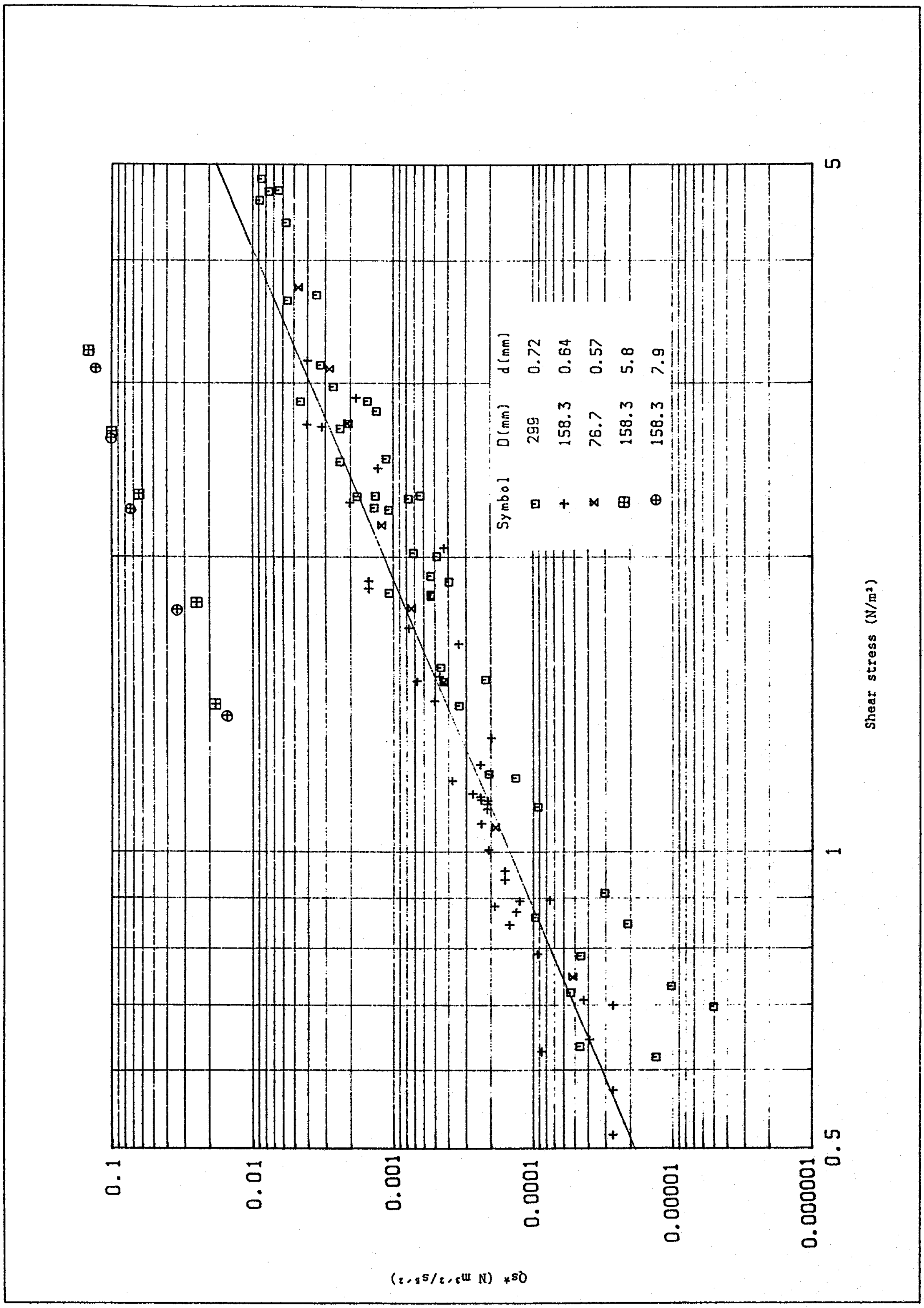

Fig 21 LIMIT OF DEPOSITION - HR data for 299 mm, 158 mm and 77 mm pipes in Macke format

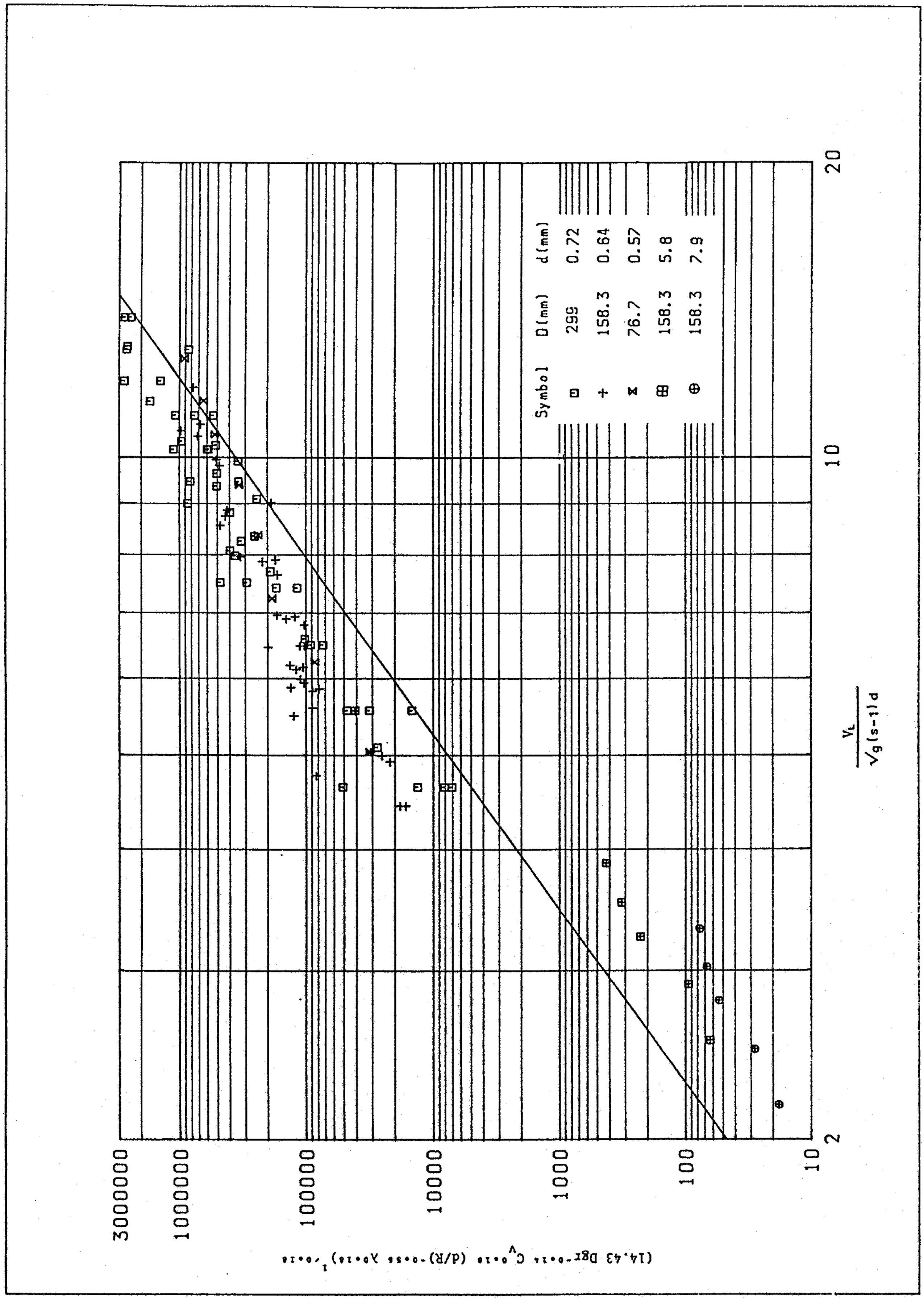

Fig 22 LIMIT OF DEPOSITION - HR data for 299 mm, 158 mm and 77 mm pipes in Mayerle & Nalluri format

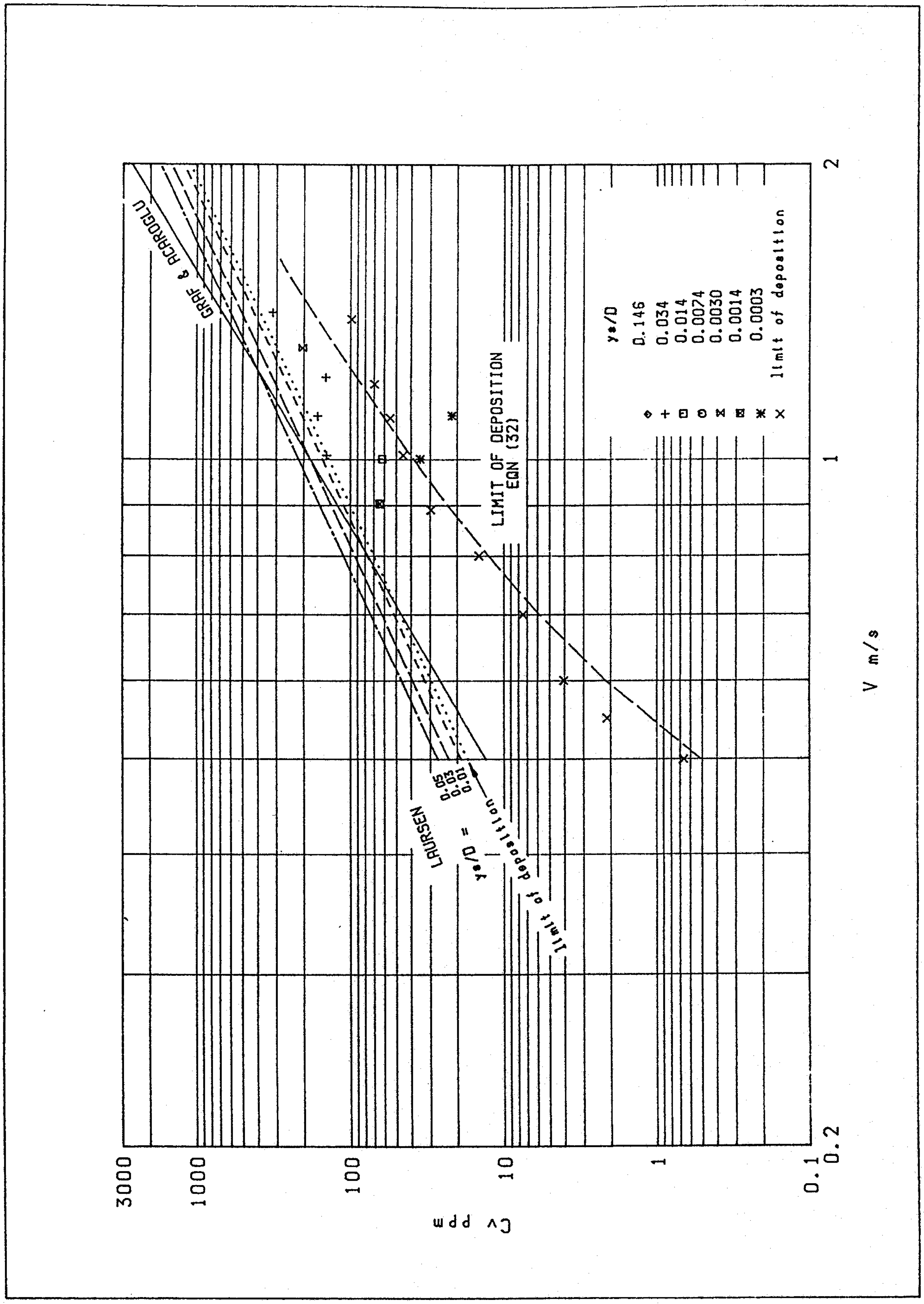

Fig 23 DEPOSITED BED - Effect of deposited bed on sediment transport rate in 299 mm pipe (pipe-full)

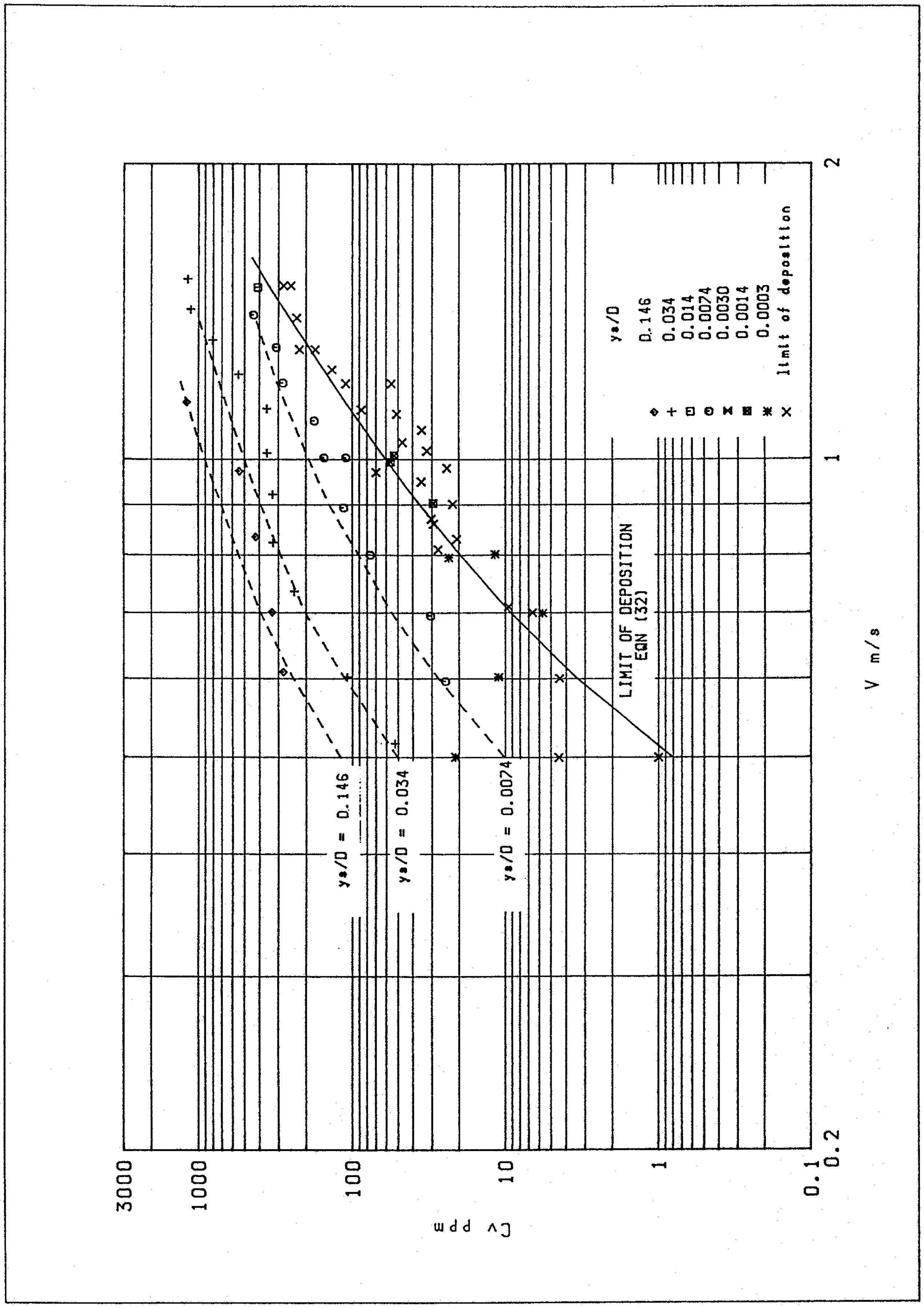

Fig 24 DEPOSITED BED - Effect of deposited bed on sediment transport rate in 299 mm pipe (pipe half-full)

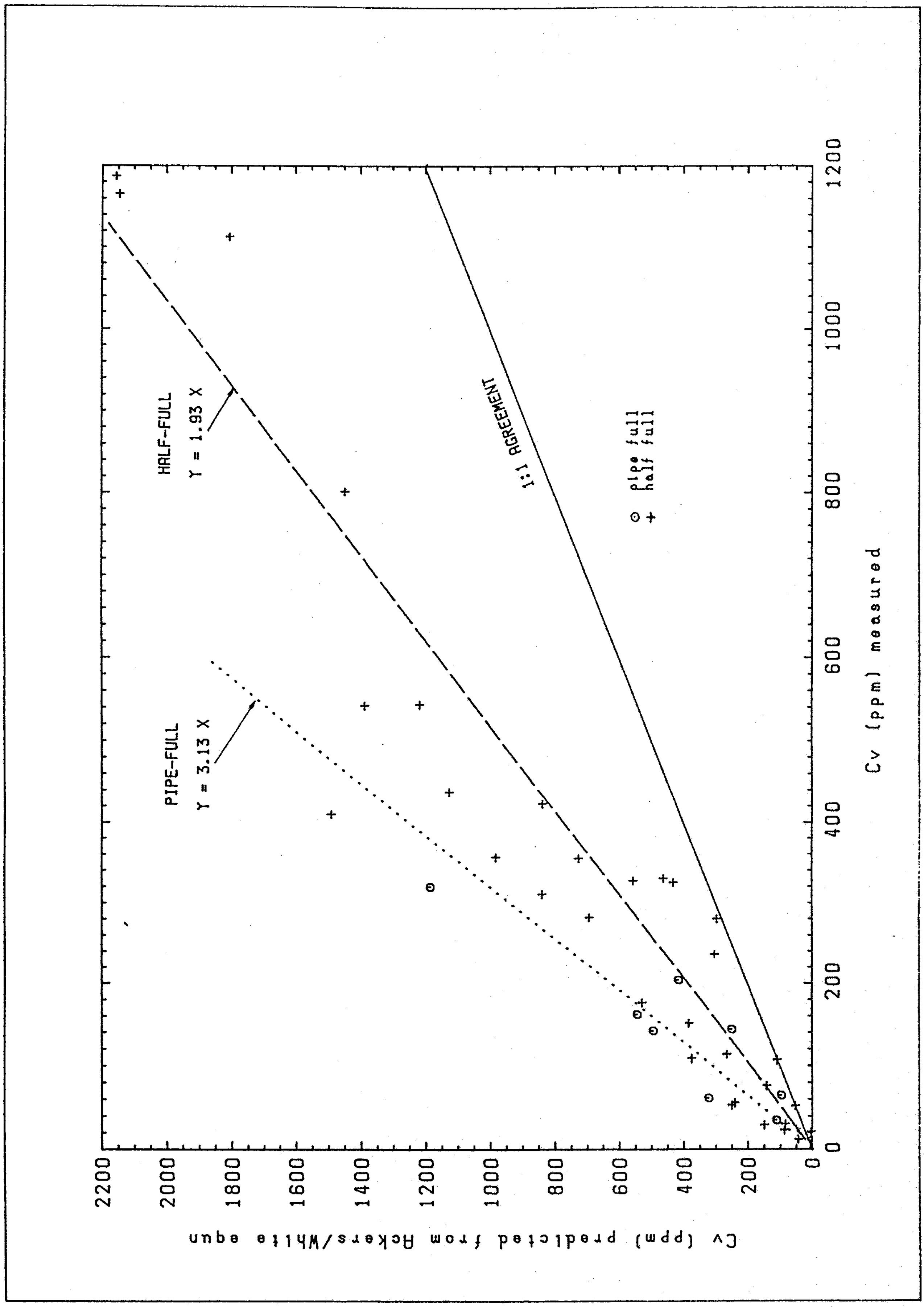

Fig 25 Comparison of measured and predicted sediment concentrations with deposited beds in 299 mm pipe

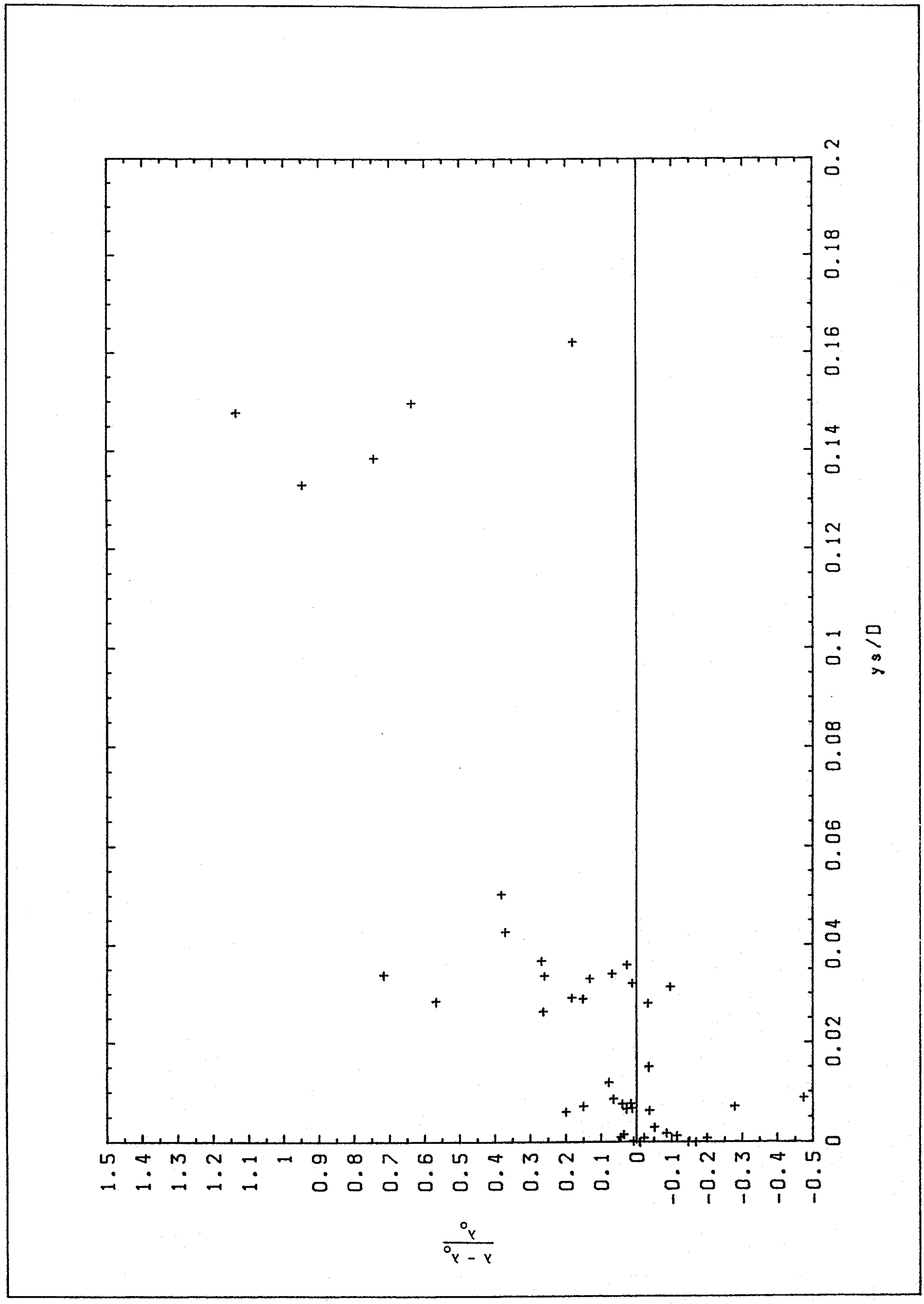

Fig 26 Proportionate change in friction factor due to deposited beds in 299 mm pipe

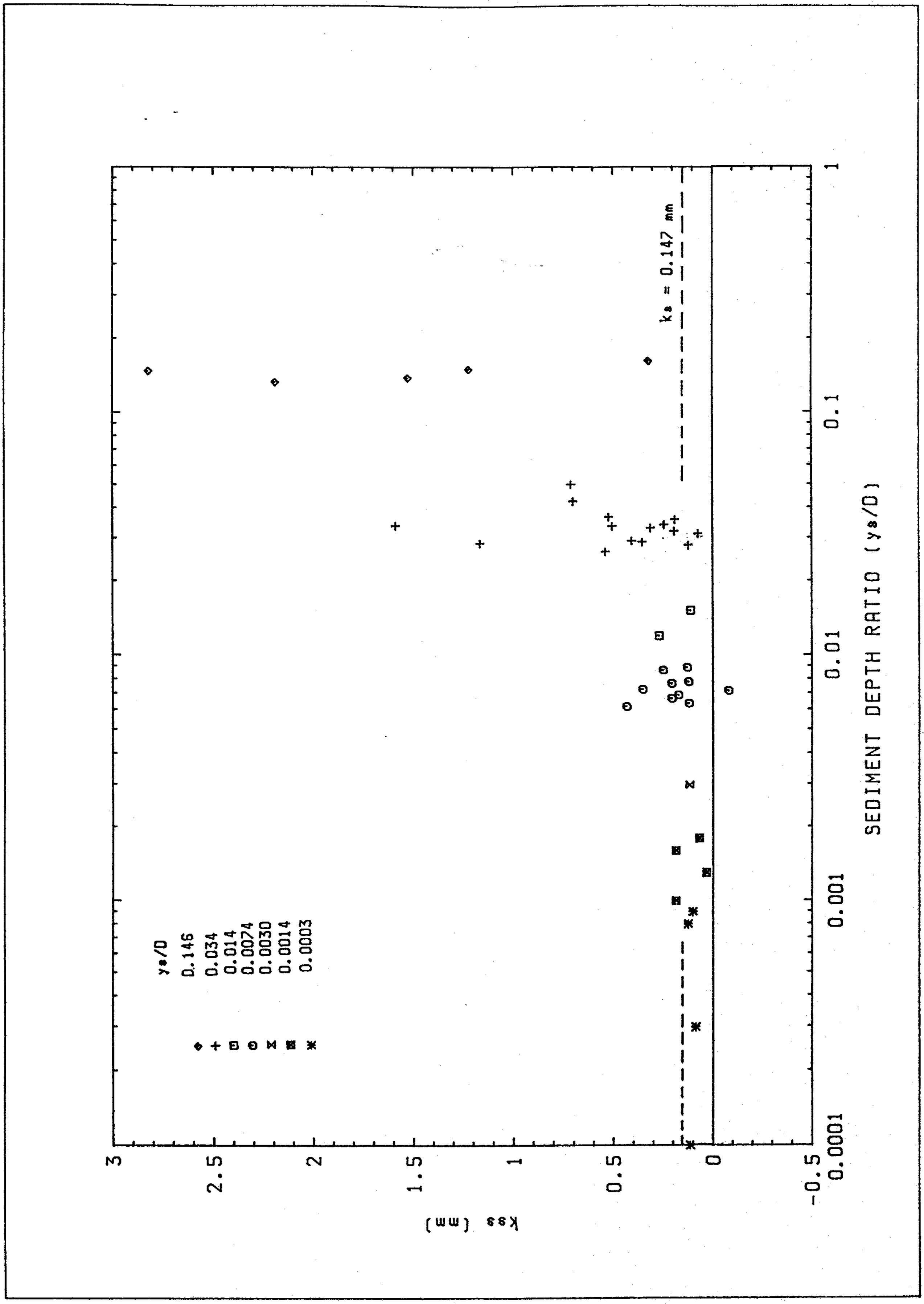

Fig 27 Change in kss roughness due to deposited beds in 299 mm pipe

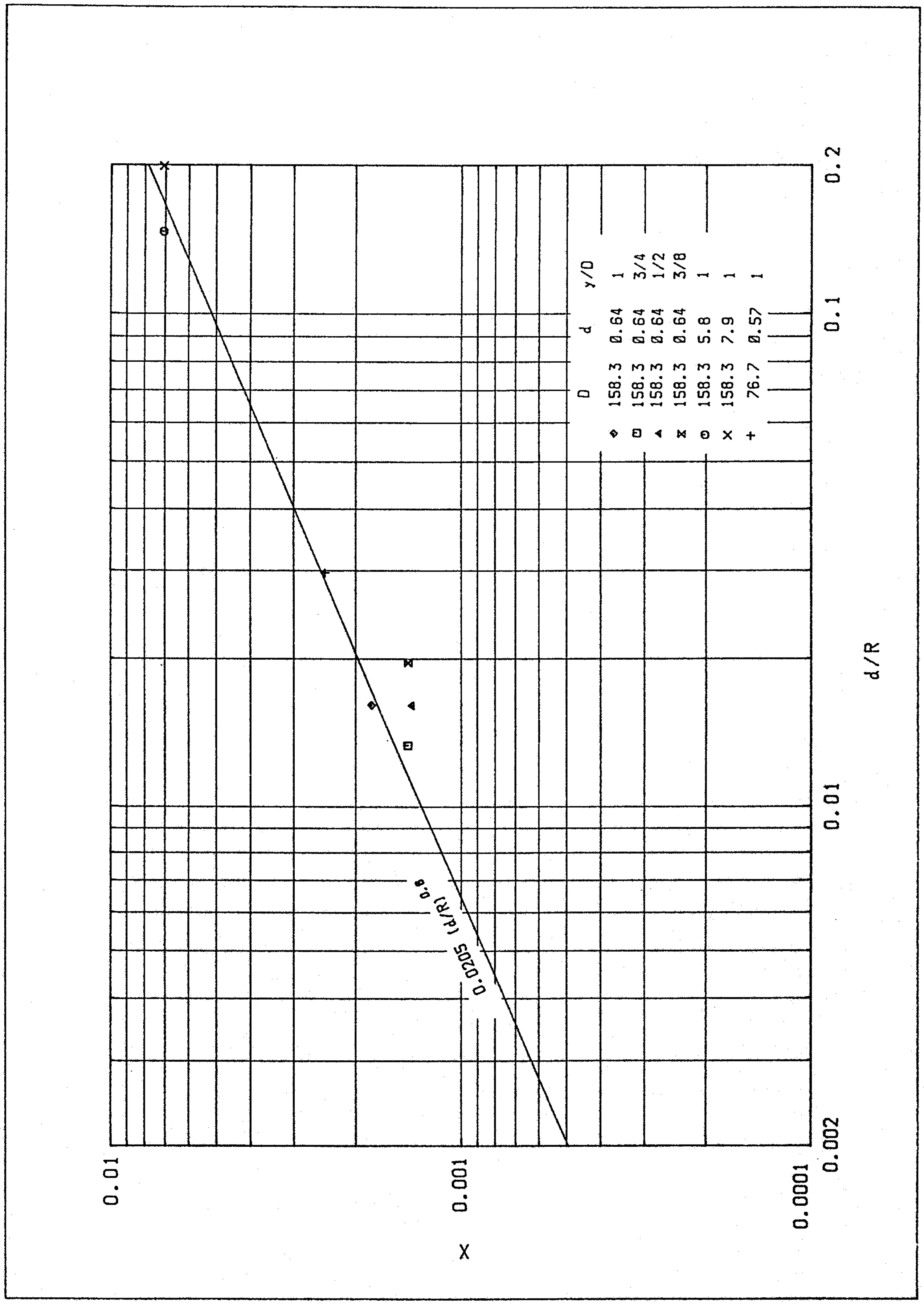

Fig 28 LIMIT OF DEPOSITION - X versus d/R

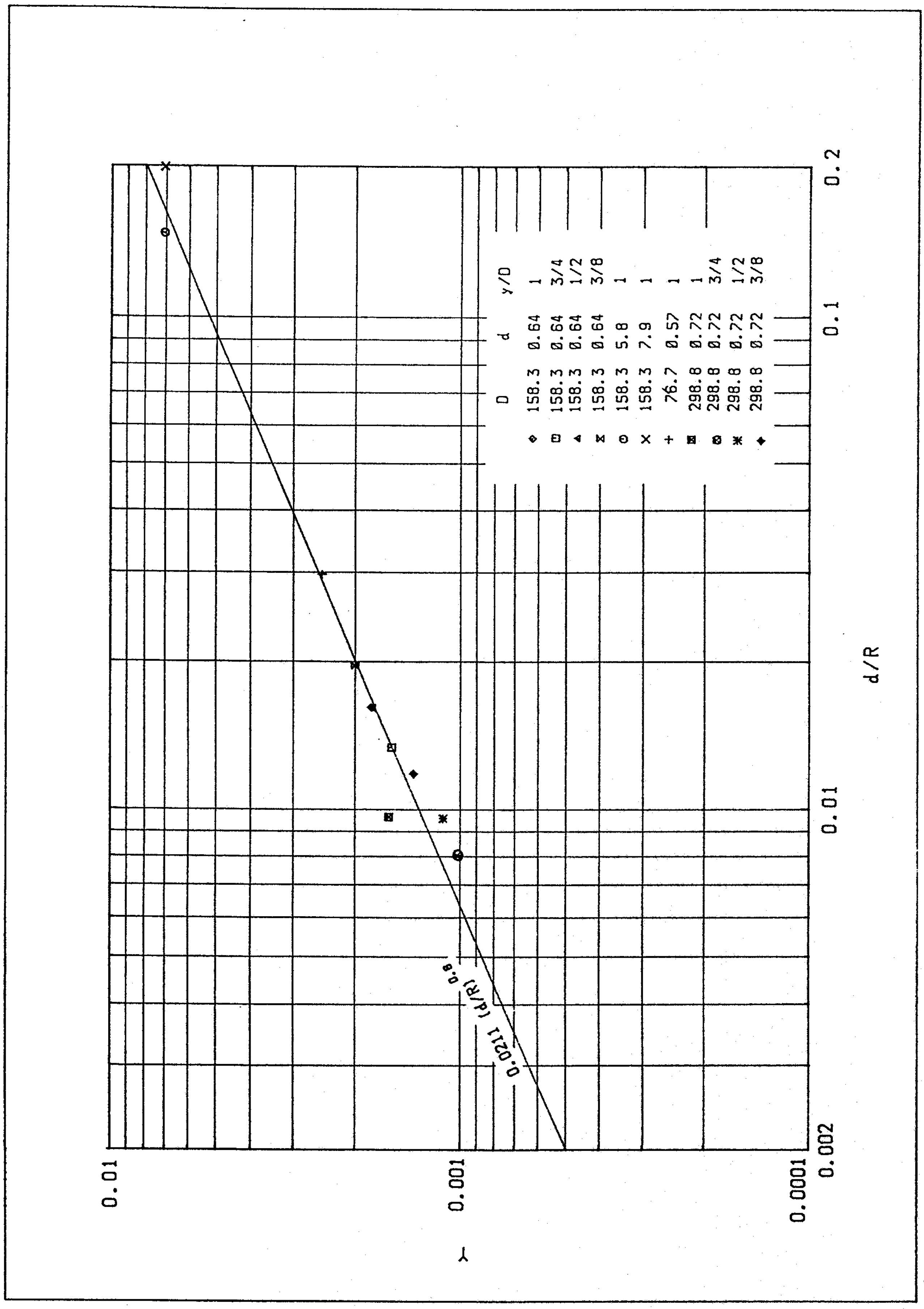

Fig 29 LIMIT OF DEPOSITION - Y versus d/R

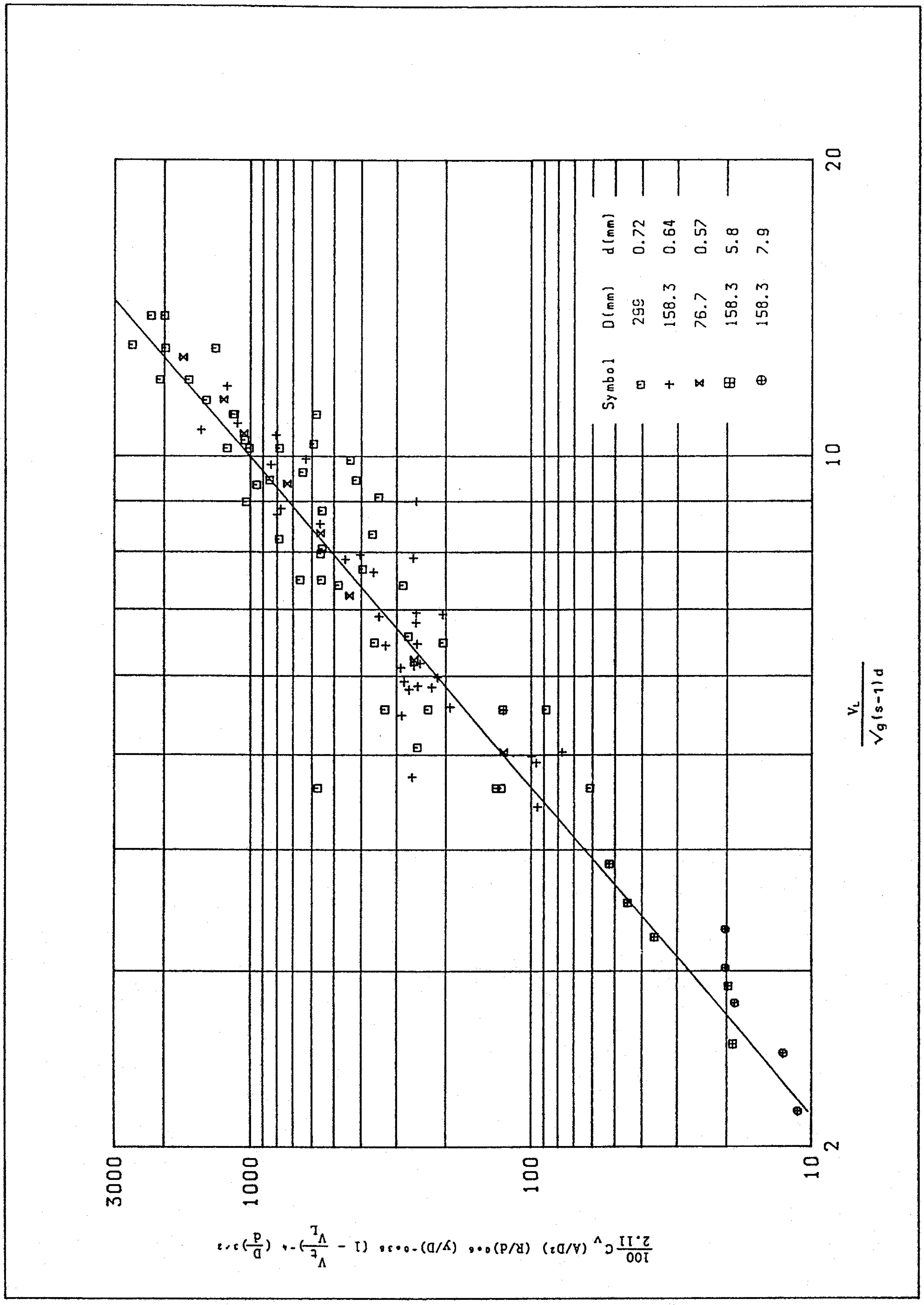

Fig 30 LIMIT OF DEPOSITION - All HR data compared with Equation (32)

APPENDIX

APPENDIX A

Formulae for fall viscosity and settling velocity

1. Kinematic viscosity, ν

$$\nu = \frac{1.79 \times 10^{-6}}{1 + 0.03368T + 0.000221T^2}$$

where T is the temperature in degrees centigrade.

2. Fall velocity of the particle, w in m/s:

$$w = \frac{\{9\,\nu^2 + 10^{-9}\,d^2\,g\,(s-1)\,(0.03869 + 0.0248d)\}^{1/2} - 3\,\nu}{[0.11607 + 0.074405\,d] \times 10^{-3}}$$

Here ν = kinematic viscosity of fluid in m^2/s

d = sediment size in mm

and s = specific gravity of sediment